QCD physics at LHC

[ATLAS-biased] [Top-biased]

Nello Bruscino

INFN Roma 1 & Sapienza Università di Roma

CTEQ School 2022 - 6-16 July 2022

This project has received funding from the European Union's Horizon 2020 research and innovation programme under the Marie Skłodowska-Curie grant agreement No. 754496

Lecture infos & disclaimers

e-mail: nello.bruscino@cern.ch

First of all, my apologies for not being there in Pittsburgh in person!

- lectures re-calibrated to be more self-explicative

Some organisational points

- ZOOM ⇾ I cannot see your doubt faces 🤔 or raised hands 🖐
- ⇾ ***I will pause after each chapter and ask for questions/comments***

Two major topics: ***QCD*** and ***top Physics*** (in this proportion! 😆)

- my background in mostly LHC > ATLAS >Top-physics oriented
- ⇾ focus on arguments I have more experience about
- ***apologies for not covering several other interesting results***

Lectures' goal? I hope to convince you that…

- **… we can perform several nice QCD tests with LHC data**
- **… ATLAS can play a leading role in such tests**
- **… top physics is a nice playground to test the Standard Model (SM) and search for new physics!**

Outline

1. The Large Hadron Collider as a gluon/top factory

2. Overview of the QCD physics program at the LHC

- what will/won't be covered

3. Experimental background

- Calibration & Tuning
- Unfolding techniques

4. Physics topics: latest experimental results on QCD

- Global quark/gluon probability density functions (PDFs)
- Exotic hadrons (charmonia and bottomonia)
- p-p quantum interference
- jet quenching in Quark gluon Plasma (QGP)
- α_S and b-fragmentation function

About the event display: One of the first heavy-ion collisions with stable beams recorded by ATLAS in November 2015. Tracks reconstructed from hits in the inner tracking detector are shown as orange arcs curving in the solenoidal magnetic field. The green and yellow bars indicate energy deposits in the Liquid Argon and Scintillating Tile calorimeters respectively. (Image: ATLAS Collaboration/CERN)

LHC as factory

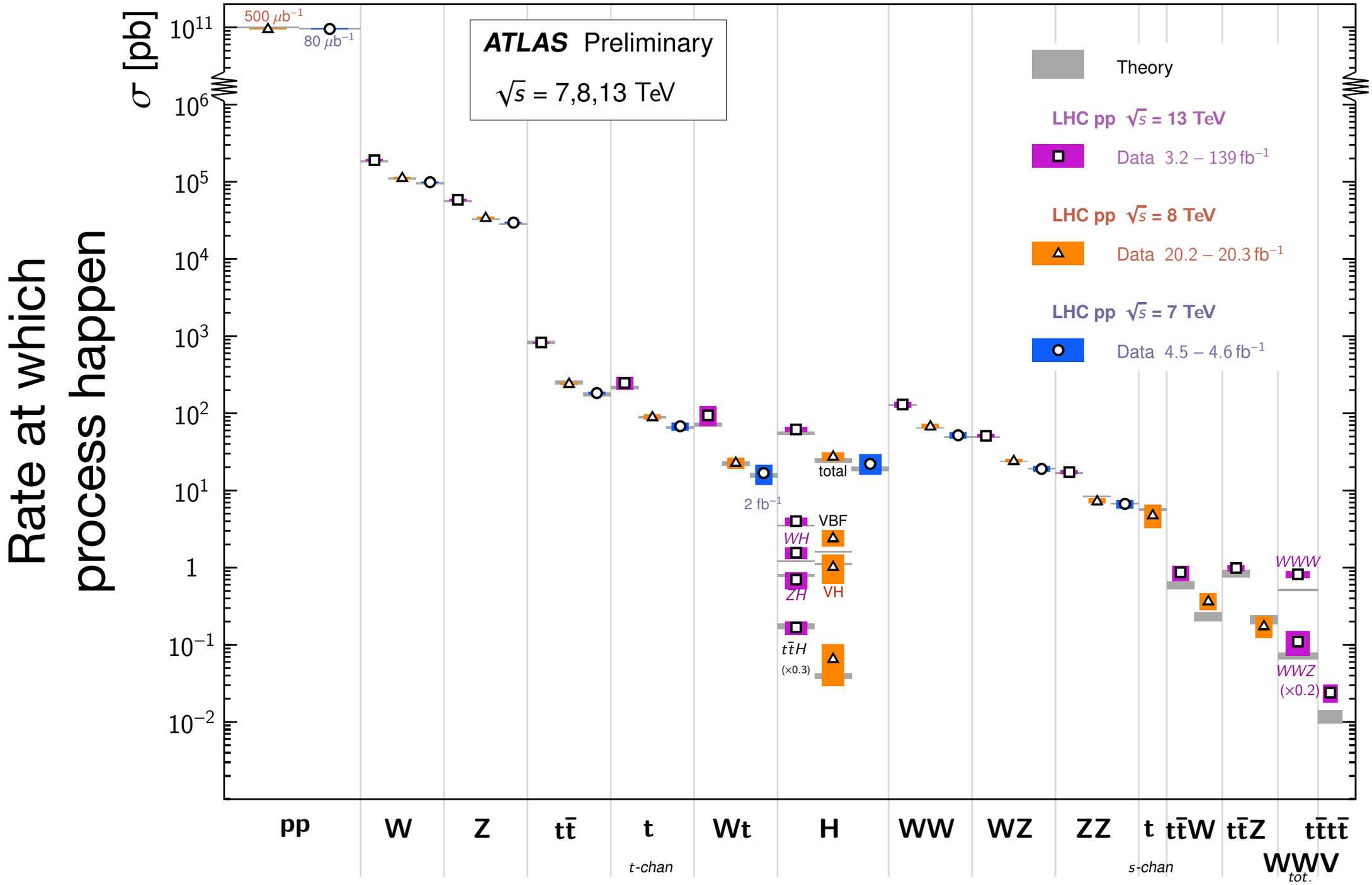

LHC as Higgs factory?

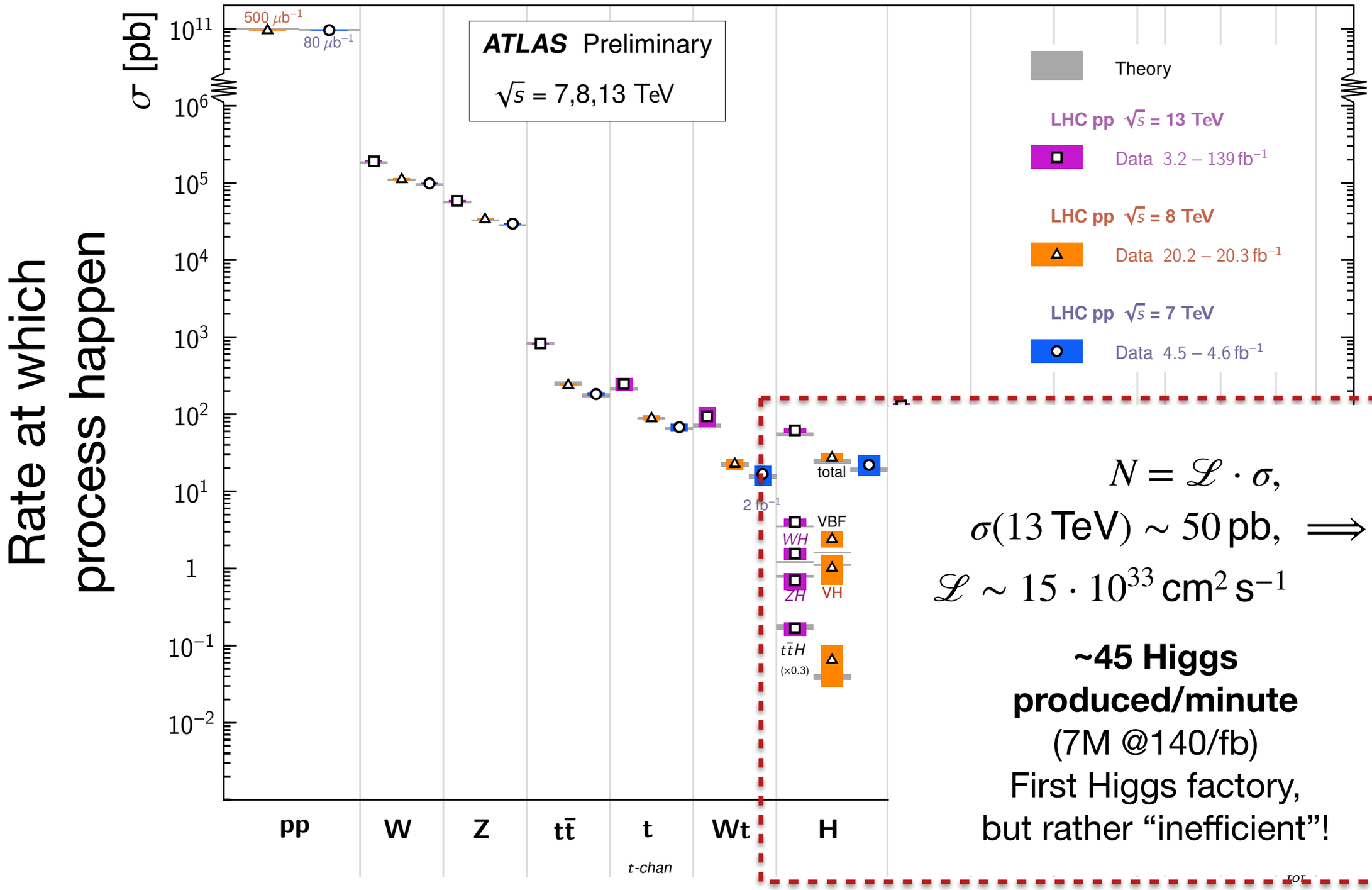

$$N = \mathscr{L} \cdot \sigma,$$

$$\sigma(13\,\text{TeV}) \sim 50\,\text{pb}, \implies$$

$$\mathscr{L} \sim 15 \cdot 10^{33}\,\text{cm}^2\,\text{s}^{-1}$$

~45 Higgs produced/minute
(7M @140/fb)
First Higgs factory,
but rather “inefficient”!

LHC as top factory?

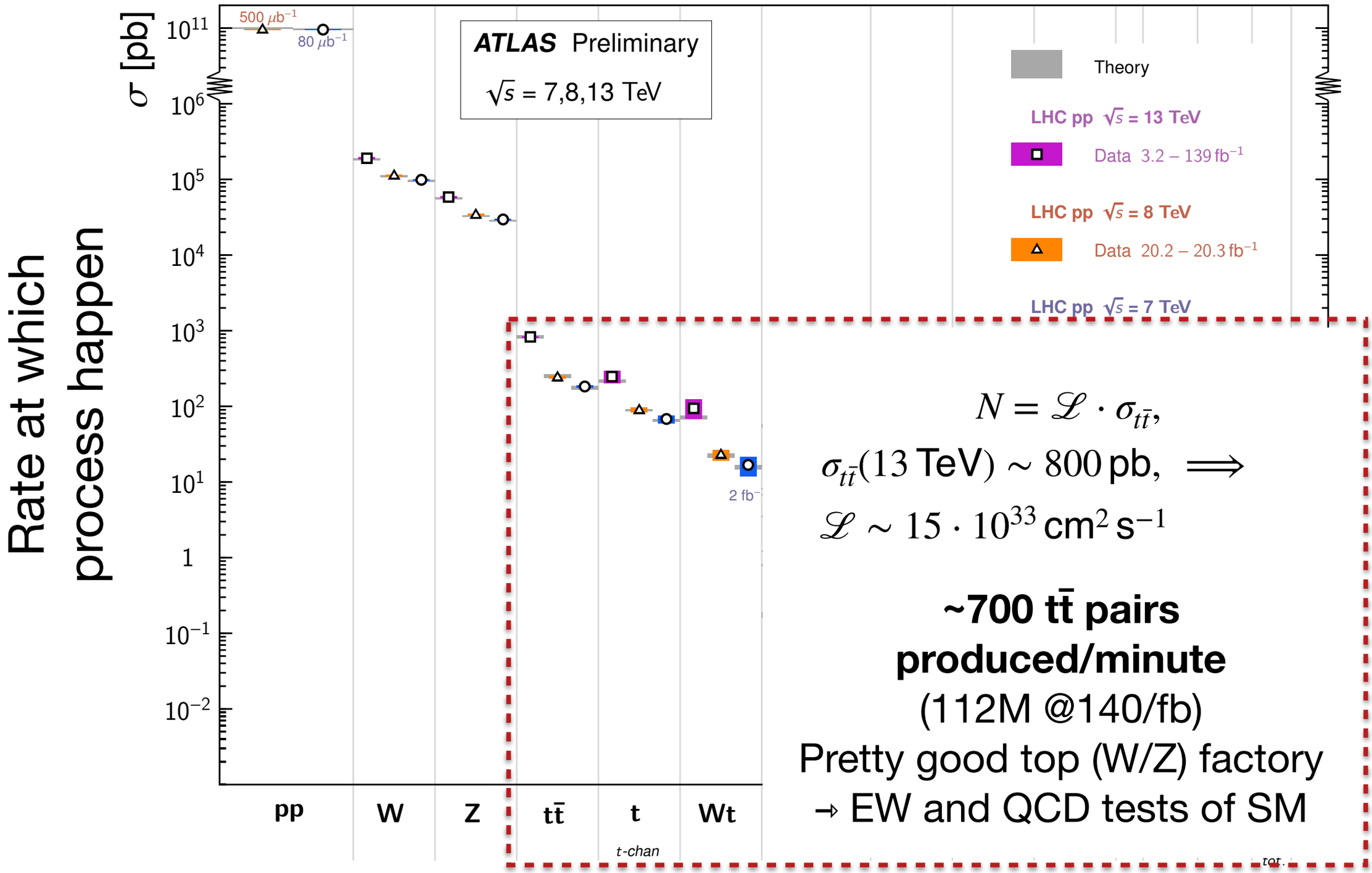

$$N = \mathscr{L} \cdot \sigma_{t\bar{t}},$$

$$\sigma_{t\bar{t}}(13\,\text{TeV}) \sim 800\,\text{pb}, \implies$$

$$\mathscr{L} \sim 15 \cdot 10^{33}\,\text{cm}^2\,\text{s}^{-1}$$

~700 $t\bar{t}$ pairs produced/minute

(112M @140/fb)

Pretty good top (W/Z) factory

➙ EW and QCD tests of SM

LHC as gluon factory?

Standard Model Production Cross Section Measurements

Status: February 2022

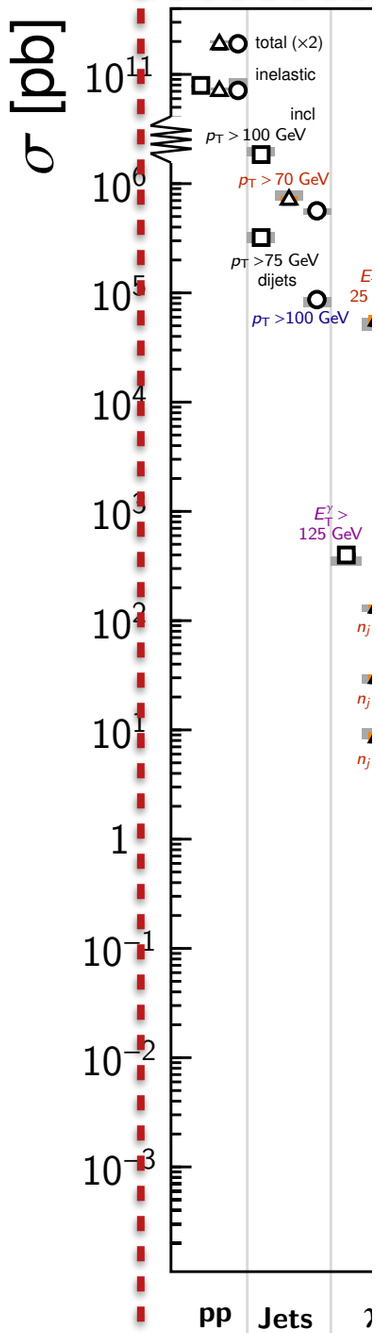

Rate at which process happen

Model	E_{CM} [TeV]	$\int \mathcal{L}\,dt$[fb^{-1}]	Measurement	Theory
pp	8	50×10^{-8}	$\sigma = 96.07 \pm 0.18 \pm 0.91$ mb	$\sigma = 99.55 \pm 2.14$ mb (COMPETE HPR1R2)
pp	7	8×10^{-8}	$\sigma = 95.35 \pm 0.38 \pm 1.3$ mb	$\sigma = 97.26 \pm 2.12$ mb (COMPETE HPR1R2)
pp inelastic	13	6×10^{-8}	$\sigma = 79.3 \pm 2.9$ mb	$\sigma = 78.4 \pm 2$ mb (Schuler/Sjöstrand)
pp inelastic	8	50×10^{-8}	$\sigma = 71.73 \pm 0.15 \pm 0.69$ mb	$\sigma = 73 \pm 2$ mb (Schuler/Sjöstrand)
pp inelastic	7	8×10^{-8}	$\sigma = 71.34 \pm 0.36 \pm 0.83$ mb	$\sigma = 71.5 + 20 - 2$ mb (Schuler/Sjöstrand)
Incl. jet **R**=0.4, **|y| < 3.0**	13	3.2	$\sigma = 1845 \pm 4 + 119 - 120$ nb	$\sigma = 1997 + 152 - 208$ nb (NLOJet++, CT14)
Incl. jet **R**=0.4, **|y| < 3.0**	8	20.2	$\sigma = 726.4 \pm 1.1 + 42.7 - 41.8$ nb	$\sigma = 800 + 59 - 100$ nb (NLOJet++, CT14)
Incl. jet **R**=0.4, **|y| < 3.0**	7	4.5	$\sigma = 563.9 \pm 1.5 + 55.4 - 51.4$ nb	$\sigma = 569.8 + 29.5 - 46.3$ nb (NLOJet++, CT10)
Dijet **R**=0.4, **|y| < 3.0**, **y* < 3.0**	13	3.2	$\sigma = 321 \pm 0.8 + 18.6 - 19$ nb	$\sigma = 340 + 17 - 54$ nb (NLOJet++, CT14)
Dijet **R**=0.4, **|y| < 3.0**, **y* < 3.0**	7	4.5	$\sigma = 86.87 \pm 0.26 + 7.56 - 7.2$ nb	$\sigma = 86.9 + 4.7 - 12.4$ nb (NLOJet++, CT10)

$$N = \mathscr{L} \cdot \sigma_{pp}^{\text{inel}},$$

$$\sigma_{pp}^{\text{inel}}(13\,\text{TeV}) \sim 80\,\text{mb}, \implies$$

$$\sigma_{pp}^{\text{dijet}}(13\,\text{TeV}) \sim 300\,\text{nb},$$

$$\mathscr{L} \sim 15 \cdot 10^{33}\,\text{cm}^2\,\text{s}^{-1}$$

~60M inelastic events produced/minute

~270k dijet events produced/minute

Great gluon factory! Immense pool of QCD processes, modulo some inefficiencies (dense environment, forward physics, SM calculations, …)

QCD physics program at LHC

Parton Distribution Functions (PDFs)

Monte Carlo parameters tuning

1. Photon/W/Z+jets

2. Jet physics

Other non-perturbative effects

3. Jet substructure

Perturbative QCD / Strong couplings

4.“Soft QCD” & Heavy Ions

5. Quarkonia

Exotic quantum phenomena

Fragmentation functions

QCD physics program at LHC

Parton Distribution Functions (PDFs) — ATLAS, CMS, LHCb, ALICE

Monte Carlo parameters tuning — ATLAS, CMS, LHCb, ALICE

1. Photon/W/Z+jets

2. Jet physics

Other non-perturbative effects — ATLAS, CMS, LHCb, ALICE

Perturbative QCD / Strong couplings — ATLAS, CMS, LHCb, ALICE

3. Jet substructure

4.“Soft QCD” & Heavy Ions

5. Quarkonia

Exotic quantum phenomena — ATLAS, CMS, LHCb, ALICE

Fragmentation functions — ATLAS, CMS, LHCb, ALICE

QCD physics program in ATLAS

The QCD cross section can be factorised in three parts: IS, HS, FS.

The ATLAS Collaboration has published important QCD results recently. Measurements are exploited to understand these three parts separately.

- Initial State $\Rightarrow$ Parton Density $f_i(x, \mu_F)$
- Hard Scattering $\Rightarrow$ Matrix Element $\hat{\sigma} \propto |\mathcal{M}|^2$
- Final State $\Rightarrow$ Fragm. Functions $D_a^h(z, Q^2)$

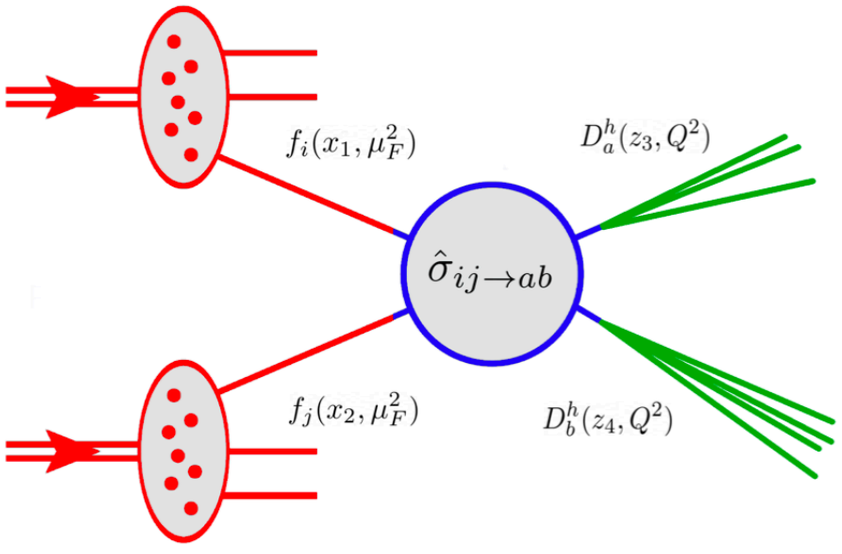

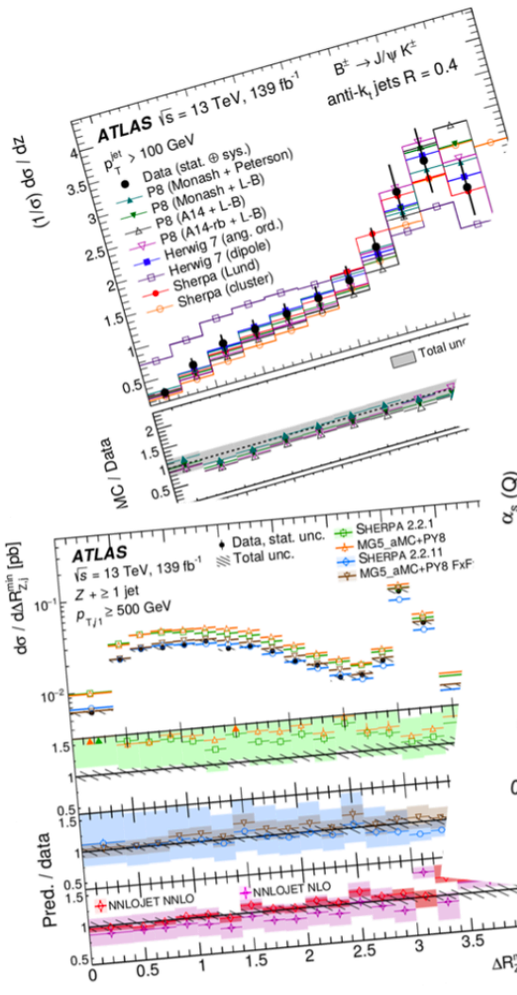

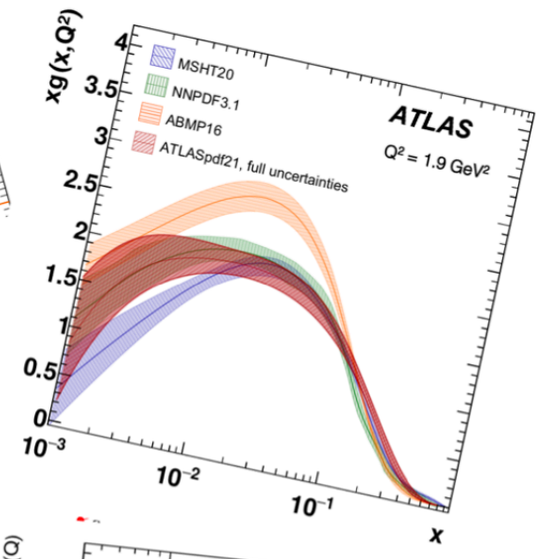

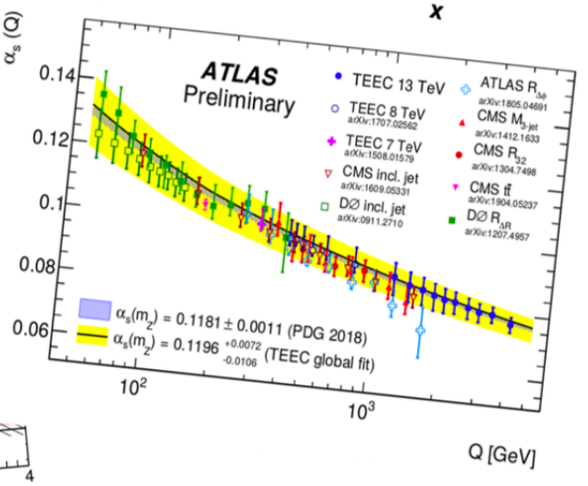

$$d\sigma = \sum_{i,j,a,b} \int_{\Omega} d^2\vec{x} d^2\vec{z}\, f_i(x_1, \mu_F^2) f_j(x_2, \mu_F^2) \times d\hat{\sigma}_{ij\to ab}(\vec{x}, \mu_R^2) \times D_a^h(z_3, Q^2) D_b^h(z_4, Q^2)$$

Questions/Comments?

Experimental background: calibration & tuning

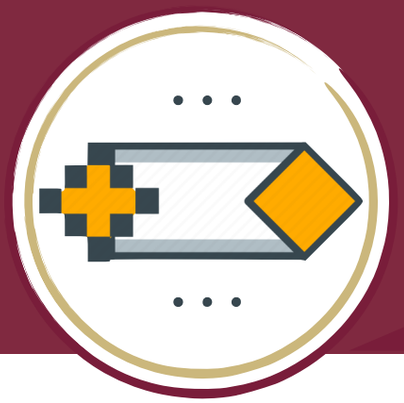

Particle detection

We don't measure particles, we measure energy deposits and then infer particle properties.

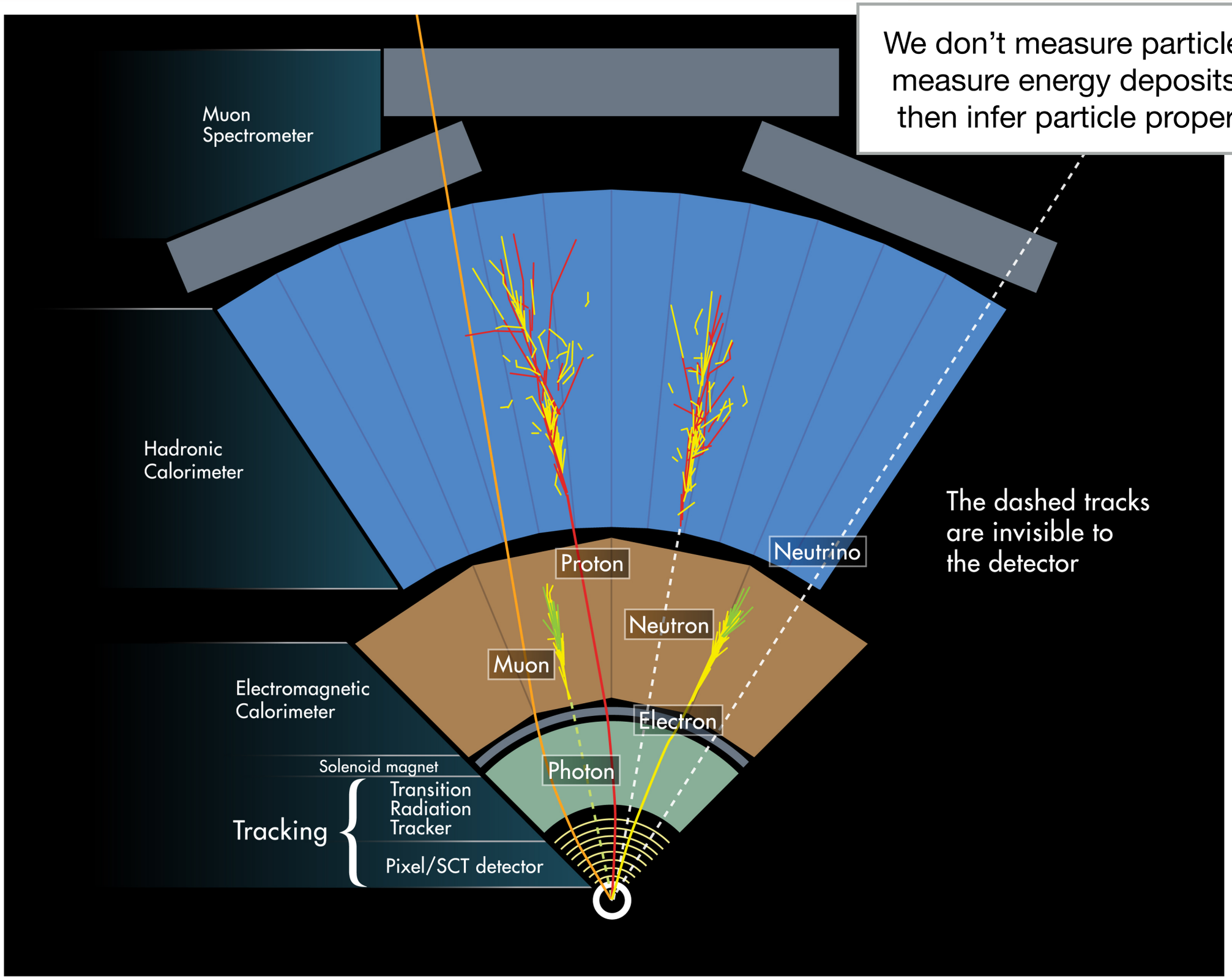

Particle detection

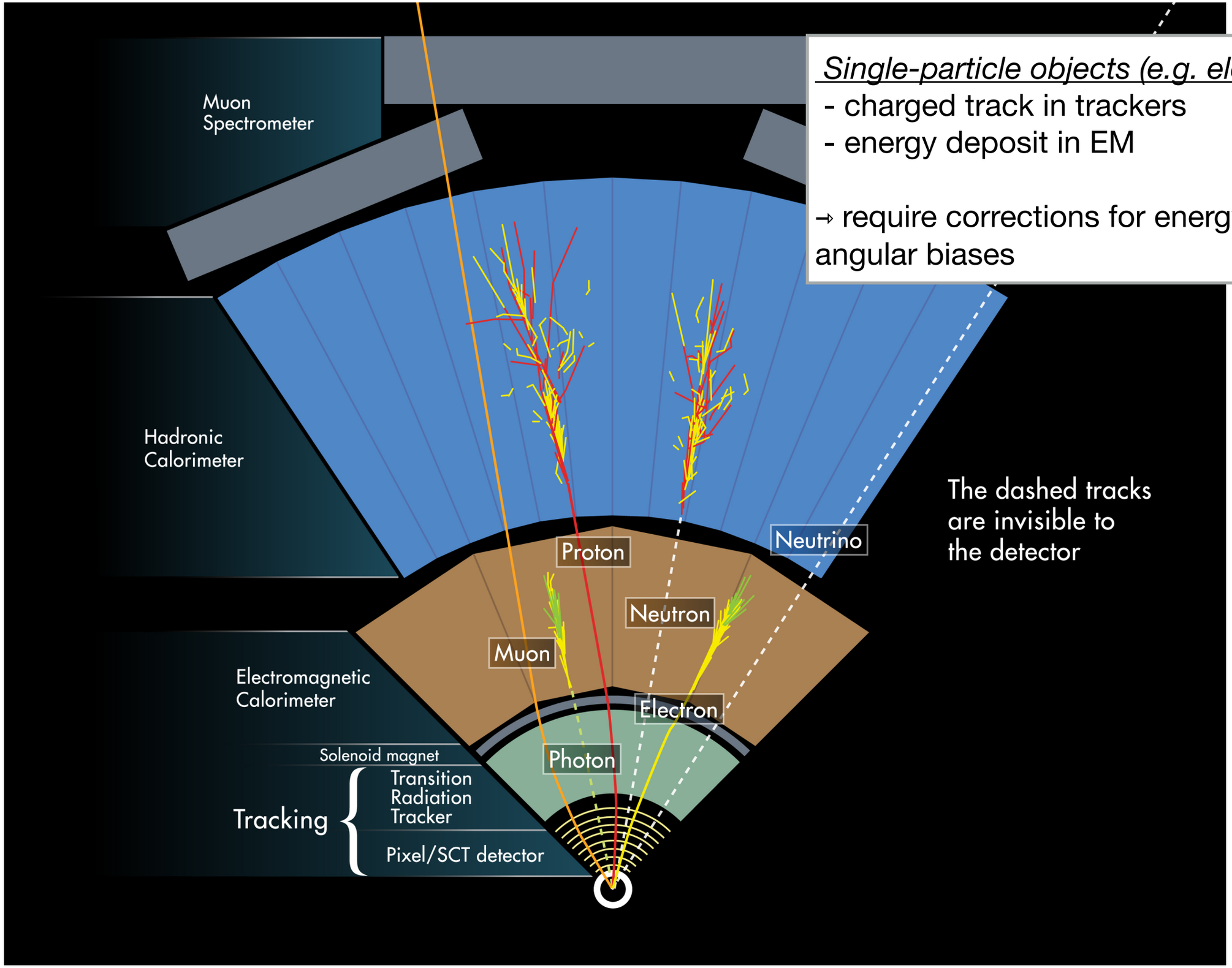

Single-particle objects (e.g. electron):
- charged track in trackers
- energy deposit in EM

⇾ require corrections for energy and angular biases

Particle detection

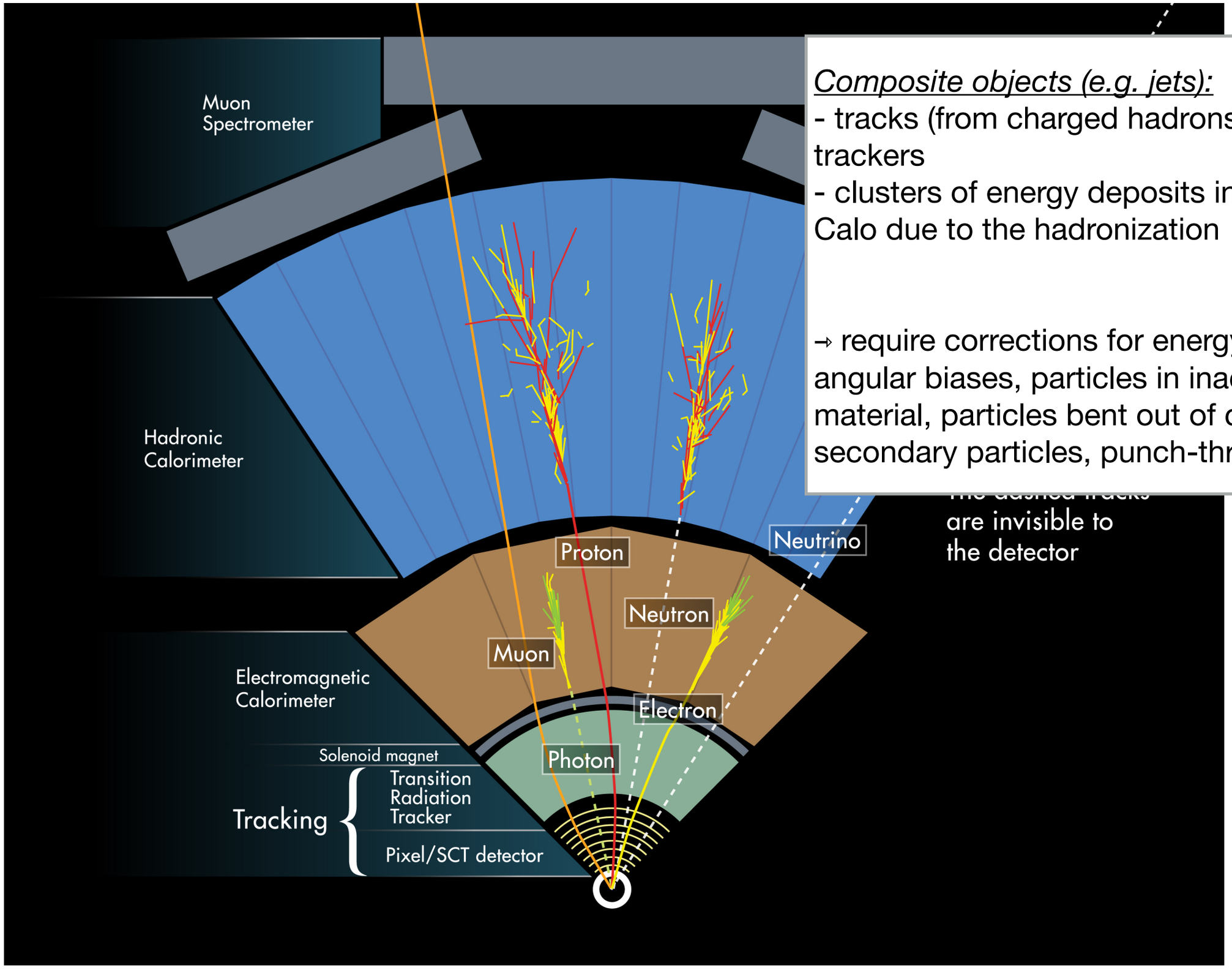

Composite objects (e.g. jets):

- tracks (from charged hadrons) in trackers
- clusters of energy deposits in Had Calo due to the hadronization

⇾ require corrections for energy and angular biases, particles in inactive material, particles bent out of cone, secondary particles, punch-through

Calibration

The nominal calibration is derived using simulation and then a residual calibration accounts for differences between data and simulation (derived using data)

- can use the balance of well- measured objects (e.g. photons) with jets to study the bias in data (e.g., Z/ɣ → ℓℓ + jets, Z → ℓℓɣ, J/Psi → ℓℓ, …)
- complex sequential calibration needed to get fully calibrated jets
  - then to be tagged to understand their likely originating particle

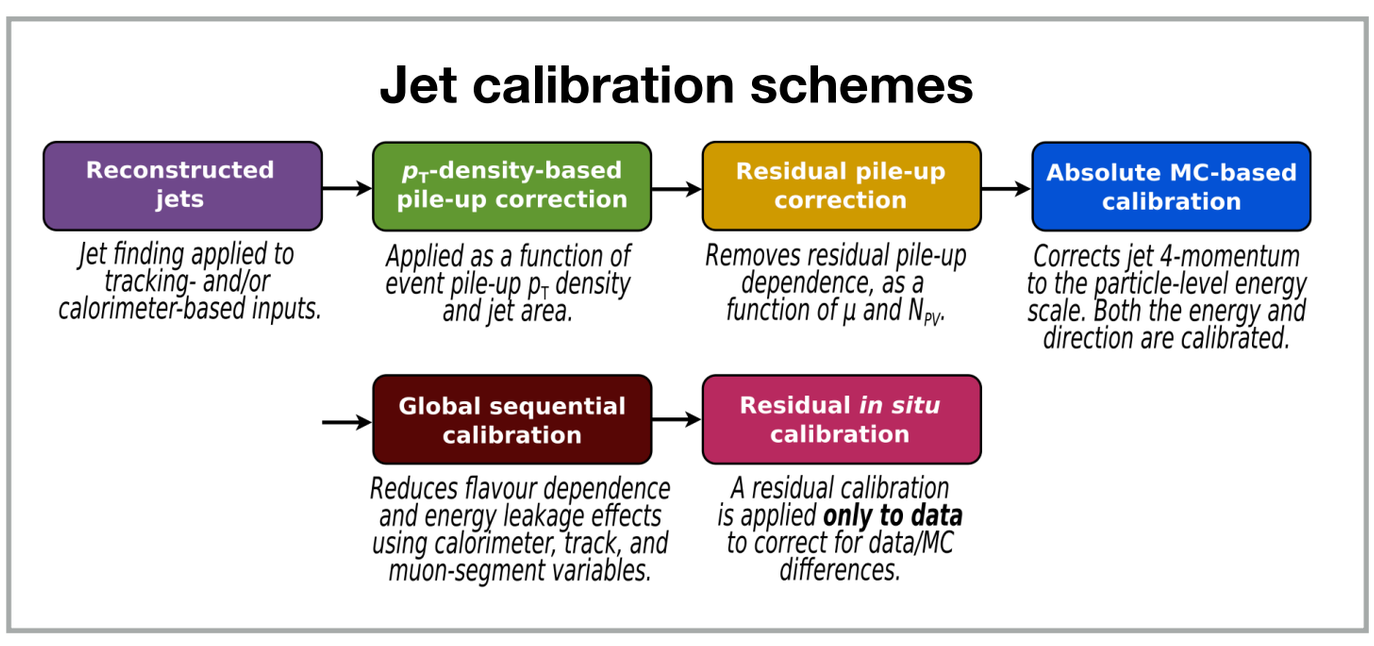

MC based

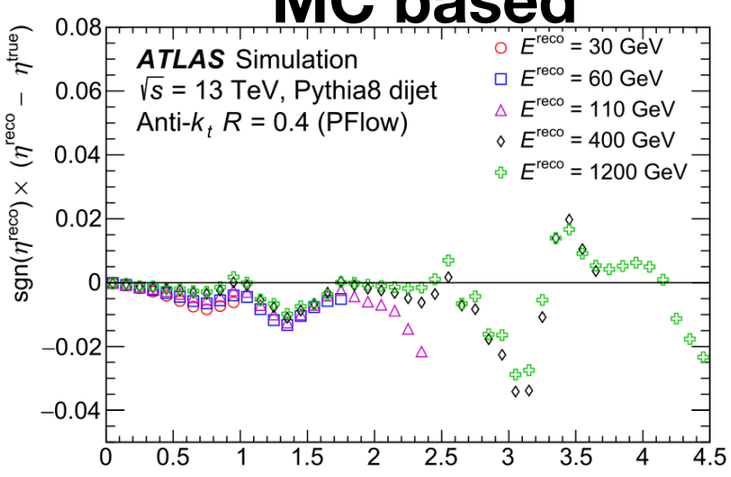

Data based (in-situ)

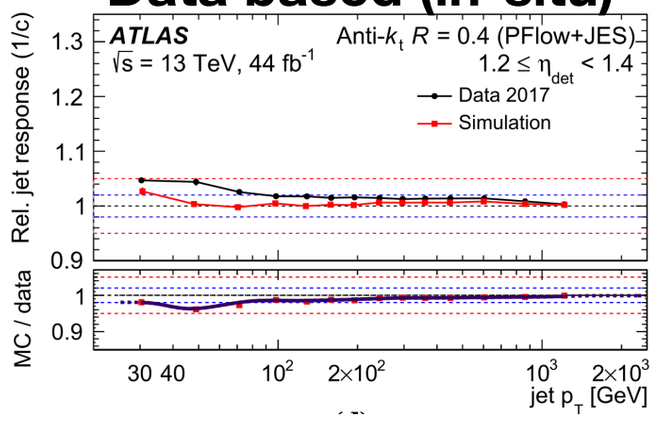

Jet energy bias uncertainty

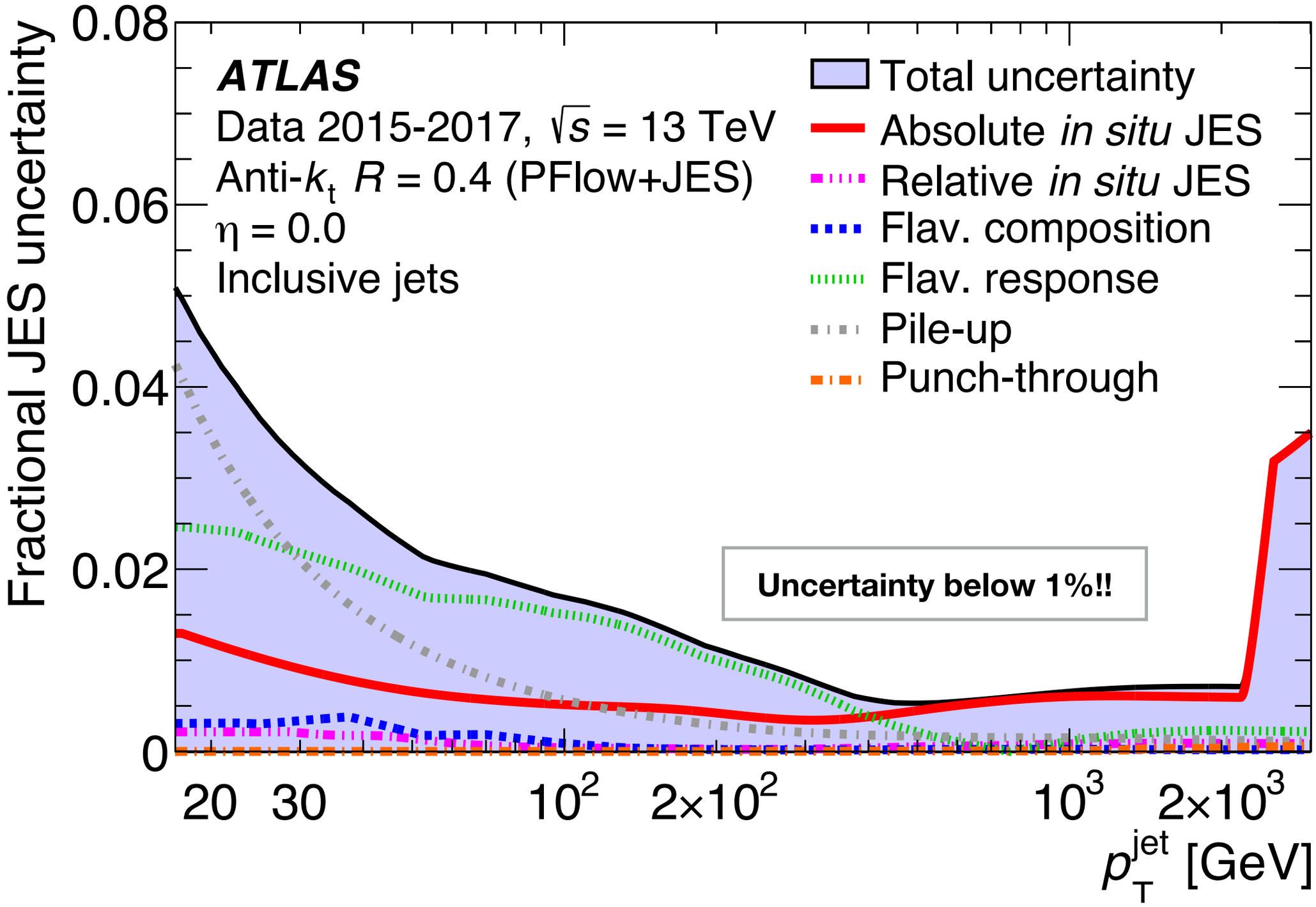

Jet energy bias uncertainty

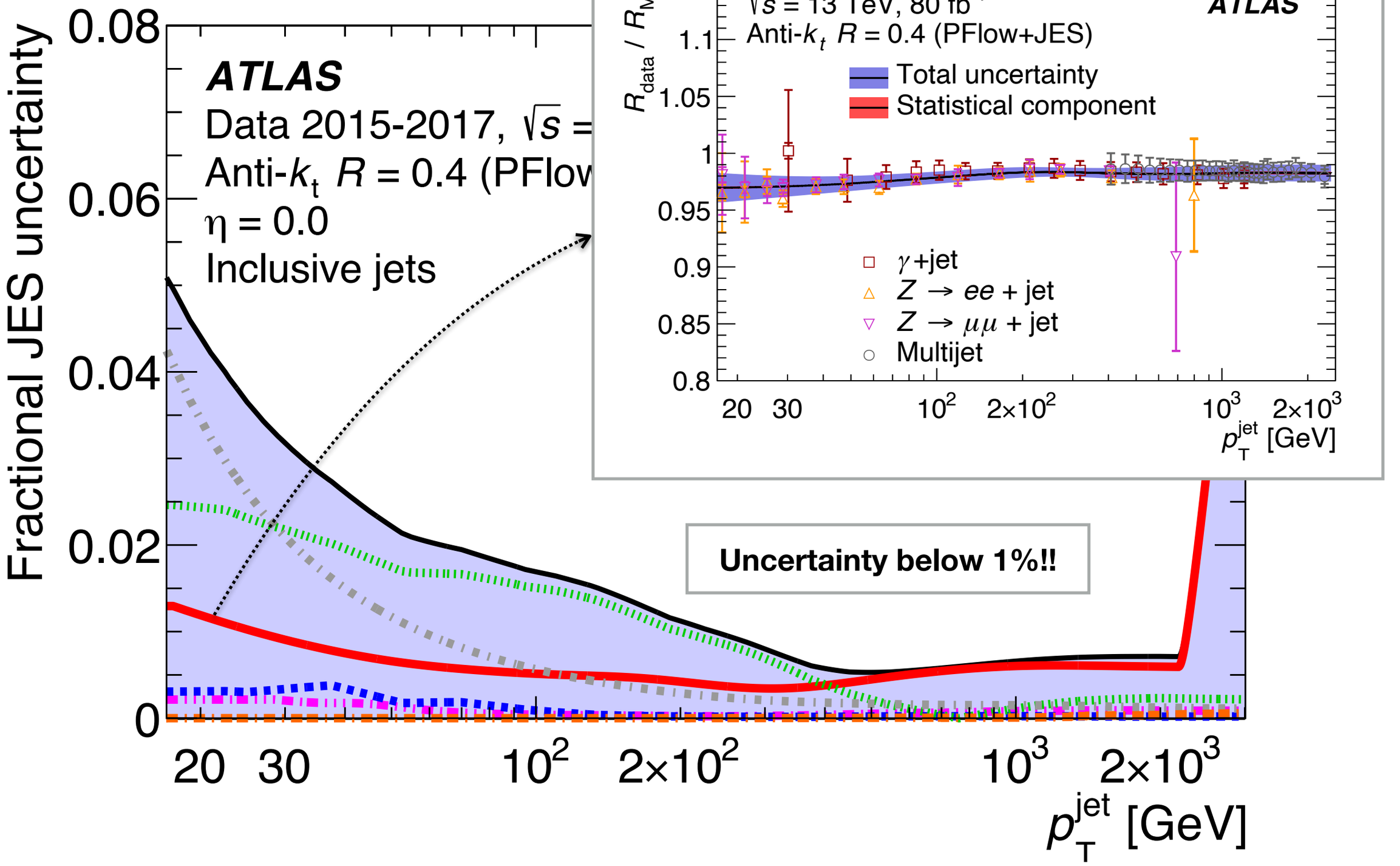

Jet energy bias uncertainty

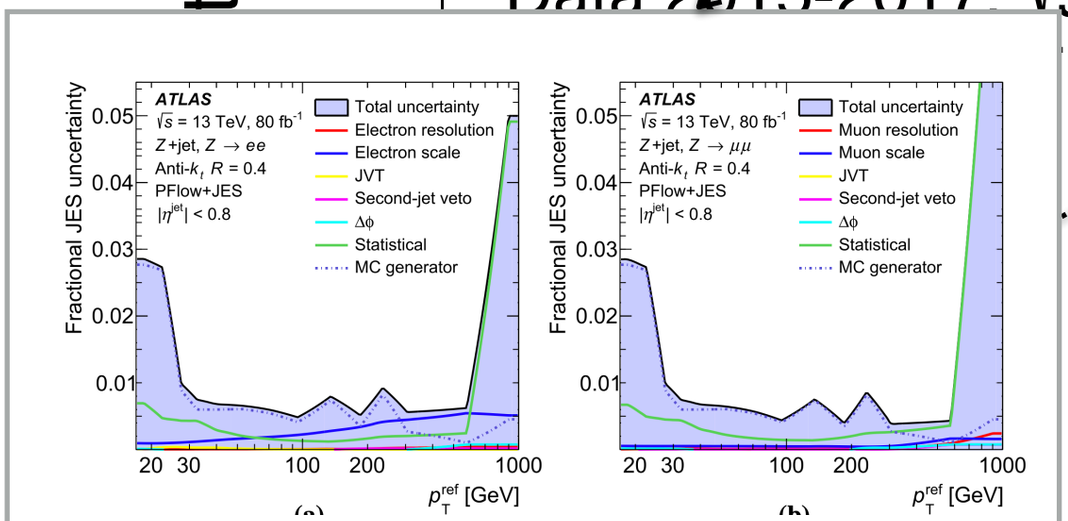

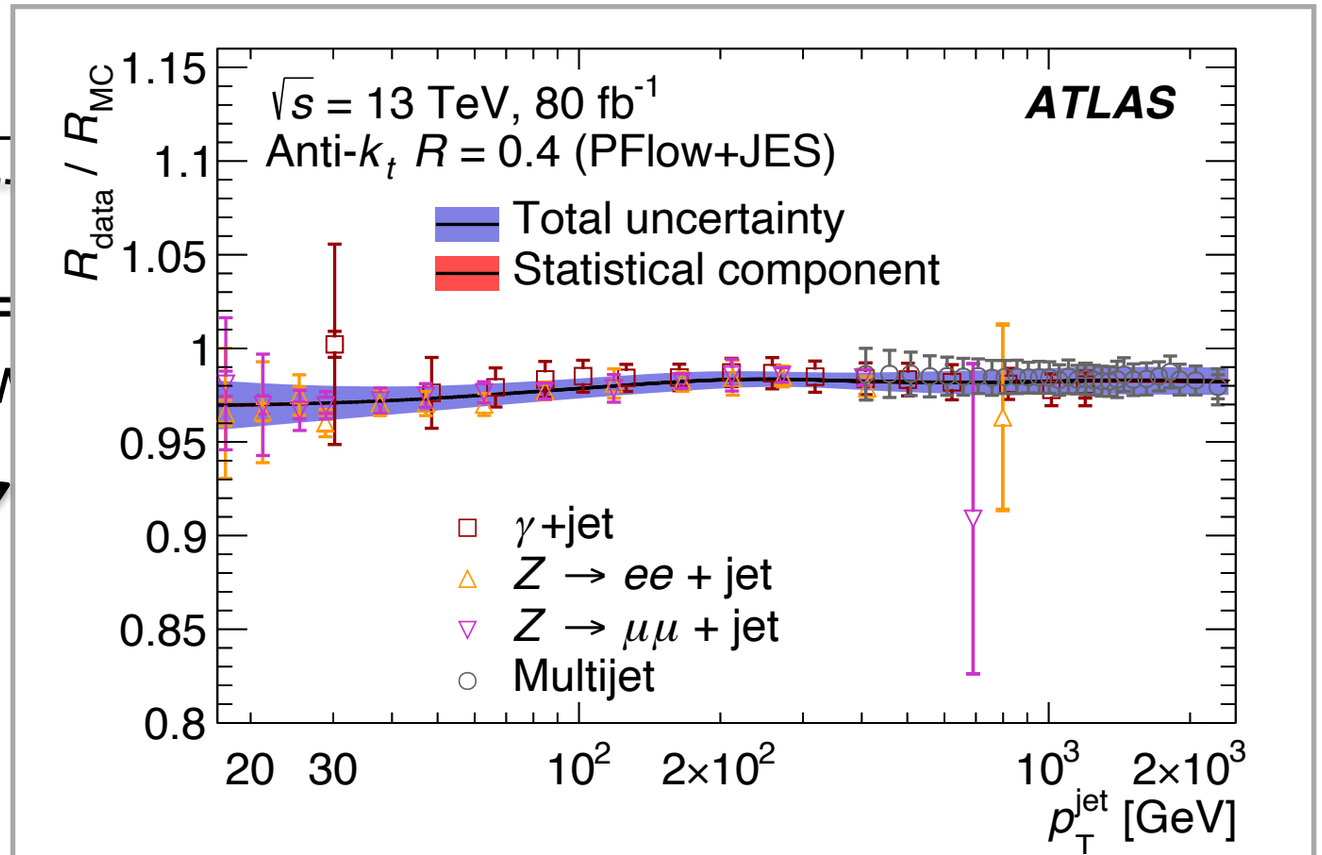

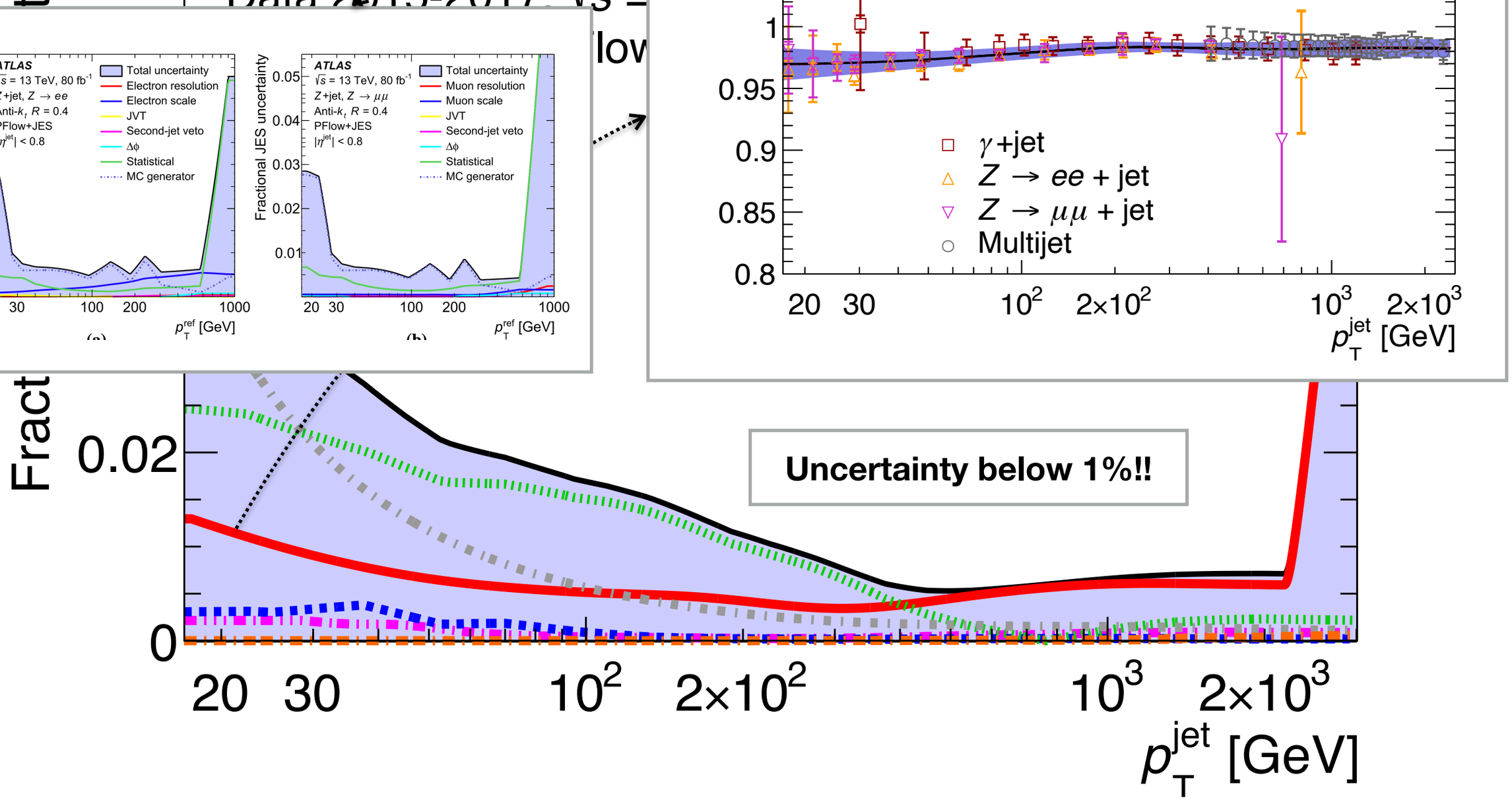

Jet energy bias uncertainty

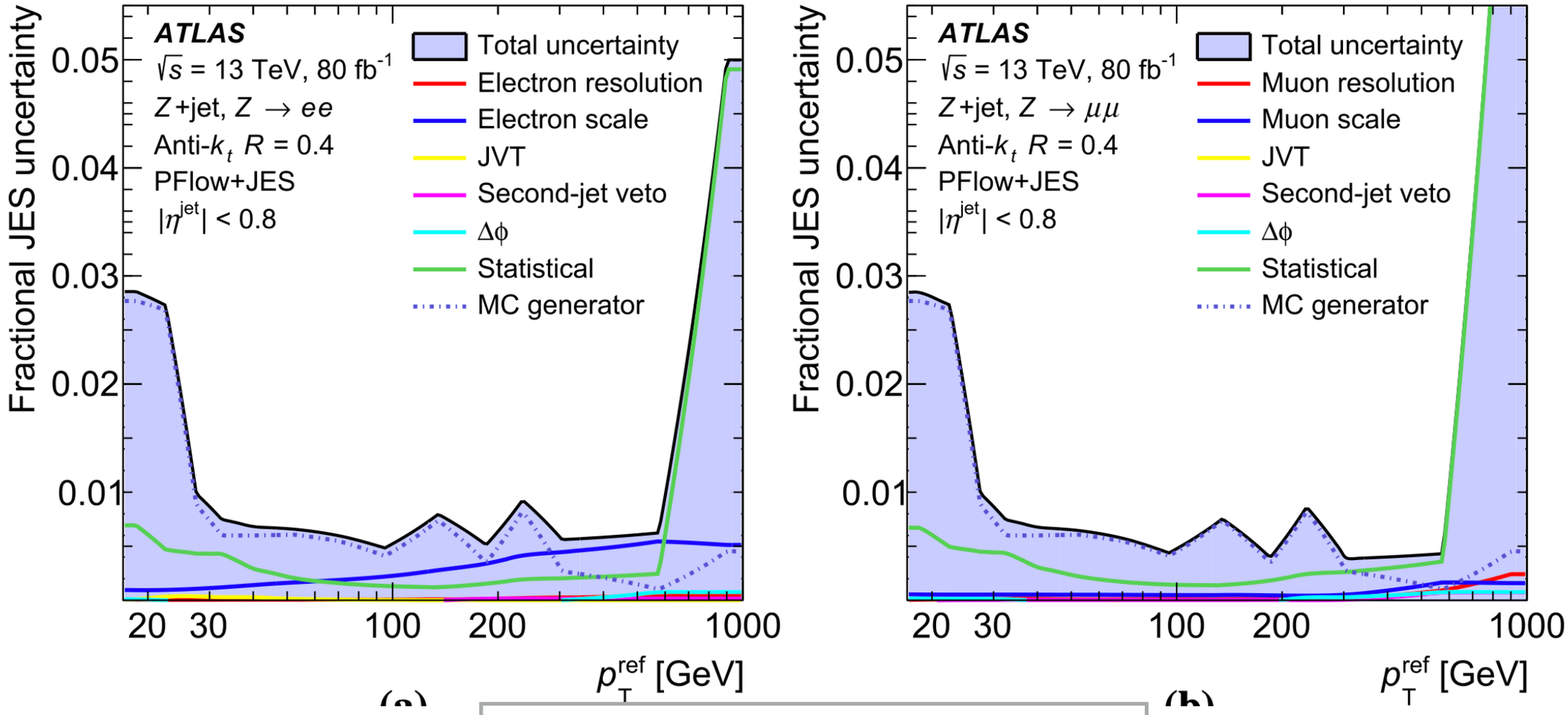

MC generator as leading source of uncertainty
Non-trivial physics in the balance beyond leading order!

Experimental background: Unfolding

What's unfolding?

When someone says they have measured a differential cross-section, they mean that it has been unfolded to parton/particle level objects

- *deconvolution of reco. spectrum to "truth" spectrum*, "removing" interrelated effects
- after unfolding data can be directly compared with theory predictions
  - + correcting data is more general and can allow for multiple theory groups to reuse the measurement

Unfolding needs to correct for interrelated effects:

- *Acceptance and efficiency* ← Particles produced may not be measured
- *Detector noise* ← Particles measured may not be from real particles
- *Background processes* ← If you want to measure process X, need to remove Y from data
- *Combinatorics* ← If N particles, chance that detector can change order
- *Detector distortions* ← Bias and resolution effects (unresolved by calibration)

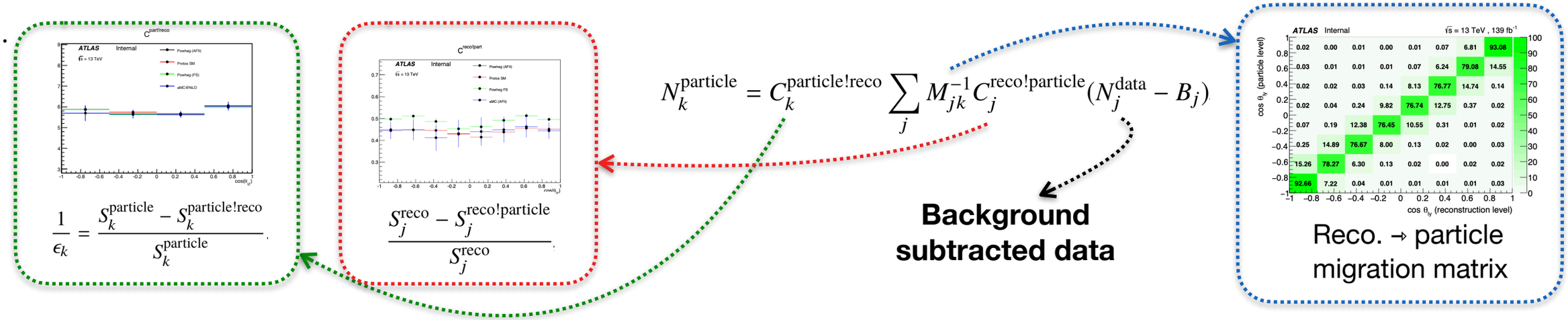

Unfolding example

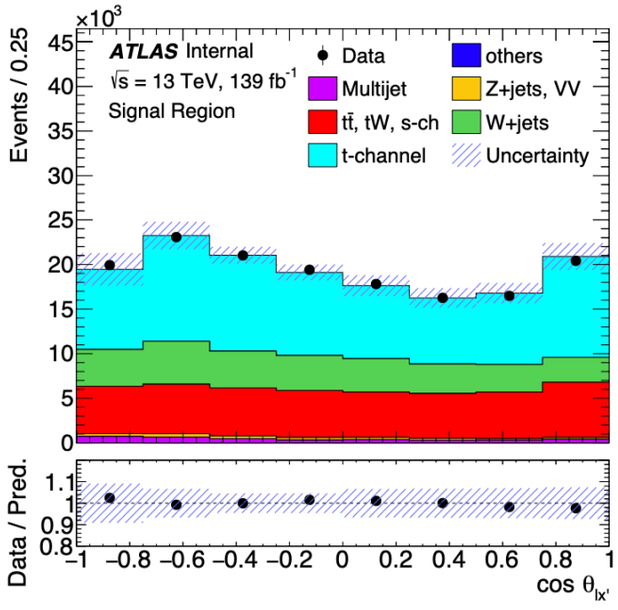

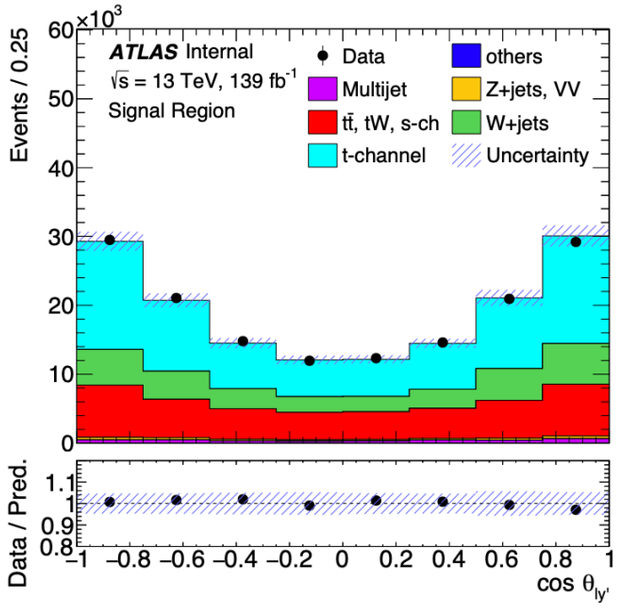

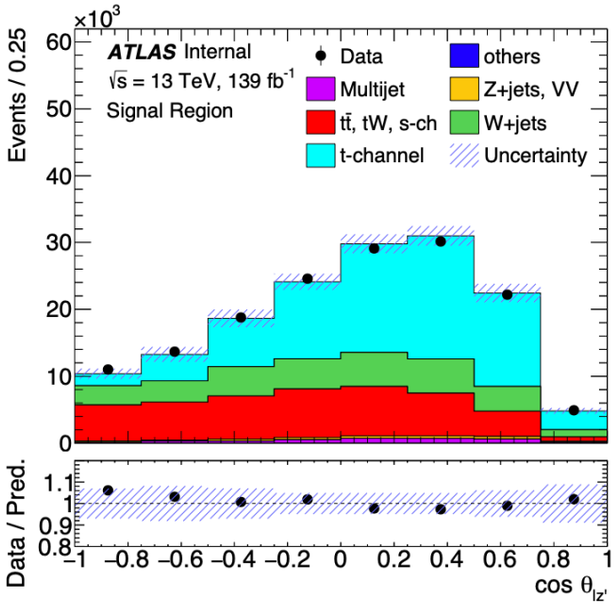

Unfolding example

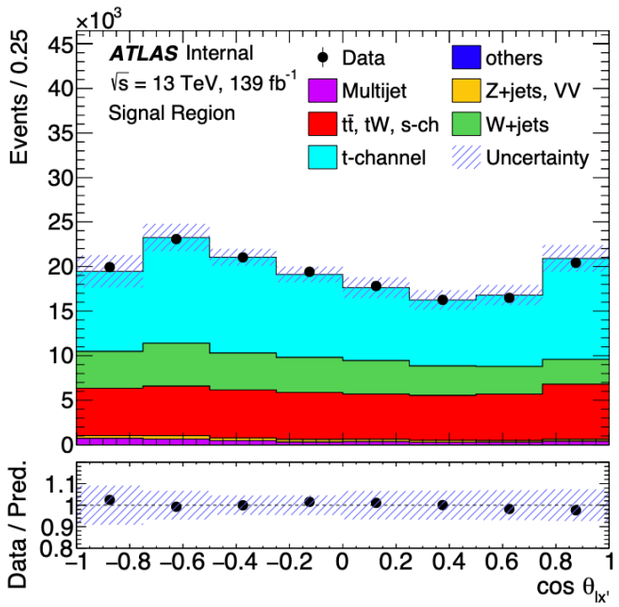

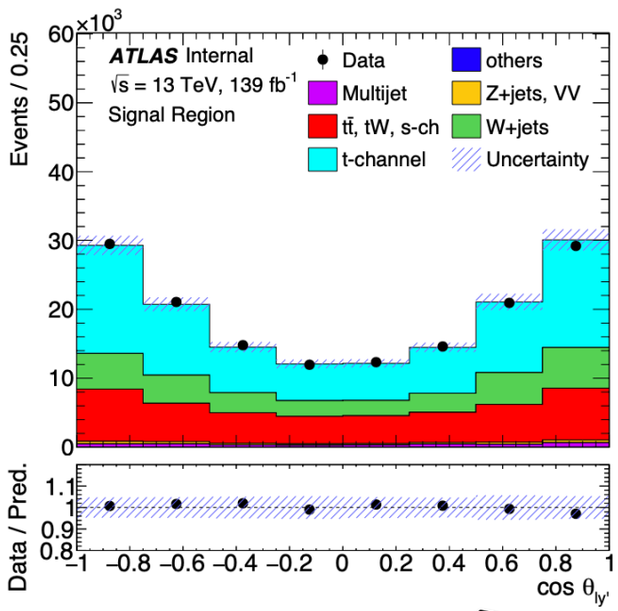

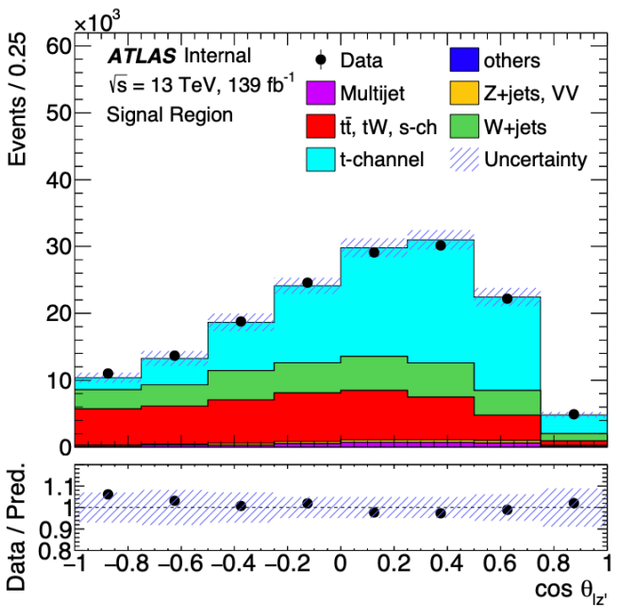

$$N_k^{\text{particle}} = C_k^{\text{particle!reco}} \sum_j M_{jk}^{-1} C_j^{\text{reco!particle}} (N_j^{\text{data}} - B_j)$$

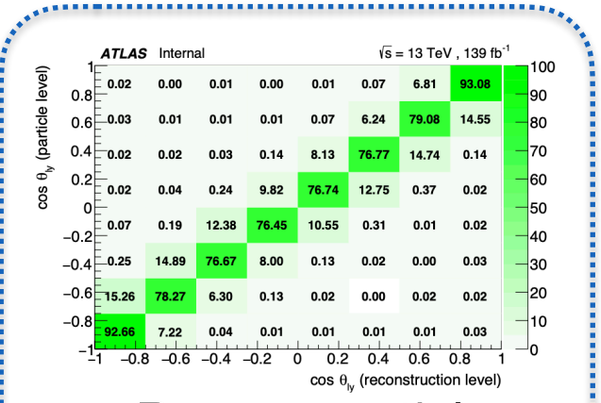

Reco. → particle migration matrix

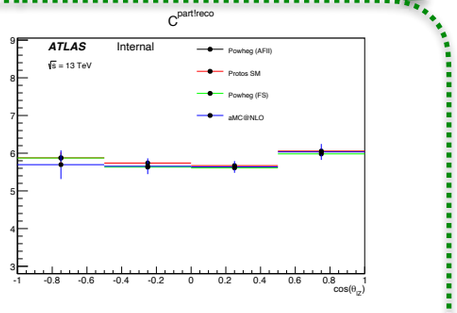

$$\frac{1}{\epsilon_k} = \frac{S_k^{\text{particle}} - S_k^{\text{particle!reco}}}{S_k^{\text{particle}}}$$

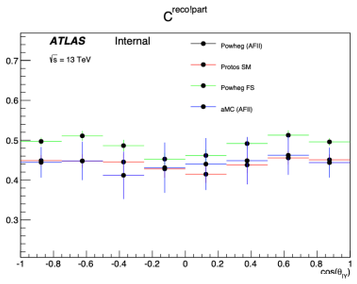

$$\frac{S_j^{\text{reco}} - S_j^{\text{reco!particle}}}{S_j^{\text{reco}}}$$

Unfolding example

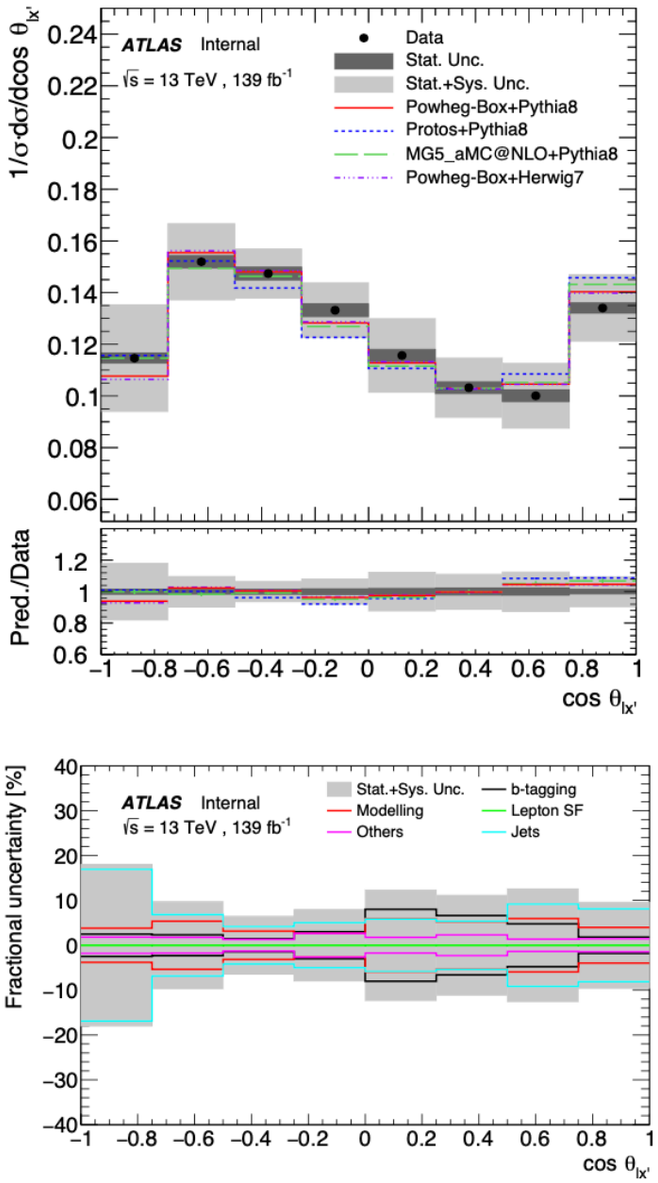

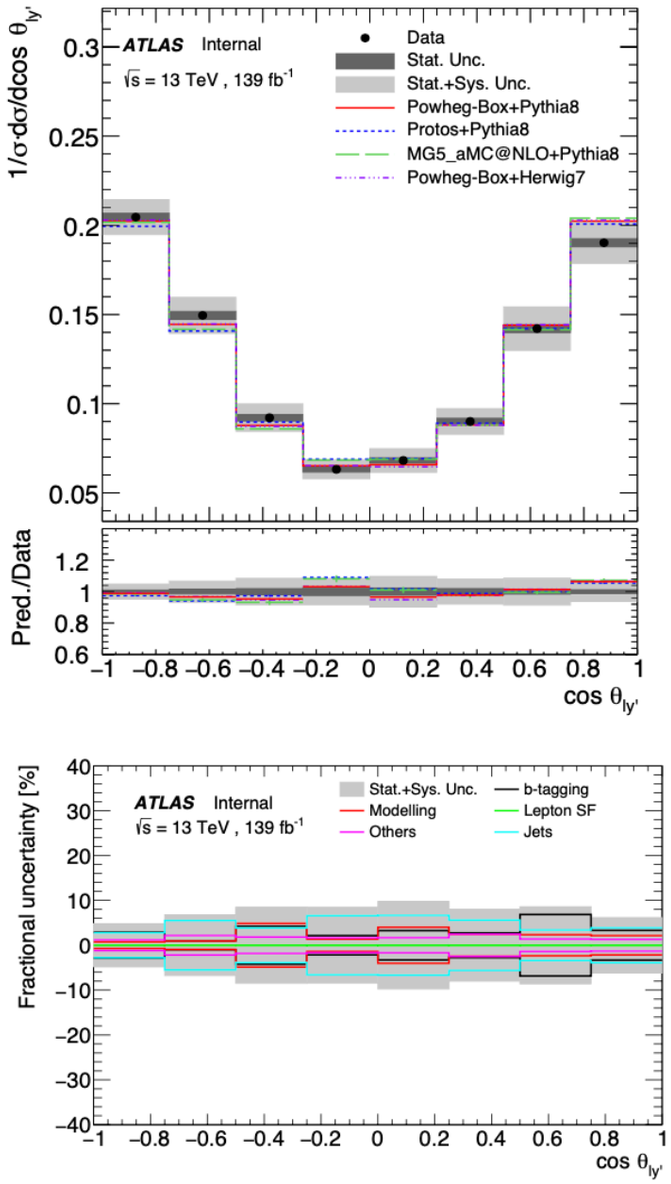

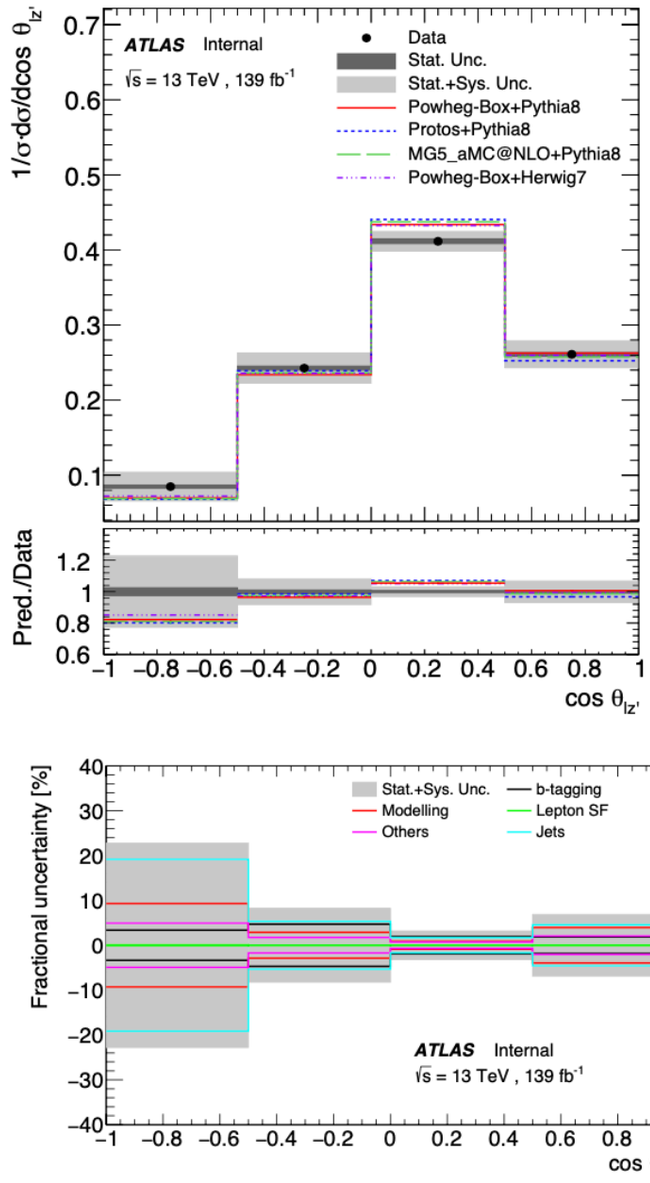

Unfolded distribution are then compared to various MC predictions (NLO, NNLO, NNLL, ….) from theorists.

Unfolding example

$$\sigma\left(\frac{c}{\Lambda^2}\right) = \underbrace{O_{SM}^2}_{\text{Pure SM}} + \frac{c}{\Lambda^2} \cdot \underbrace{O_{SM} O_{dim6}}_{\text{Interference term}} + \frac{c^2}{\Lambda^4} \cdot \underbrace{O_{dim6}^2}_{\text{Pure BSM}}$$

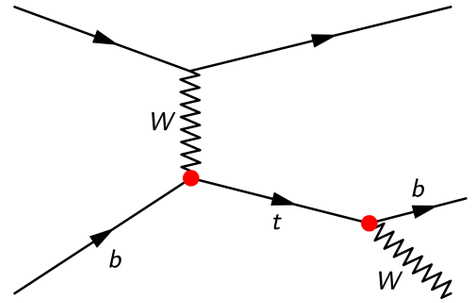

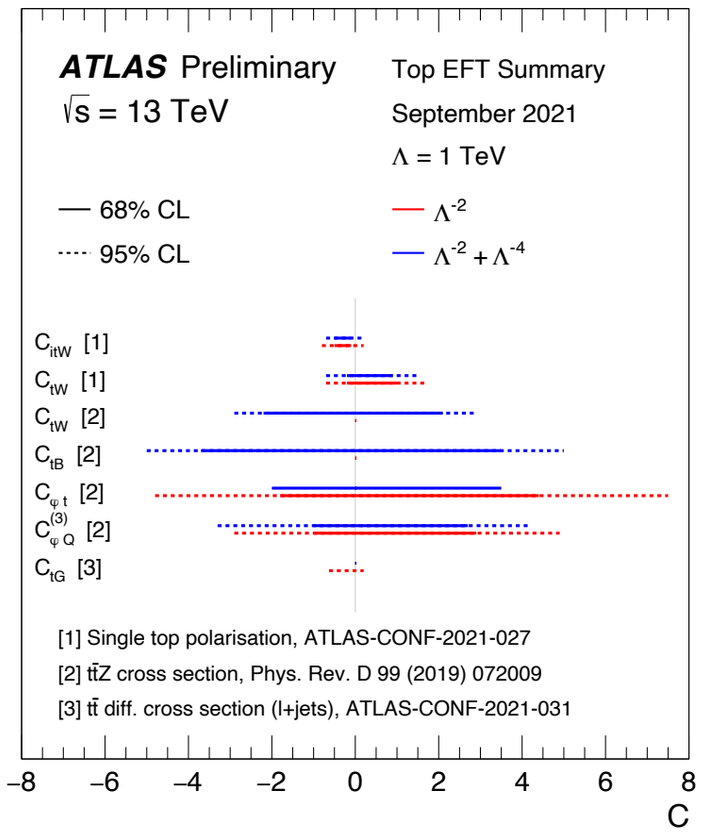

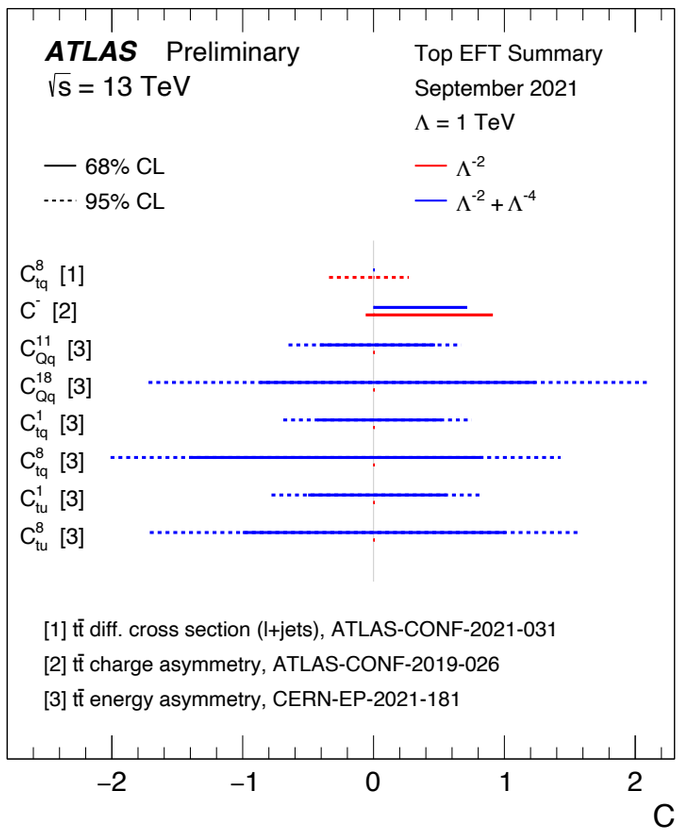

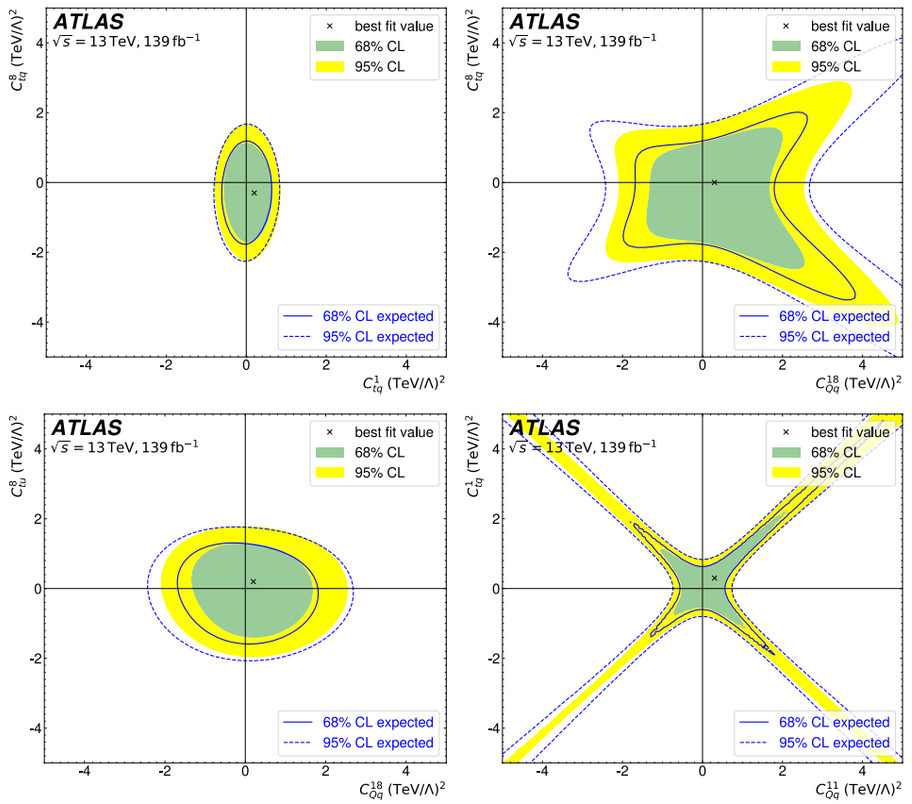

Reinterpreted in terms of Effective Field Theory (EFT)
→ set limits on New Physics operators!

Which unfolding?

$$N_k^{\text{particle}} = C_k^{\text{particle!reco}} \sum_j M_{jk}^{-1} C_j^{\text{reco!particle}} (N_j^{\text{data}} - B_j)$$

Tool: RooUnfold

IBU

D'Agostini Iterative Bayesian Unfolding
Nucl. Inst. Meth. A 362 (1995) 487

Tool: PyFBU

FBU

Fully Bayesian Unfolding
arxiv.org/1201.4612

Tool: RooUnfold

SVD

Singular Value Decomposition
Nucl. Inst. Meth. A 372 (1995) 469

Tool: TRExFitter (ATLAS)

PLU

Profile Likelihood Unfolding
CMS reference

Which unfolding?

Tool: RooUnfold

IBU

D'Agostini Iterative Bayesian Unfolding
Nucl. Inst. Meth. A 362 (1995) 487

$$N_k^{\text{particle}} = C_k^{\text{particle!reco}} \sum_j M_{jk}^{-1} C_j^{\text{reco!particle}} (N_j^{\text{data}} - B_j)$$

$$\theta_{ij} = \frac{\Pr(m_j|t_i) \cdot \Pr(t_i)}{\sum_i \Pr(m_j|t_i) \cdot \Pr(t_i)}$$

response matrix

regularization = number of iterations

$$\Pr_{k+1}(t_i) = \sum_j \theta_{ij} \Pr_k(t_i)$$

Answer: an estimator θ_{ij} and its covariance matrix

It involves iterations and depend on a convergence criterion

- first point of an iterative procedure, named "prior".
- converges towards some of the possible solutions
- Regularization by interrupting iterations

Which unfolding?

Tool: PyFBU

FBU

Fully Bayesian Unfolding
arxiv.org/1201.4612

$$P(T|D,\mathcal{M}) \propto \mathcal{L}(D|T,\mathcal{M})\pi(T),$$

$$\mathcal{L}(D|T,\mathcal{M},B) = \prod_{i=1}^{N_\mathrm{r}} \frac{(r_i+b_i)^{d_i}}{d_i!}\mathrm{e}^{-(r_i+b_i)},$$

$$r_i(T,\mathcal{M}) = \sum_{j=1}^{N_\mathrm{t}} m_{ij}t_j, \qquad m_{ij} = \frac{\epsilon_{t_j}P(r_i|t_j)}{f_{\mathrm{acc},r_i}}$$

Nuisance parameters (NP) directly encapsulated in the likelihood definition

$$\mathcal{L}(D|T) = \int \mathcal{L}(D|R(T;\boldsymbol{\theta}_s),B(\boldsymbol{\theta}_s,\boldsymbol{\theta}_b))G(\boldsymbol{\theta}_s)G(\boldsymbol{\theta}_b)\mathrm{d}\boldsymbol{\theta}_s\mathrm{d}\boldsymbol{\theta}_b$$

Answer: a posterior probability density defined in the space of possible spectra

- pdf which does not have to be Gaussian, which is important especially in bins with small Poisson event counts.

No matrix inversion and computation of eigenvalues, which makes it more stable numerically

No iterations (⇢ no convergence criterion)

- If more than one answers are equally likely, as can happen when the reconstructed spectrum has fewer bins than the inferred one, then FBU reveals all of them, while IBU converges towards some of the possible solutions.

Regularization by choosing a prior which favors certain characteristics, such as smoothness

Which unfolding?

Tool: RooUnfold

SVD

Singular Value Decomposition
Nucl. Inst. Meth. A 372 (1995) 469

$$R = USV^T$$

U, *V*, orthogonal, *S* diagonal & non-negative

$$d = U^T m \quad z_i(\tau) = \frac{d_i}{s_i} \cdot \frac{s_i^2}{s_i^2 + \tau}$$

$$t = Vz$$

regularization parameter

Answer: an estimator θ_{ij} and its covariance matrix

- migrations matrix is distorted by singular value decomposition (SVD)
- works in the Gaussian regime only
- it involves a matrix inversion ⇾ sometimes numerically unstable ⇾ requires some curvature regularisation

Tool: TRExFitter (ATLAS)

PLU

Profile Likelihood Unfolding
CMS reference

$$L(\boldsymbol{\lambda}) = p(\mathbf{y}|\boldsymbol{\lambda}) = \prod_{i=1}^{n} p(y_i|\boldsymbol{\lambda}) = \prod_{i=1}^{n} \frac{\left(\sum_{j=1}^{p} K_{ij}\lambda_j\right)^{y_i}}{y_i!} e^{-\sum_{j=1}^{p} K_{ij}\lambda_j}, \quad \boldsymbol{\lambda} \in \mathbb{R}_+^p$$

Similar to FBU in terms of prior for regularisation, but it involves a Profile Likelihood fit too.

Questions/Comments?

Latest experimental results on QCD physics at LHC [ATLAS-baised]

Global PDF fit in ATLAS

EPJC 82, 438 (2022)

Knowledge of PDFs traditionally from lepton–proton colliders (like HERA @ DESY)

- point-like particles, such as electrons, to directly probe the partons within the proton
- revealed that, in addition to up and down valence quarks, there is also a sea of $q\bar{q}$ pairs
  - + theoretically made of all types of quarks, bound together by gluons

ATLAS global PDF fit at $\sqrt{s}$ = 7, 8, 13 TeV provides a detailed look into PDFs

- using HERA + ATLAS data at different p-p centre-of-mass (c.o.m.) energies
- Theoretical predictions at NNLO QCD + NLO EW (current state-of-the-art)
- Uncertainties on (μ_R, μ_F) treated as correlated in the fit where they are sizeable with respect to experimental systematics
- extended PDF parameterisation using 21 parameters → ***ATLASPDF21***

Data set	$\sqrt{s}$ [TeV]	Luminosity [fb^{-1}]	Decay channel	Observables entering the fit
Inclusive $W, Z/\gamma^*$	7	4.6	e, μ combined	η_ℓ (W), y_Z (Z)
Inclusive Z/γ^*	8	20.2	e, μ combined	$\cos\theta^*$ in bins of $y_{\ell\ell}$, $m_{\ell\ell}$
Inclusive W	8	20.2	μ	η_μ
$W^\pm$ + jets	8	20.2	e	p_{T}^W
Z + jets	8	20.2	e	$p_{\mathrm{T}}^{\mathrm{jet}}$ in bins of $\lvert y^{\mathrm{jet}}\rvert$
$t\bar{t}$	8	20.2	lepton + jets, dilepton	$m_{t\bar{t}}$, p_{T}^t, $y_{t\bar{t}}$
$t\bar{t}$	13	36	lepton + jets	$m_{t\bar{t}}$, p_{T}^t, y_t, $y_{t\bar{t}}^{\mathrm{b}}$
Inclusive isolated γ	8, 13	20.2, 3.2	-	E_{T}^γ in bins of η^γ
Inclusive jets	7, 8, 13	4.5, 20.2, 3.2	-	$p_{\mathrm{T}}^{\mathrm{jet}}$ in bins of $\lvert y^{\mathrm{jet}}\rvert$

Global PDF fit in ATLAS

EPJC 82, 438 (2022)

ATLAS diff. x-section measurements considered:

- inclusive W± and Z/γ* boson production
- W± and Z boson production in association with jets
- $t\bar{t}$ production
- inclusive jet production
- direct photon production

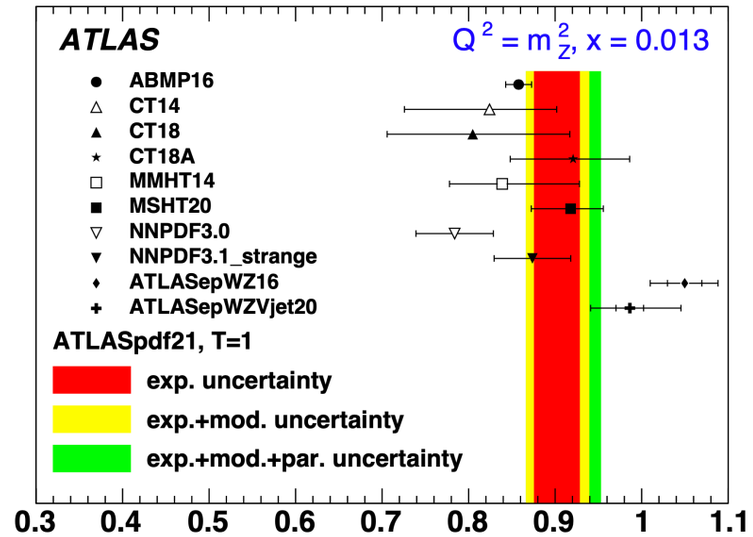

$R_S = x(s + \bar{s})/x(\bar{u} + \bar{d})$

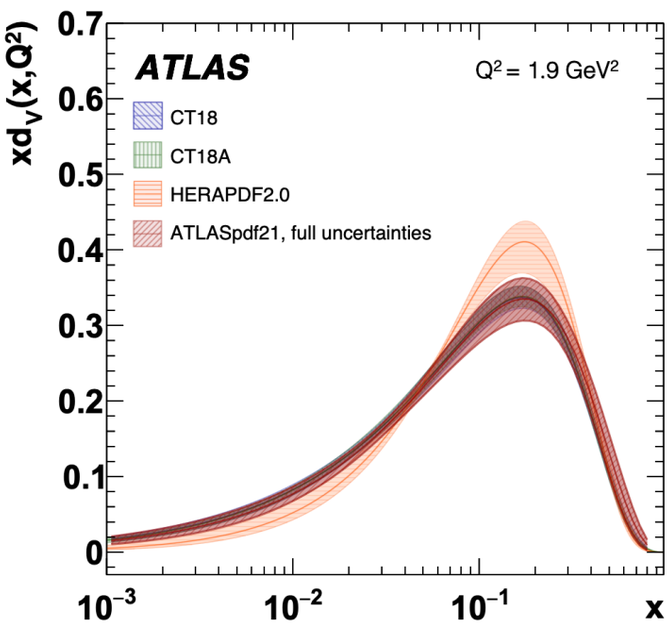

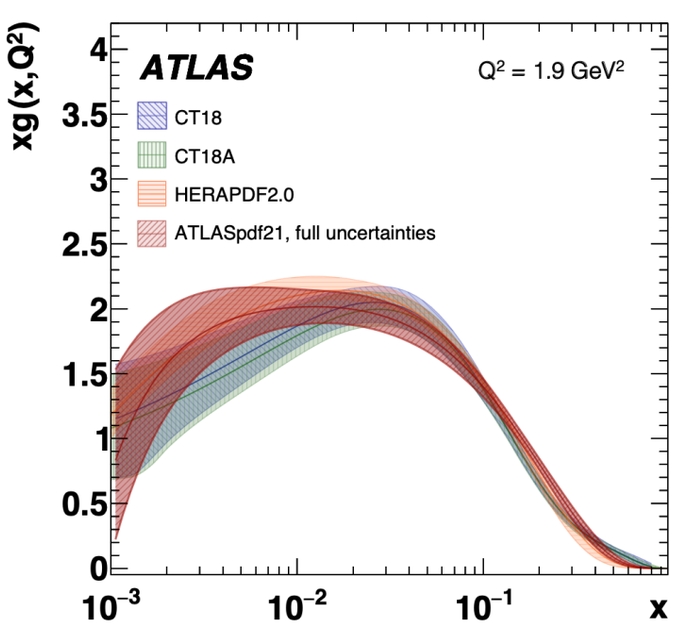

Comparison to global PDF sets (CT18, NNPDF, MSHT20, ...)
→ Inclusion of ATLAS data brings ATLAS PDF closer to global PDF sets than to HERAPDF.

The Paper describes effective techniques for assessing data uncertainties – providing a new "vademecum" for PDF groups around the world.

ATLAS Physics Briefing

Exotic hadrons

1960s: Gell-Mann and Zweig independently proposed the existence of quarks

- their model successfully described hadrons ($q\bar{q}$ and qqq) and the strong force
- theorists also predicted the existence of exotic hadrons (>3q)

≥2003: Belle discovered X(3872) tetraquark, followed by a series of tetraquark candidates observed by several experiments

- ⇾ new understandings of strong force at low energy scales

2020: a possible tetraquark with mass 6.9 GeV observed by LHCb (2J/Psi -> 4μ)

- called X(6900), an exotic hadron which may consist of two charm quarks and two charm antiquarks in a bound state
- narrow peak in $m_{4\mu}$ and broad structure alongside (whose nature remains unclear)
  - J/ψ+ψ(2S) ?

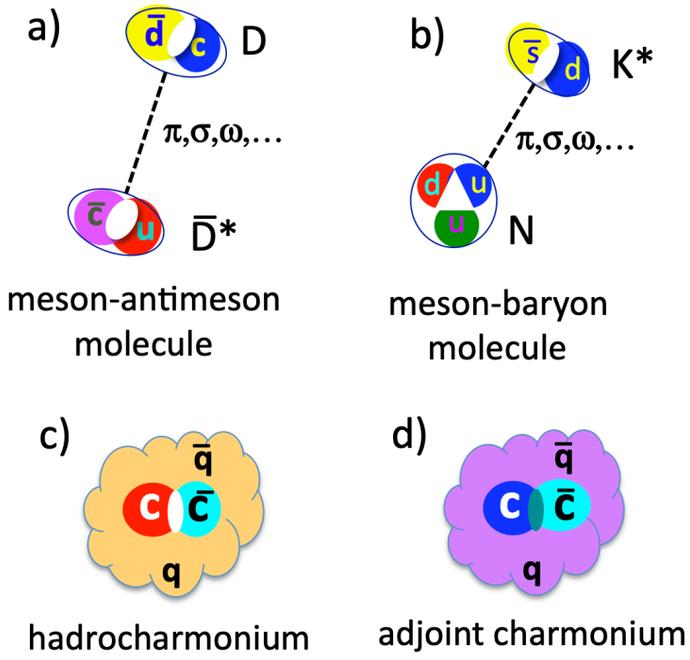

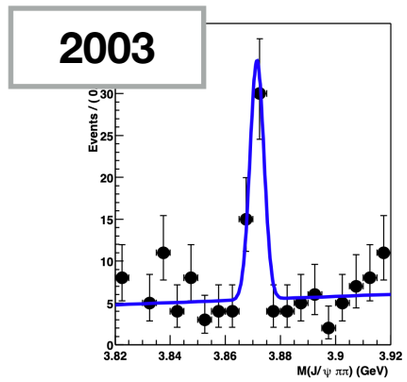

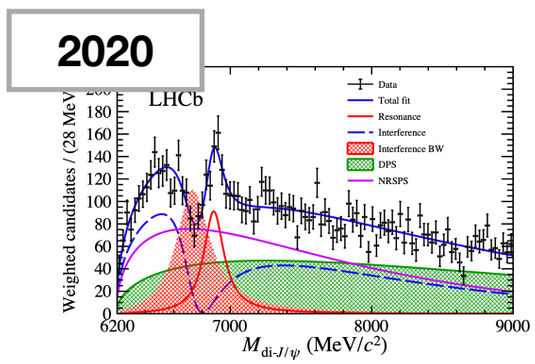

Potential 4-charmioun tetraquark

ATLAS-CONF-2022-040

ICHEP 2022 conference: ATLAS physicists found evidence of "di-charmonium" excess

- J/ψ pair and J/ψ+ψ(2S) decay channels in events with four muons in the final state

Thanks to ATLAS' excellent muon ID and dedicated B-physics selection system

- reconstructed di-charmonium candidates using two pairs of $\mu^+\mu^-$, whose inner detector tracks originate from a common vertex
- constraints on di-muon mass for the best mass resolution
- combination of MC simulations and data-driven methods to estimate backgrounds

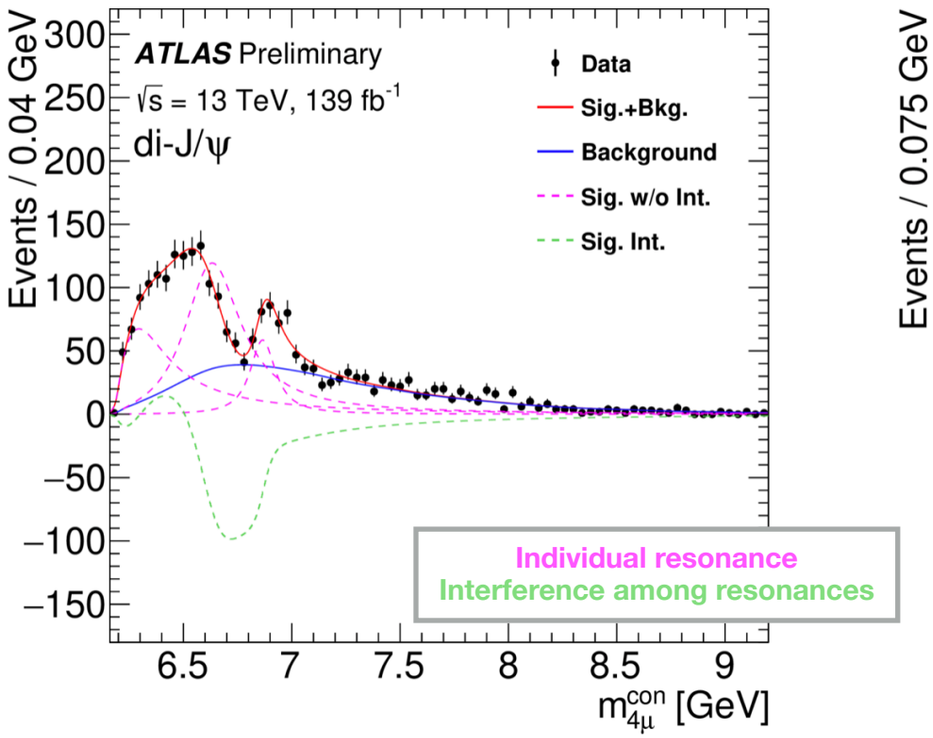

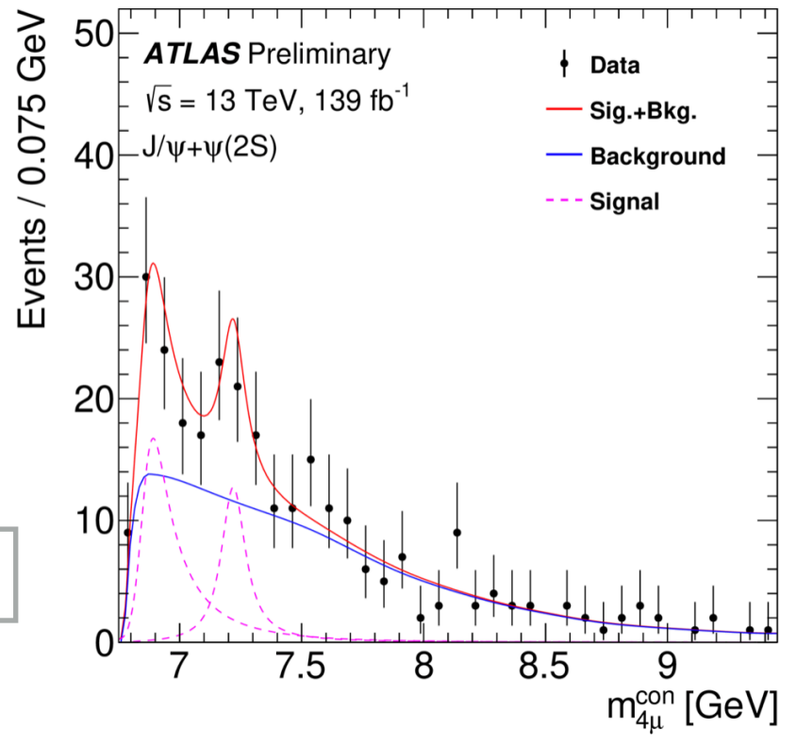

Evidence (left plot), like LHCb, of X(6900) and a broad structure at threshold: model of 3 interfering resonances describes the spectrum well.

Excess composed of 4.6σ in J/ψ+ψ(2S) channel (right plot)

More data needed!!!

ATLAS Physics Briefing

Nature of p-p collisions at LHC

p-p collisions at LHC can be elastic and inelastic

- inelastic: Sometimes, hundreds of tiny particles, like π's
- inelastic: on rare occasions, heavy particles, like Higgs
- elastic: rather unspectacular collisions – protons bounce off each other and change directions of their momenta
  - + the kinematics may be quite simple, their study can reveal the complex dynamics that govern proton interactions

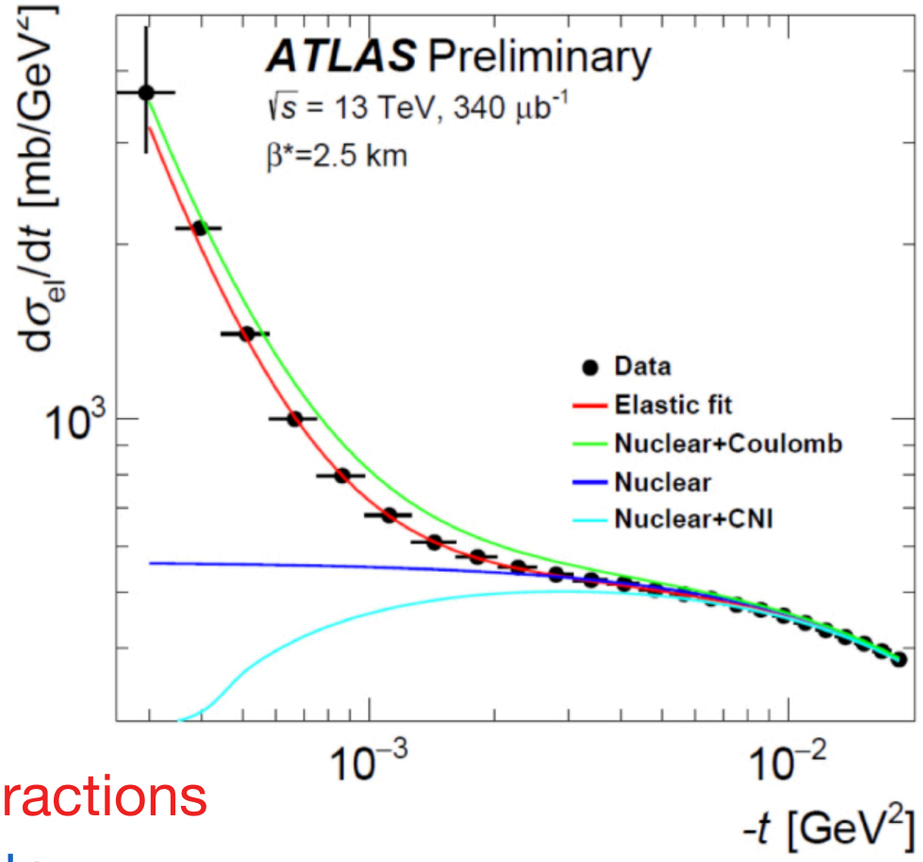

"Mandelstam" variable t (related to the scattering angle)

- θ_{pp}<5 μrad (|t| < 0.001GeV²): dominated by Coulomb interactions
- θ_{pp}>15 μrad (|t| > 0.01 GeV²), nuclear interactions dominate
- 5 μrad<θ_{pp}<15 μrad (0.001<|t| <0.01 GeV²), Coulomb and nuclear interactions contribute with similar magnitude.
  - + effects cannot be distinguished for single event ⇾ quantum-mechanical interference occurs
- The magnitude and sign of this interference depends on the complex phase between the Coulomb and nuclear scattering amplitudes

p-p quantum interference in scattering

STDM-2018-08

Measurement of p-p scattering at μrad angles and study this quantum interference

- dedicated experimental setup:
- LHC magnets tuned to a special “high-β* optics'' setting
  - which gives the proton beams a very small angular spread
- special detectors needed far away from the central interaction point but very close to the proton beam (ALFA detectors)
  - installed ~240 metres on either side of the ATLAS cavern inside “Roman pots”, and can take measurements just a few mm from the beam centre

$$\mathscr{L} = \frac{N_1 N_2 f_{\mathrm{rev}} N_{\mathrm{b}}}{4\pi \sigma_x \sigma_y}$$

$$\varepsilon_0^{x,y} = \frac{(2\sigma_{x,y}^2)}{\beta_{x,y}},$$

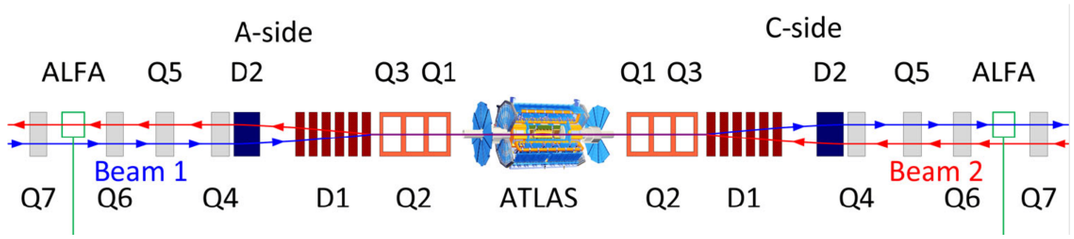

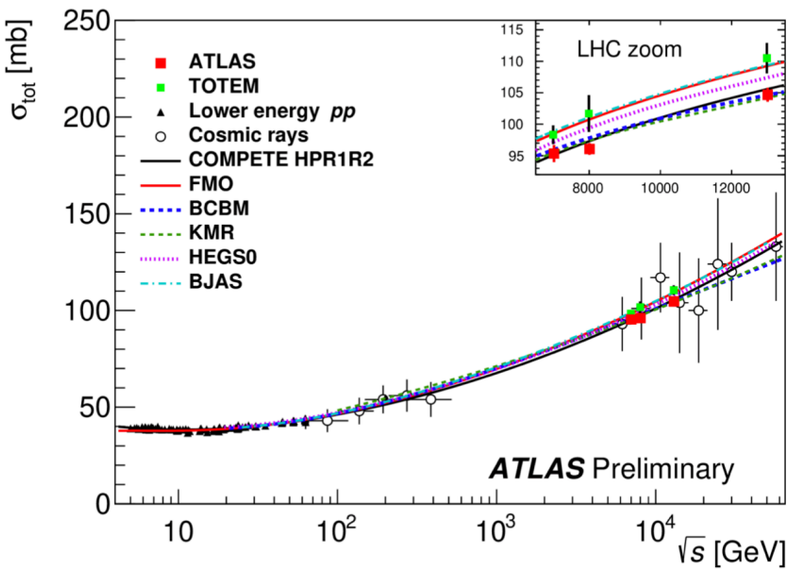

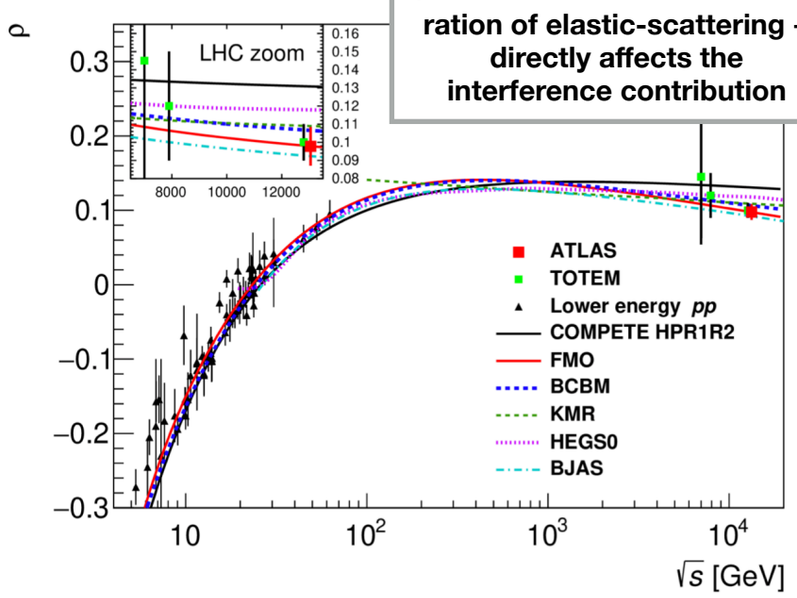

ρ = real/imaginary amplitude ration of elastic-scattering → directly affects the interference contribution

ρ disagrees with pre-LHC theoretical expectations

→ either the increase of σ_{tot} with c.o.m. energy will eventually slow down

→ or the hadronic interactions of p-$\bar{p}$ remain different at high c.o.m. energies.

ATLAS Physics Briefing

Dijet suppression in HI collisions

HION-2019-02

Heavy-ion (HI) collisions at LHC to study quark-gluon plasma (QGP)

- very hot and dense state of nuclear matter
- extreme conditions like the early Universe during the first μs after Big Bang

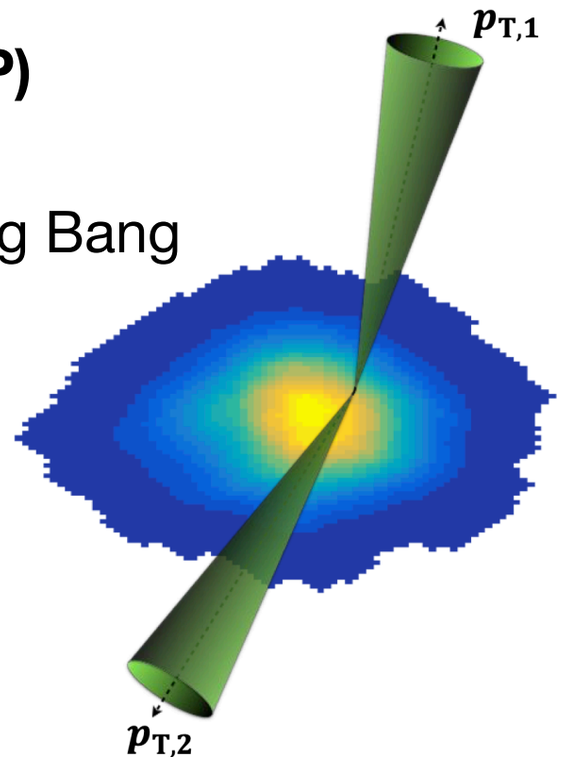

ATLAS new study of "jets" of particles travelling through QGP

- achieved with heavy-ion collisions (Pb-Pb)
- overlap between colliding nuclei (⇾ QGP size) characterised experimentally by "centrality"
  - + 0-10% centrality corresponds to maximal overlap
  - + larger numbers correspond to more "peripheral" or "glancing" collisions
- jets modified while travelling through QGP ⇾ can vary widely depending on centrality
  - + new insight into dijet suppression due to interactions with nuclear medium previously seen in Pb-Ion

Jets typically formed from elastic scattering of quarks and gluons

- ⇾ 2 back-to-back jets with same p_T travelling different trajectories through QGP
- p_T balance (x_J) as probe for path-length dependence to jet energy loss

Pb-ion and p-p collision data used (at $\sqrt{s}$ = 5.02 TeV)

ATLAS Physics Briefing

Dijet suppression in HI collisions

HION-2019-02

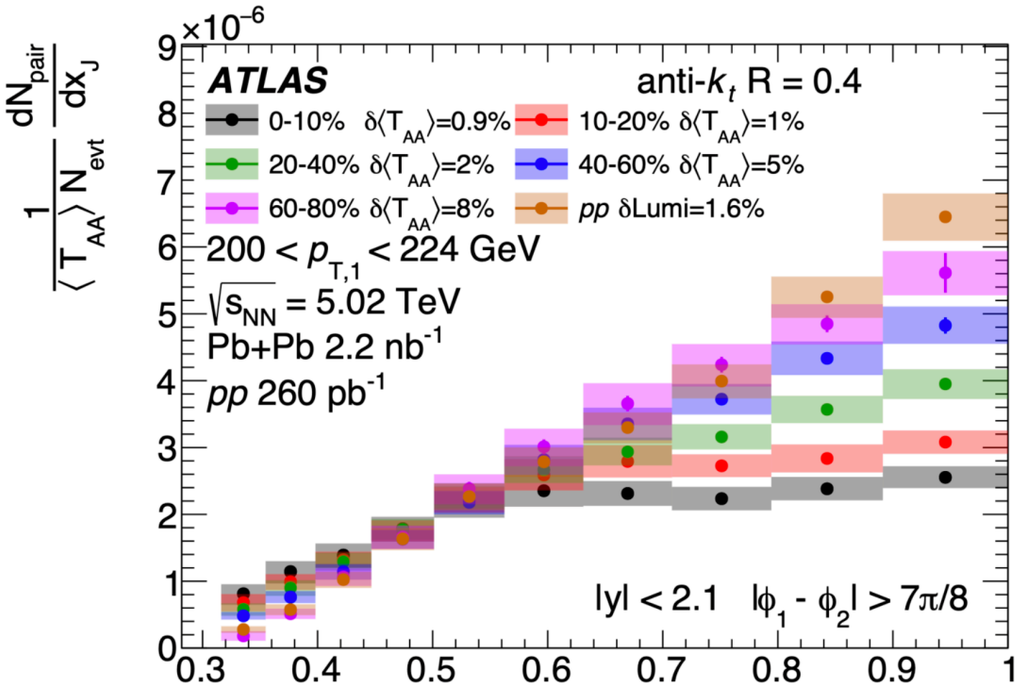

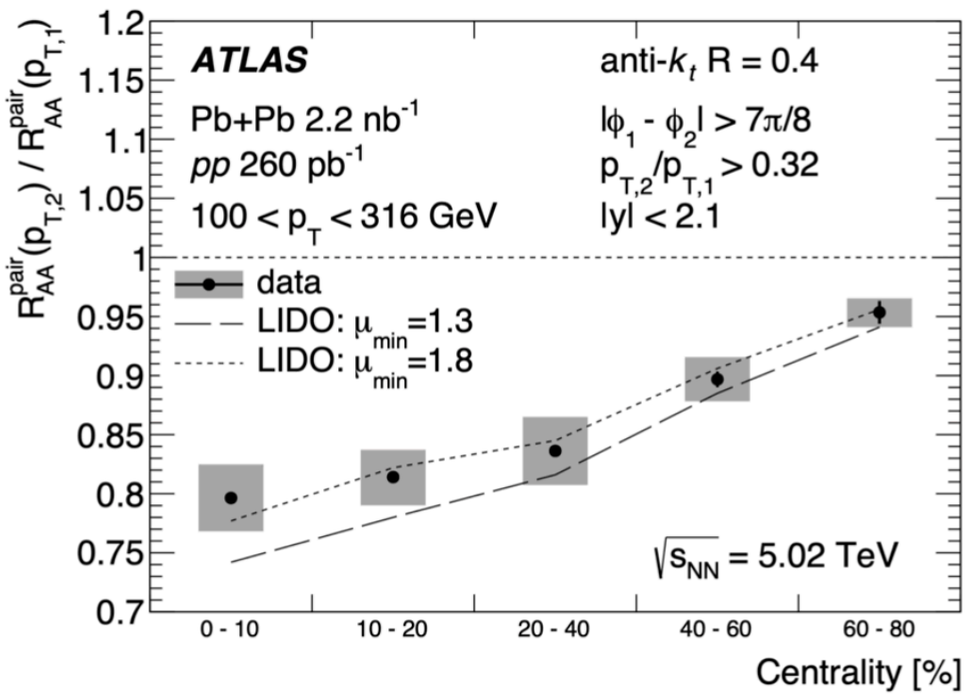

Significant suppression of symmetric jet pairs ($x_J \approx 1$) at low centrality (→ big QGP)

Highly unbalanced dijets (low x_j) unchanged

New constraint for theoretical models

Significant suppression of subleading jets relative to leading jets for all lead-ion-collision centrality. Most peripheral collisions having a 3σ sigma significant relative suppression

Clear indications that jet suppression occurs when jets have similar p_T

- more unbalanced jets, instead, produced at similar rates to p-pp collisions
- unprecedented access to jet quenching in planned collisions of oxygen ions in Run 3

ATLAS Physics Briefing

Questions/Comments?

ATLAS+CMS $t\bar{t}$ combination at 7+8 TeV

arXiv:2205.13830

Quick spoiler on top physics
More details provided tomorrow!

Uncert. (%)	σ_{tt}(7 Tev)	σ_{tt}(8 Tev)
ATLAS	3.5	3.2
CMS	$^{+3.6}_{-3.5}$	$^{+3.7}_{-3.5}$
Comb^{n}	$^{+2.7}_{-2.6}$	$^{+2.5}_{-2.4}$

Legacy eμ results from ATLAS+CMS at √s=7, 8 TeV combined

- minimisation with Convino tool
- careful accounting of correlations between experiments and beam energies
- total uncertainties (25/28% better c.f. most precise input)

Measured $\sigma_{t\bar{t}}$ used to extract α_s, assuming a value of m_t^{pole}

- or vice versa - assume α_s and extract m_t^{pole}
- $\sigma_{t\bar{t}}$ results depend on assumed MC mass as acceptance/kinematics depend on m_t
  - + assume mt^{pole} and m_t^{MC} are equal within a few GeV

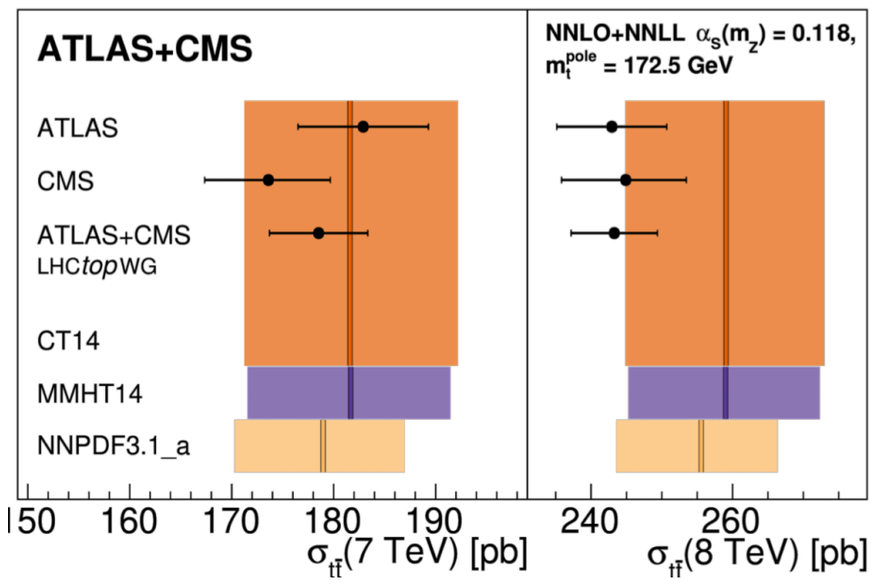

Results compatible with recent PDFs

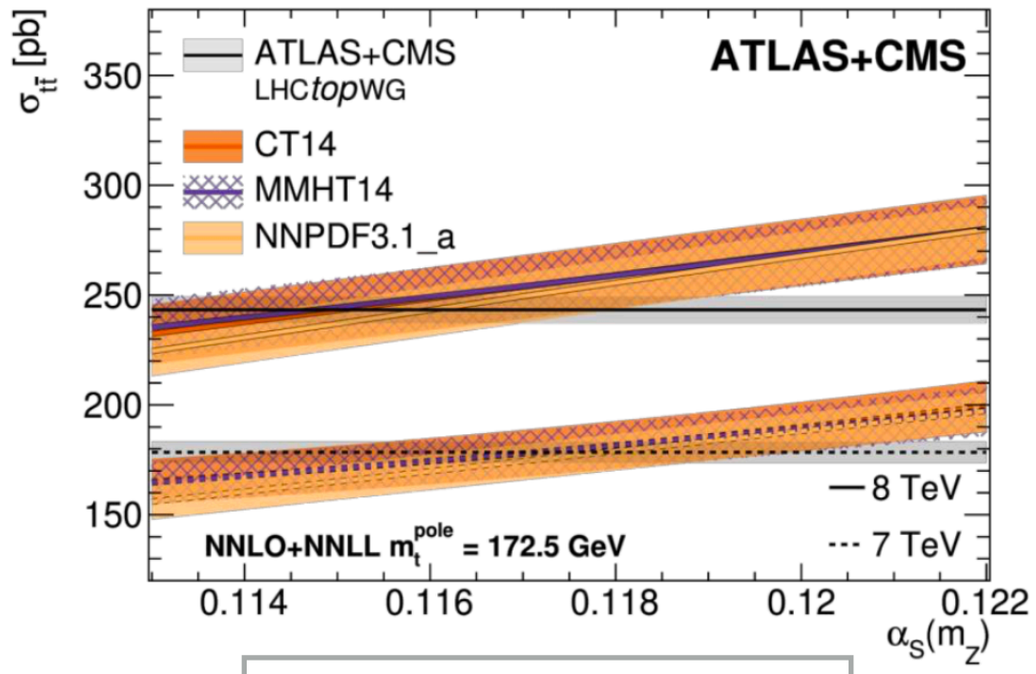

Most precise α_S extraction from top events

b-fragmentation with ATLAS data

[JHEP 12 (2021) 131](#)
[arXiv:2202.13901](#)

Quick spoiler on top physics
More details provided tomorrow!

b-quarks fragmentation in hadrons is of interest for many reasons

- 1. precise probe of QCD (from Z → $b\bar{b}$ decays)
  - + function tuned to e+e– collider ⇾ extrapolation to LHC environment correct?
- 2. precision top-mass measurements via b ⇾ leptons play a role in the LHC's long-term m_t strategy
  - + top-quark → b-hadron momentum transfer is key!
- 3. best physics results with b-jets (b-tagging response)

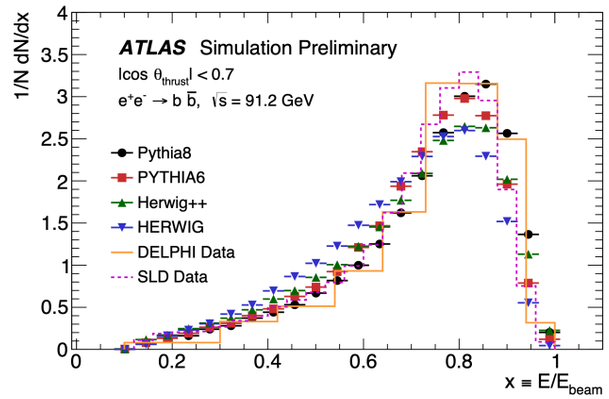

some tension between e^+e^-⇾ bb measurements of b-fragmentation parton-shower generators are also not in good agreement

Two recent measurements at ATLAS in dijet and tt final states

- provide excellent coverage where LEP data can't reach (complementary to each other)
- unfold related observables to particle level
- $z_{(L)} = \vec{p}_B \cdot \vec{p}_{jet} / p_{jet}^2$, $p_T^{rel} = |\vec{p}_B \times \vec{p}_{jet}| / |p_{jet}|$ (dijet only)
- $\rho = p_T^B / \mathrm{avg}(p_T^\ell)$ ($t\bar{t}$ only), charged particle multiplicity, n_{ch}^B ($t\bar{t}$ only)
- dijet: measure full B ⇾ μμK and full jet momentum
- $t\bar{t}$: only measure "charged momentum" of B and jet

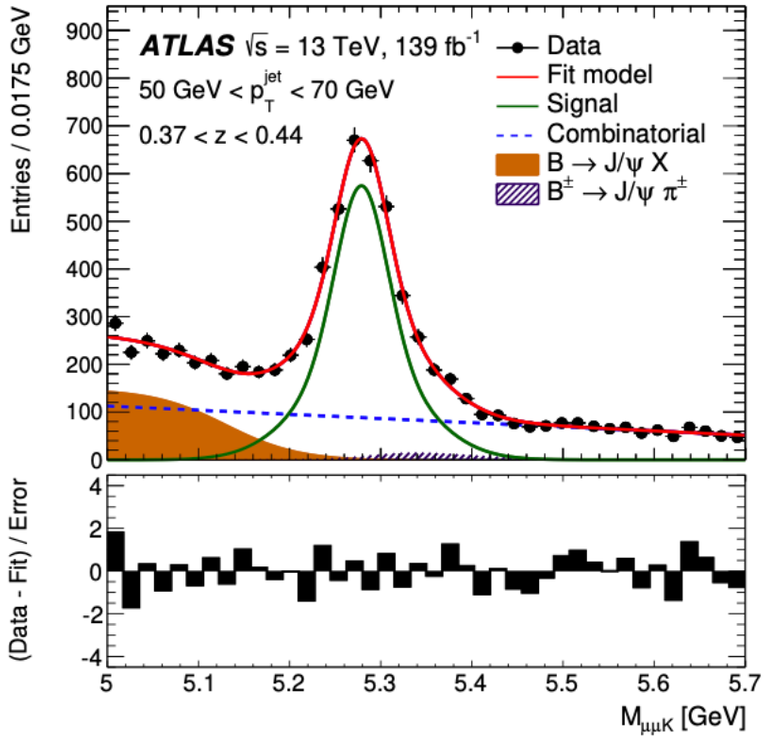

b-fragmentation with ATLAS data

JHEP 12 (2021) 131
arXiv:2202.13901

Quick spoiler on top physics
More details provided tomorrow!

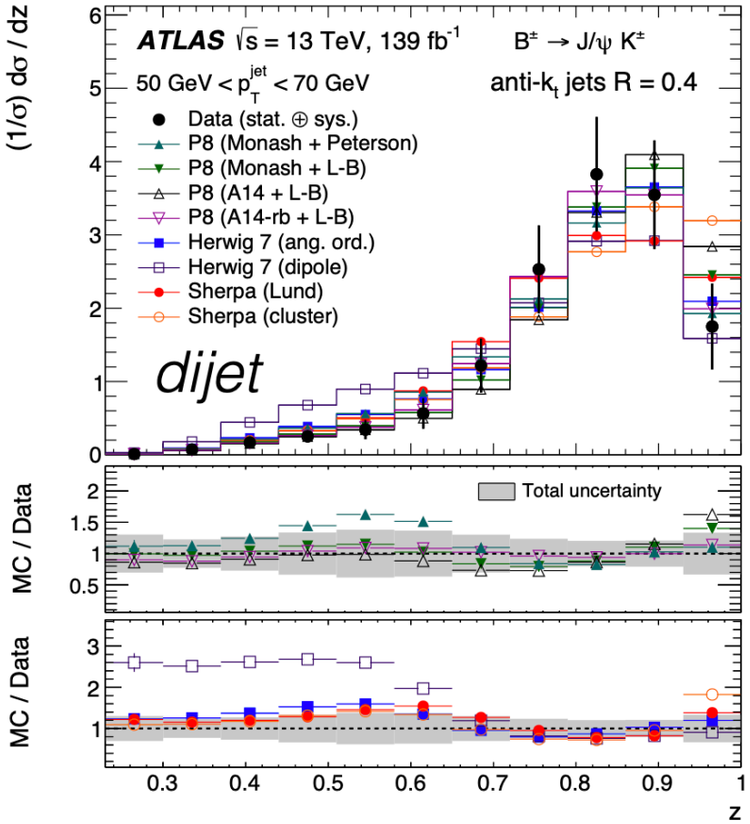

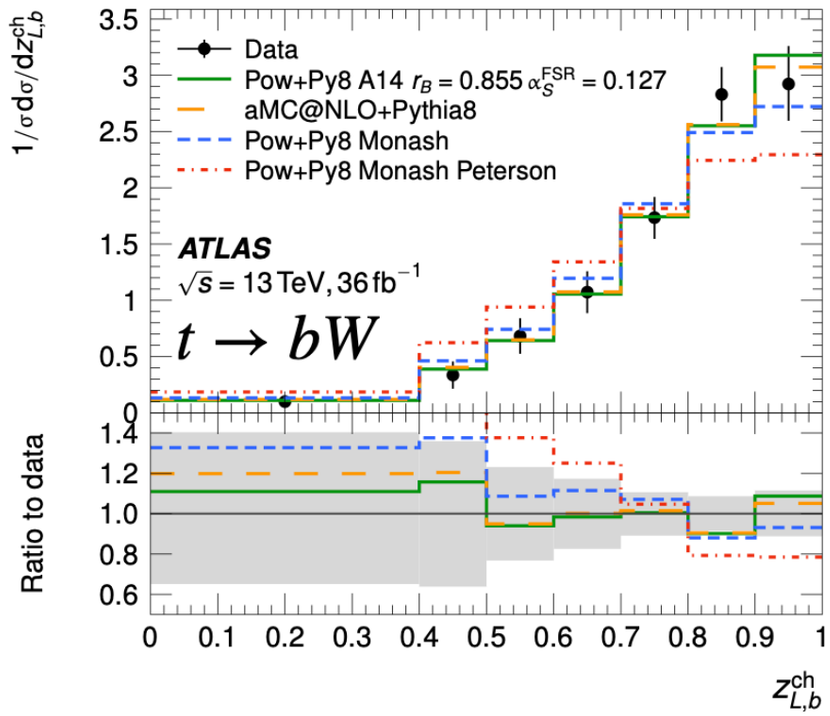

b-fragmentation with ATLAS data

[JHEP 12 (2021) 131](#)
[arXiv:2202.13901](#)

Quick spoiler on top physics
More details provided tomorrow!

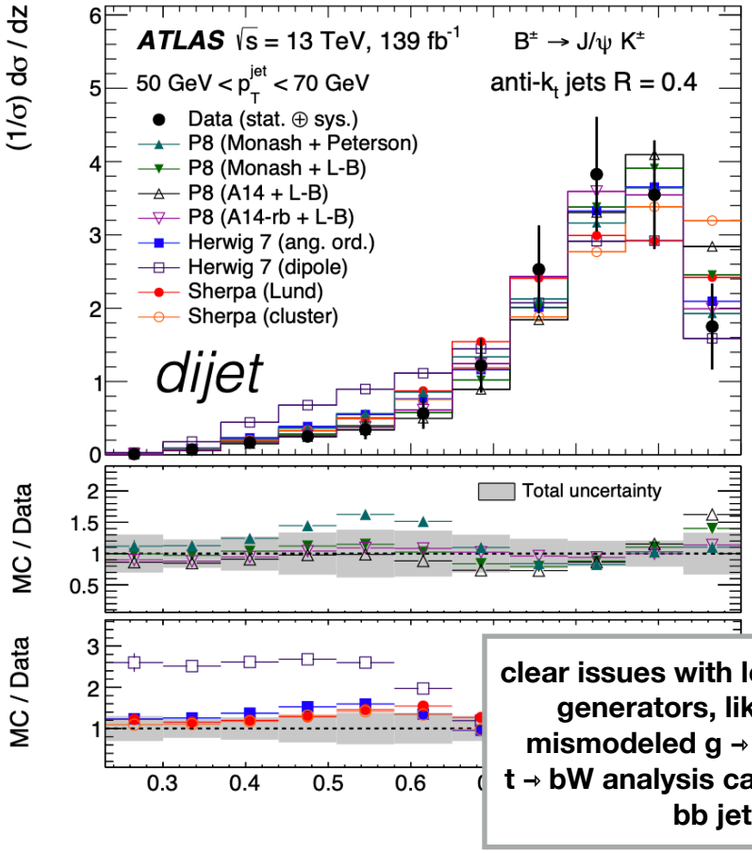

clear issues with low-z for some generators, likely due to mismodeled g → bb fractions
t → bW analysis can help (no g → bb jets)

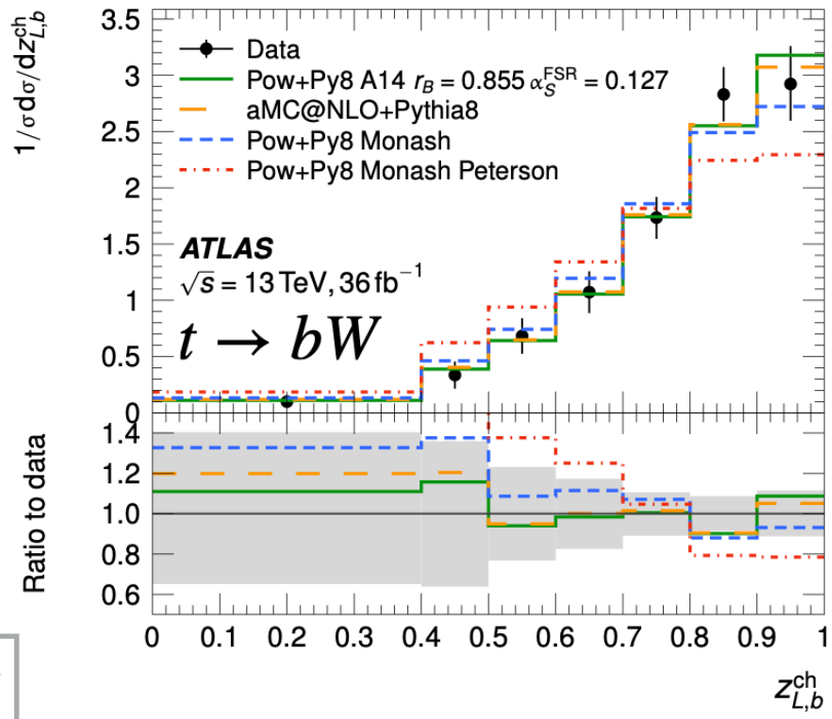

ATLAS A14 tune + Lund-Bowler fragmentation tuned to A14 α_{FSR} performs best

Peterson model strongly disfavoured in both measurements

Herwig7.0 also disfavoured, but improvement in later versions

b-fragmentation with ATLAS data

JHEP 12 (2021) 131
arXiv:2202.13901

Quick spoiler on top physics
More details provided tomorrow!

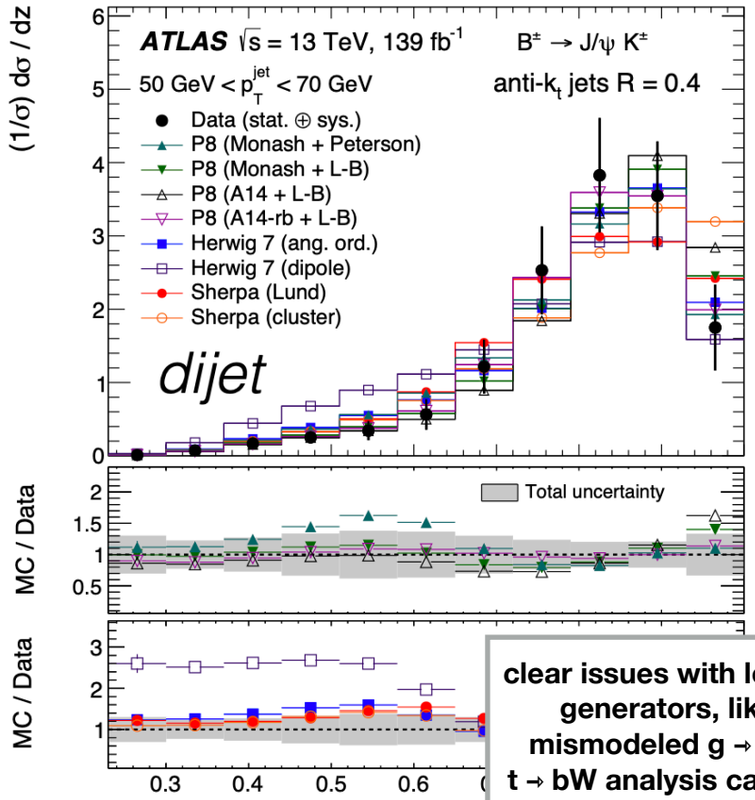

clear issues with low-z for some generators, likely due to mismodeled g → bb fractions
t → bW analysis can help (no g → bb jets)

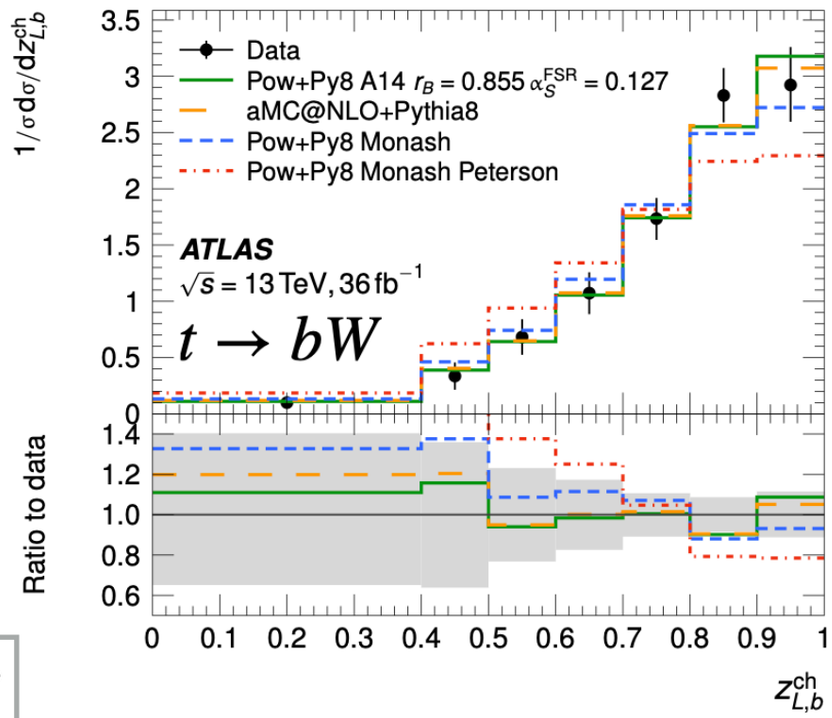

ATLAS A14 tune + Lund-Bowler fragmentation tuned to A14 α_{FSR} performs best

Peterson model strongly disfavoured in both measurements

Herwig7.0 also disfavoured, but improvement in later versions

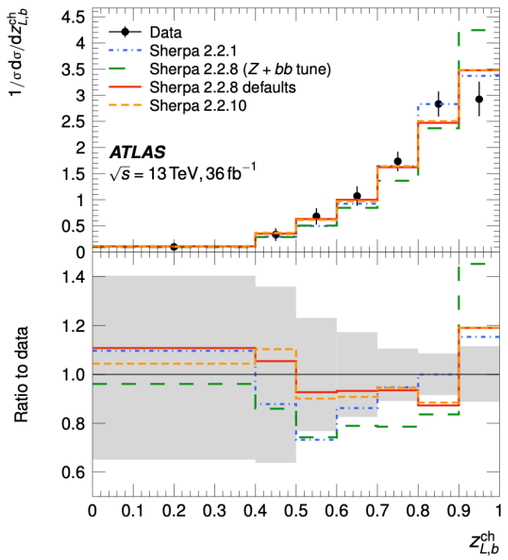

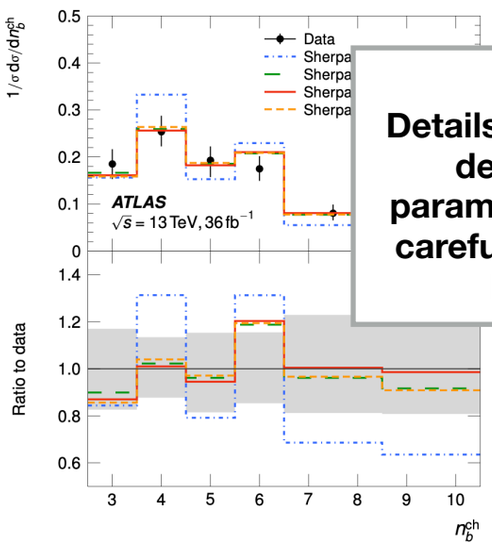

Beware!
Details of top-quark decays depend strongly on parameters that need to be carefully chosen in current MC generators

b-fragmentation with ATLAS data

JHEP 12 (2021) 131
arXiv:2202.13901

Quick spoiler on top physics
More details provided tomorrow!

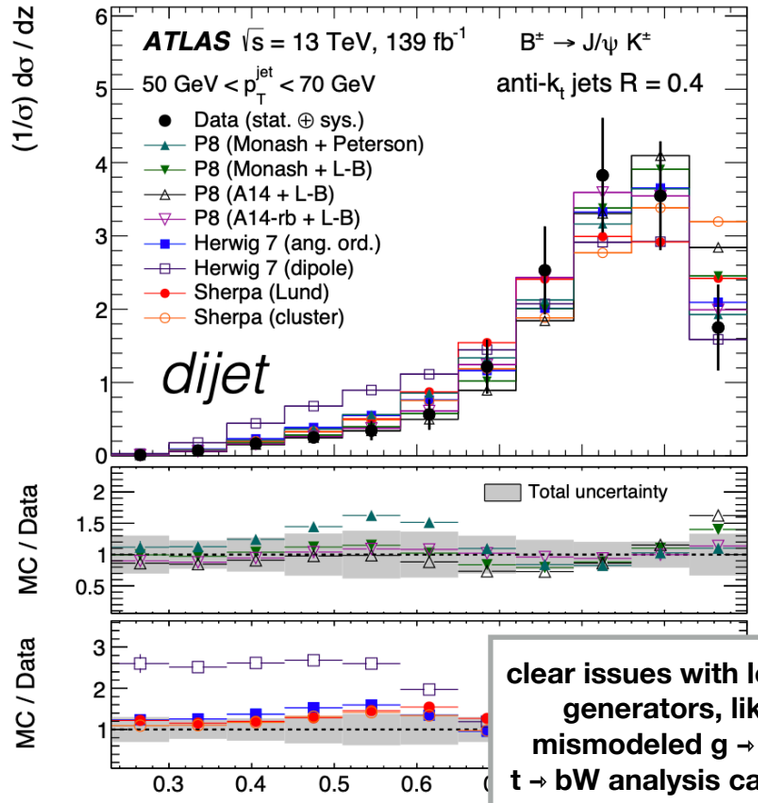

clear issues with low-z for some generators, likely due to mismodeled g → bb fractions
t → bW analysis can help (no g → bb jets)

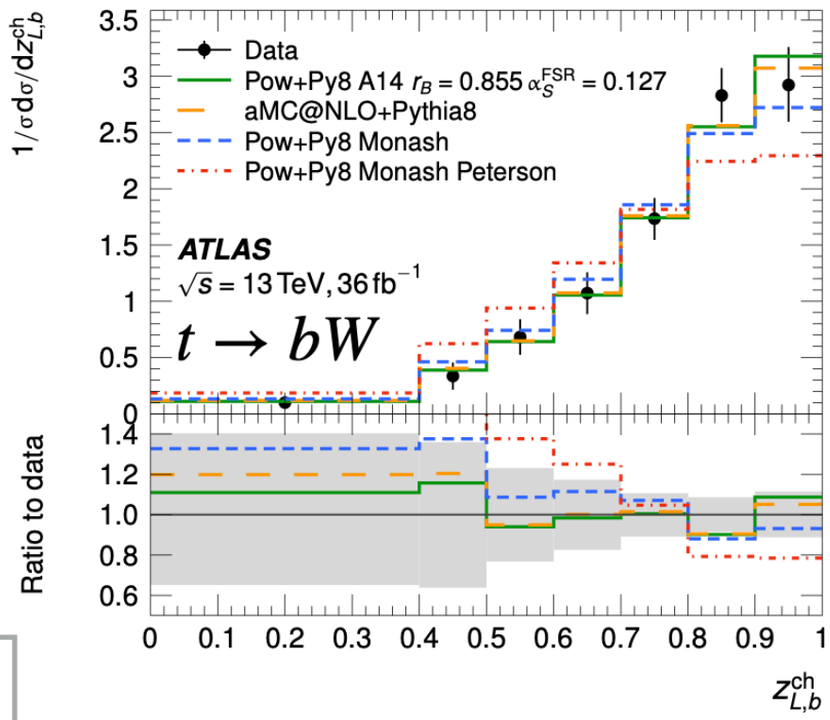

ATLAS A14 tune + Lund-Bowler fragmentation tuned to A14 α_{FSR} performs best

Peterson model strongly disfavoured in both measurements

Herwig7.0 also disfavoured, but improvement in later versions

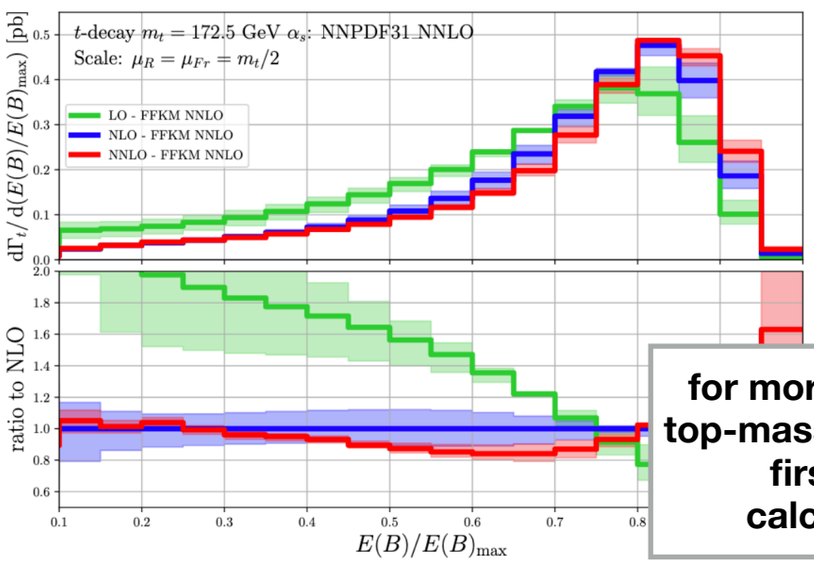

for more precise direct top-mass measurements, first ~analytic calculations of z

arxiv:2102.08267

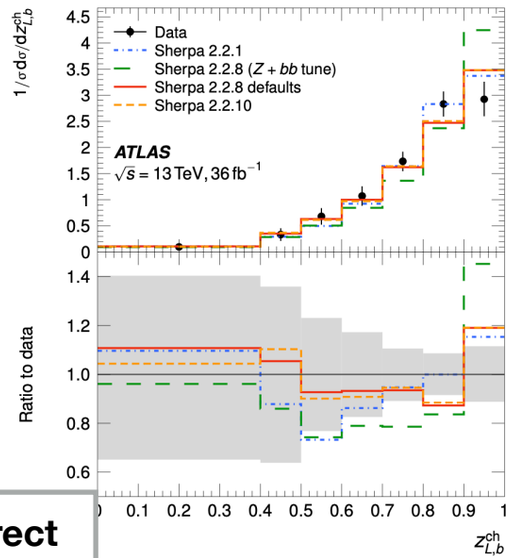

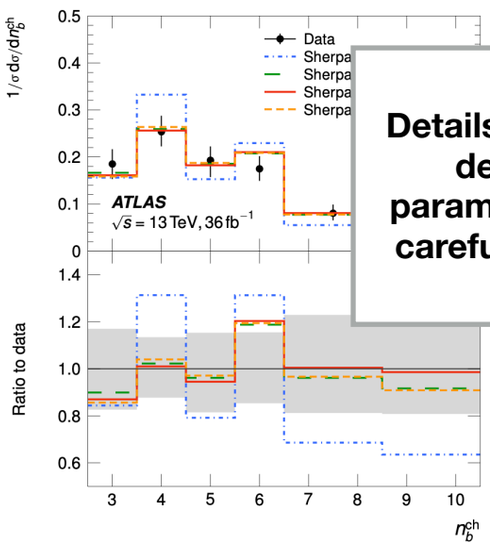

Beware!
Details of top-quark decays depend strongly on parameters that need to be carefully chosen in current MC generators

b-fragmentation with ATLAS data

JHEP 12 (2021) 131
arXiv:2202.13901

Quick spoiler on top physics
More details provided tomorrow!

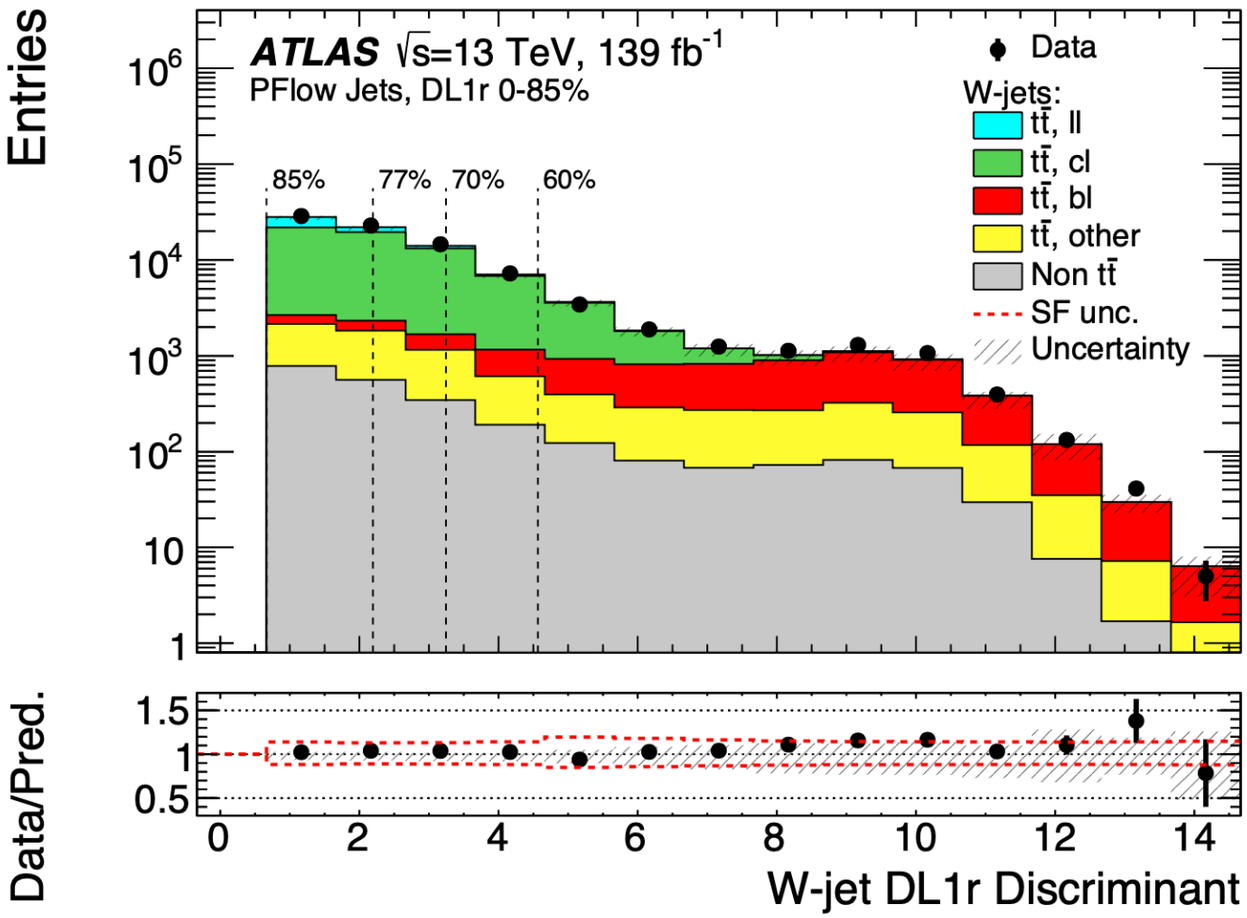

Could we measure charm fragmentation in t → bW → b(cq) decays?
Could be very important for H →cc̄

Fairy general experimental techniques developed for t → bW measurement.
We know how to obtain a reasonably clean sample of charm jets from W decays.

Summary and overview

QCD has much more to offer

- I've offered a (biased) collection of results, but there are many more!
- More on PDFs, fixed-order effects, resummation, non-global effects ("entanglement"), quark and gluon properties, W/Z/H hadronic decays, collective effects, connections with heavy ions, ...

Even though QCD has only ~1 free parameter, it is a rich theory with various regimes that we can probe at the LHC

- Studying QCD is inherently interesting as a quantum theory of nature
- Understanding it is also critical for precise SM measurements and new particles searches
- there are also many exciting connections to modern machine learning (ML4Jets 2022)!

Summary and overview

QCD has much more to offer

- I've offered a (biased) collection of results, but there are many more!
- More on PDFs, fixed-order effects, resummation, non-global effects ("entanglement"), quark and gluon properties, W/Z/H hadronic decays, collective effects, connections with heavy ions, ...

Even though QCD has only ~1 free parameter, it is a rich theory with various regimes that we can probe at the LHC

- Studying QCD is inherently interesting as a quantum theory of nature
- Understanding it is also critical for precise SM measurements and new particles searches
- there are also many exciting connections to modern machine learning (ML4Jets 2022)!

Last call for comments or questions?

Hints for questions...

Last call for comments or questions?

1. what's a b-fragmentation function?
2. what are exotic quantum phenomena?
3. what are the other non perturbative effects?

4. regarding particle identification, what punch-through means?
5. parton and particle level objects?

6. what are the Roman pots?
7. $\langle T_{AA} \rangle$ normalized ratio for Pb-Pb collisions
8. Convino tool, strengths and shortcomings

Backup

ATLAS Calorimetry

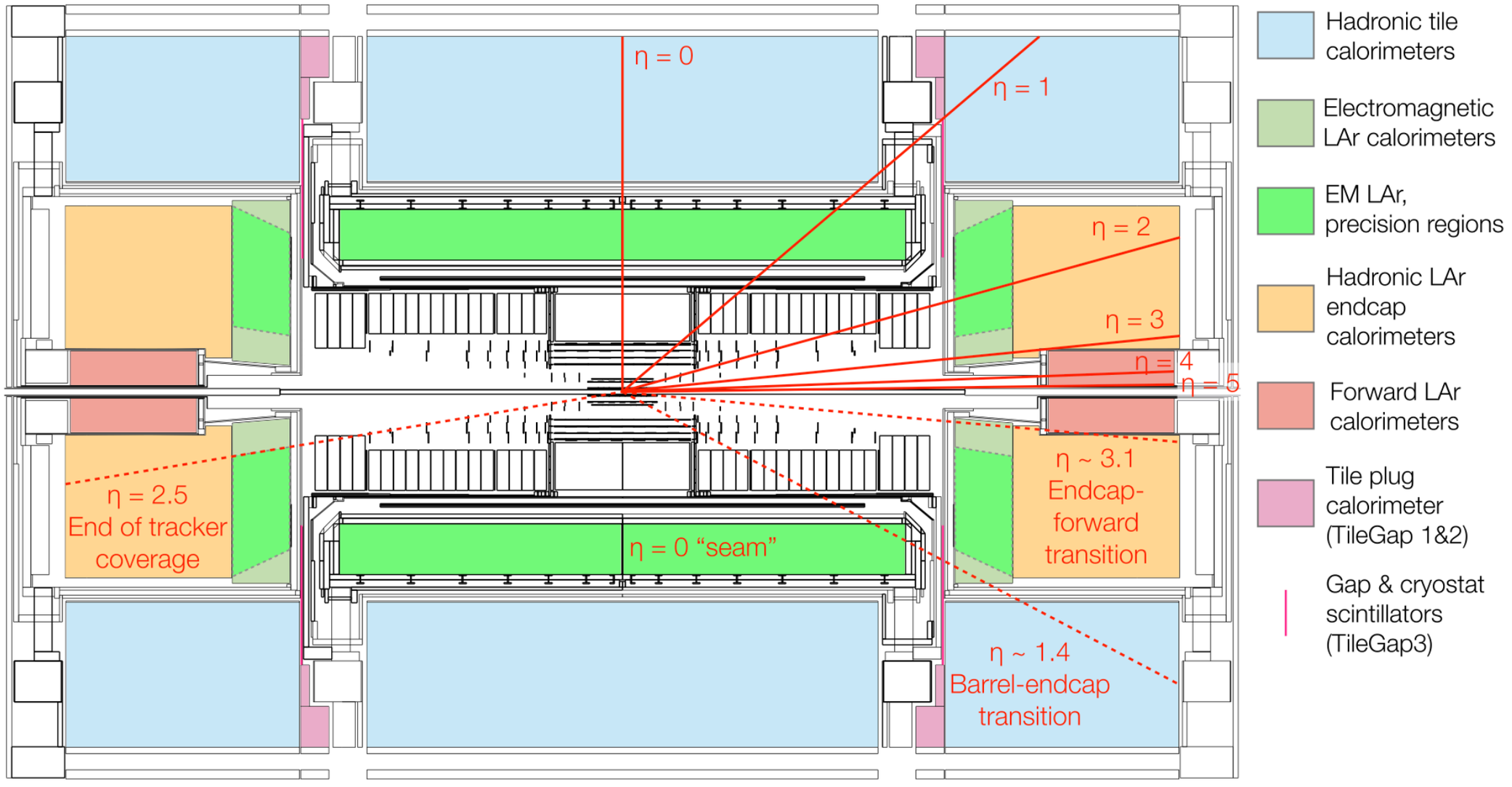

Fig. 1 Layout of the ATLAS calorimeters with pseudorapitidy (η) values marked for reference. The inner detector systems can be seen in black-and-white in the center of the diagram; tracking is provided up to $\eta = 2.5$. The electromagnetic (EM) barrel and endcap calorimeters are shown in green. The EM barrel has consistent performance throughout, but has a seam in the construction at $\eta = 0$ which can impact jet energy resolution. The EM endcap has a precision region marked in darker green and an extended region in light green, and the transition from one to the other around $\eta \sim 2.5$ involves a dramatic change in the material layers. The hadronic Tile calorimeter is shown in light blue while the hadronic endcap calorimeters based on liquid argon are illustrated in light orange. The forward calorimeters are shown in dark orange. Pink filled regions represent the tile plug calorimeter, often referred to as TileGap1 and TileGap2. The thin hot pink line marks the location of the very narrow gap and cryostat scintillators (TileGap3). The regions corresponding to the transition from barrel to endcap ($\eta \sim 1.4$) and from endcap to forward calorimeter ($\eta \sim 3.1$) are given for reference

Jet calibration

Small-R and Large-R Calibration schemes

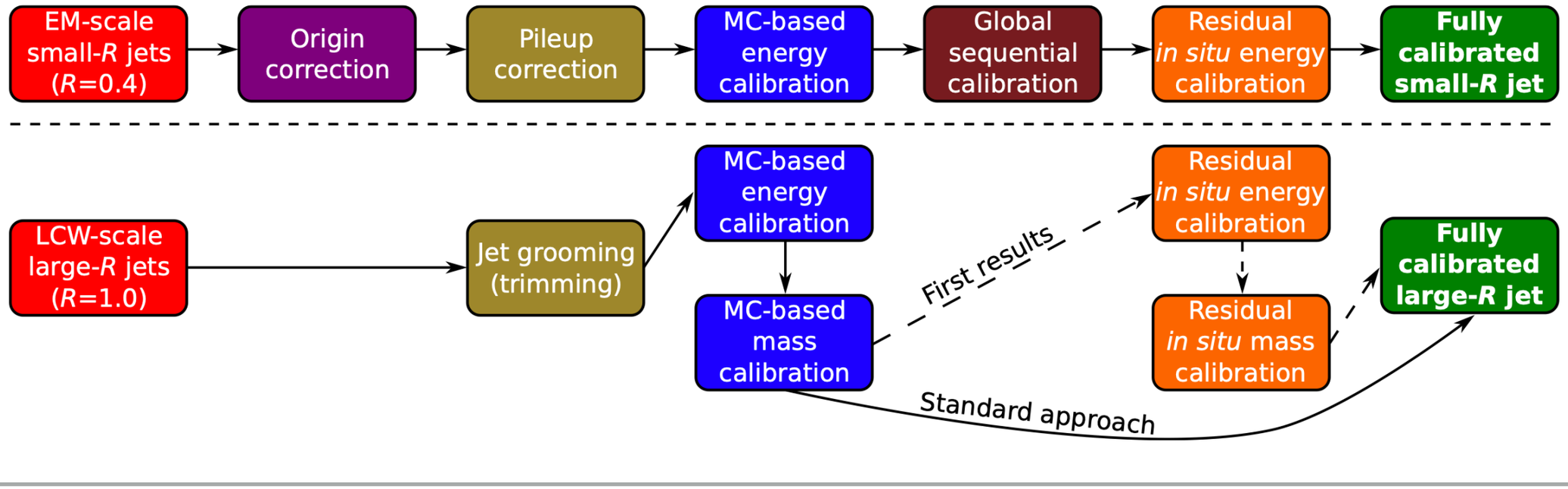

FullJER is your friend

JES and JER uncertainties are computed from a combination of many different measurements comparing data and MC

- The ‘full’ set of nuisance parameters is ~100 for JES and 34 for JER

The Jet/ETMiss group provides ‘reductions’ which combine related NP to reduce the burden on analysis

Sophisticated analyses (like those in Top Group) have a huge number of bins and signal regions

- does a wiggle in, e.g., bin1 corresponds to a wiggle in bin 107, or anti-wiggle?
- “Everything wiggles together” in the case of 1 NP: obviously overly simplistic!
- **Could result in too aggressive (or too conservative) application of uncertainties**

The more NP are combined, the more information on the correlation structure between the SRs you lose

JES/JER uncertainty

JES corrects Data to match MC, which itself is calibrated to “truth scale”

- MC reco jets calibrated to truth jets
- then, data jets calibrated to MC reco jets
- JES uncertainties correspond to how sure we
- are that data and MC are *actually* at the same scale

JES recommendation is “Category Reduction”

- ⇾ 30 NPs (UP and DOWN variations)

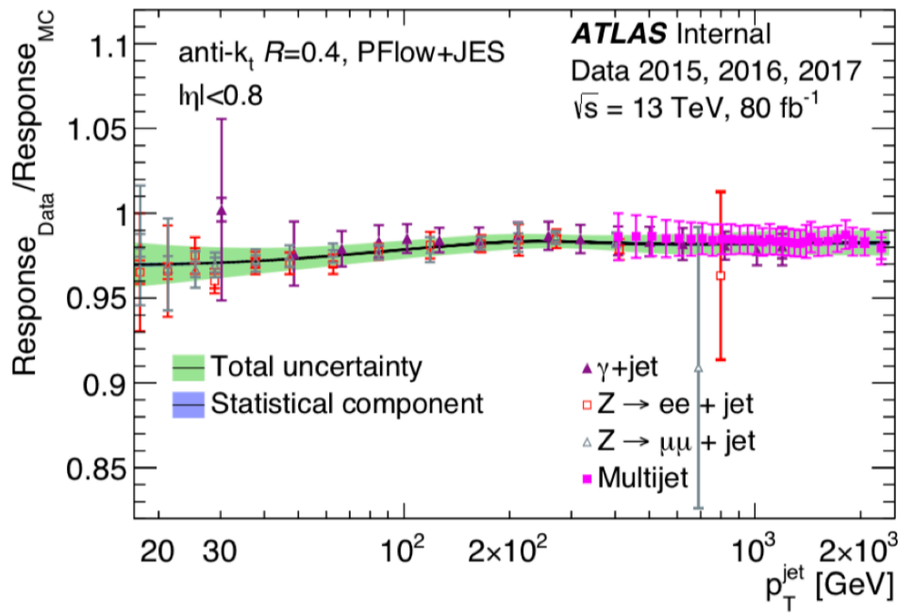

JER is a more complicated story...

- Not so easy to apply a correction like for the scale!
- You *can* smear the MC to match data,
  if MC resolution is better than data
- But if data resolution is better than MC,
  don’t want to degrade the data!

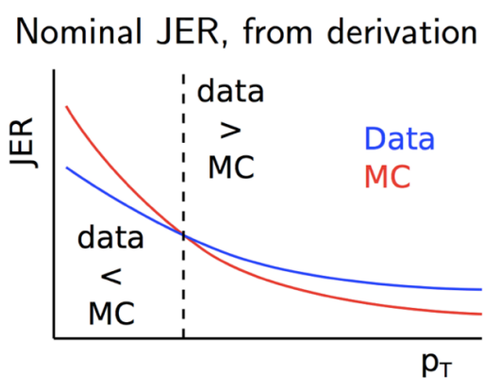

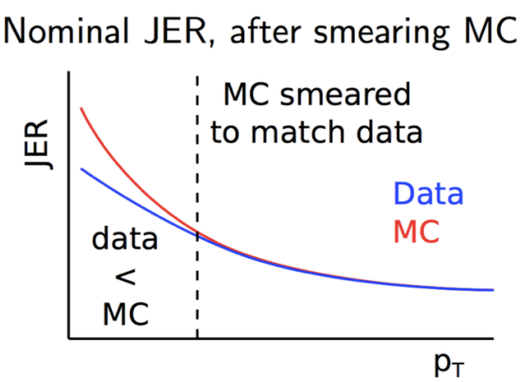

JER smearing

Uncertainties on JER propagated by smearing jets by a Gaussian width σ_{smear}:

$$(\sigma_{smear})^2 = (\sigma_{nominal}-\sigma_{NP})^2 - (\sigma_{nominal})^2$$

- If $\sigma_{NP} > 0$, smear MC; If $\sigma_{NP} < 0$, smear data (or pseudo-data)
- When **JER(data) < JER(MC)**, take full difference as uncertainty *in addition* to other JER uncertainties ($\sigma_{NP} = \sigma_{nominal,data} - \sigma_{nominal,MC}$)

This means that:

- **green** uncertainties are applied everywhere
- **gold** are extra uncertainties to cover cases when data resolution is better than MC

Smearing (pseudo-)data preserves anti-correlations when uncertainty components cross zero

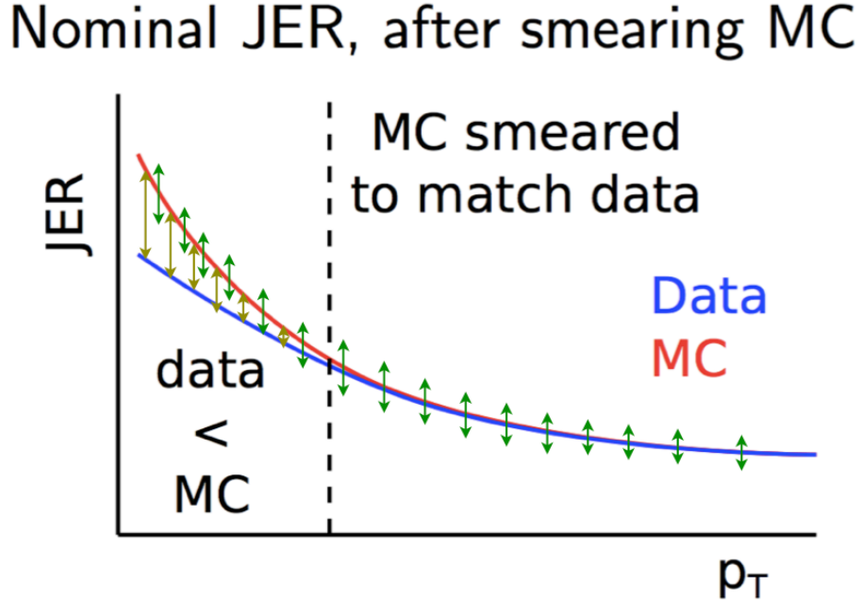

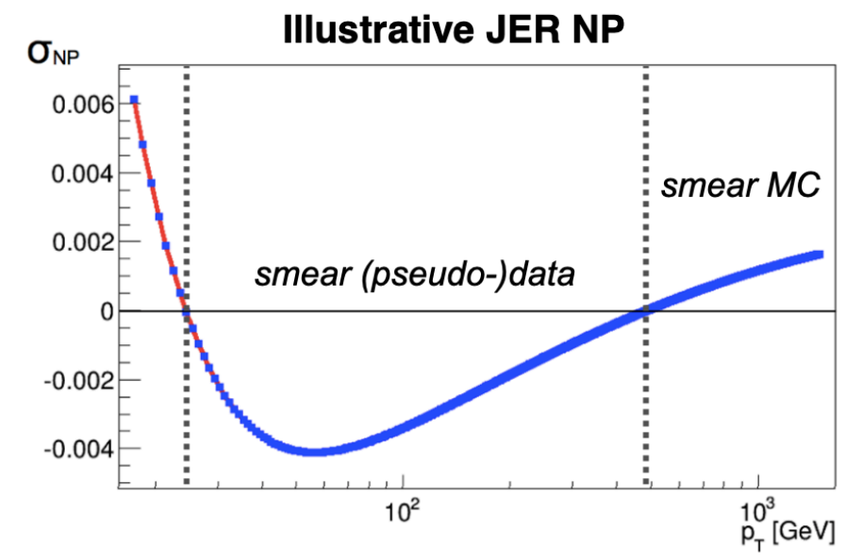

JER In Practice...

(Pseudo-)data smearing may not always be desirable

- e.g. searches insensitive to the JER
- ⇾ provide two correlation schemes:
  - **Full correlations** (*data or MC* smearing): crossing zero = anti-correlation
    Recommended for analyses sensitive to JER.
  - **Simple correlations** (*MC-only* smearing): crossing zero = correlation
    Recommended only for analyses insensitive to JER.

Further details about the application **here**

Benefits of using FullJER:

- Before using FullJER:
  - *"We unblinded and see a large pull in the JER.We need to talk to Jet/ ETMiss and understand in detail what is happening and understand our analysis sensitivity to this pull.This will slow down our analysis so much and we will miss our deadlines* 😭"
- After using FullJER:
  - *"We unblinded and we see a large pull in the JER.We implemented FullJER, so we can trust this instrumental pull.We should probably still mention this to Jet/ETMiss so they can think about why our phase space has such sensitivity to the CP NP, and they will be grateful for providing feedback on the effects of the JER on analyses.We will make our deadlines!* 😎"

IBU vs. FBU vs. SVD vs. PLU

Reference: arxiv.org/1201.4612

FBU differs from *D'Agostini's iterative unfolding (IBU)* despite both using Bayes' theorem.

- In FBU the answer is not an estimator and its covariance matrix, but a posterior probability density defined in the space of possible spectra.
- FBU does not involve iterations, thus does not depend on a convergence criterion, nor on the first point of an iterative procedure, which in IBU is named "prior".
  - If more than one answers are equally likely, as can happen when the reconstructed spectrum has fewer bins than the inferred one, then FBU reveals all of them, while IBU converges towards some of the possible solutions.
- Regularization is not done by interrupting iterations, but by choosing a prior which favors certain characteristics, such as smoothness.
  - Thus, FBU offers intuition and full control of the regularizing condition, which makes the answer easy to interpret.

FBU differs significantly also from *SVD unfolding*.

- In FBU the migrations matrix is not distorted by singular value decomposition (SVD), therefore FBU assumes the intended migrations model.
- The answer of FBU is a probability density function which does not have to be Gaussian, which is important especially in bins with small Poisson event counts.
- FBU does not involve matrix inversion and computation of eigenvalues, which makes it more stable numerically.
- SVD imposes curvature regularization, while FBU offers the freedom to use different regularization choices. This freedom becomes necessary when the correct answer actually has large curvature, or when the answer has only two bins, thus curvature is not even defined.

PLU is similar to *FBU* in terms of prior for regularisation, but it involves a Profile Likelihood fit too.

Global PDF fit in ATLAS

EPJC 82, 438 (2022)

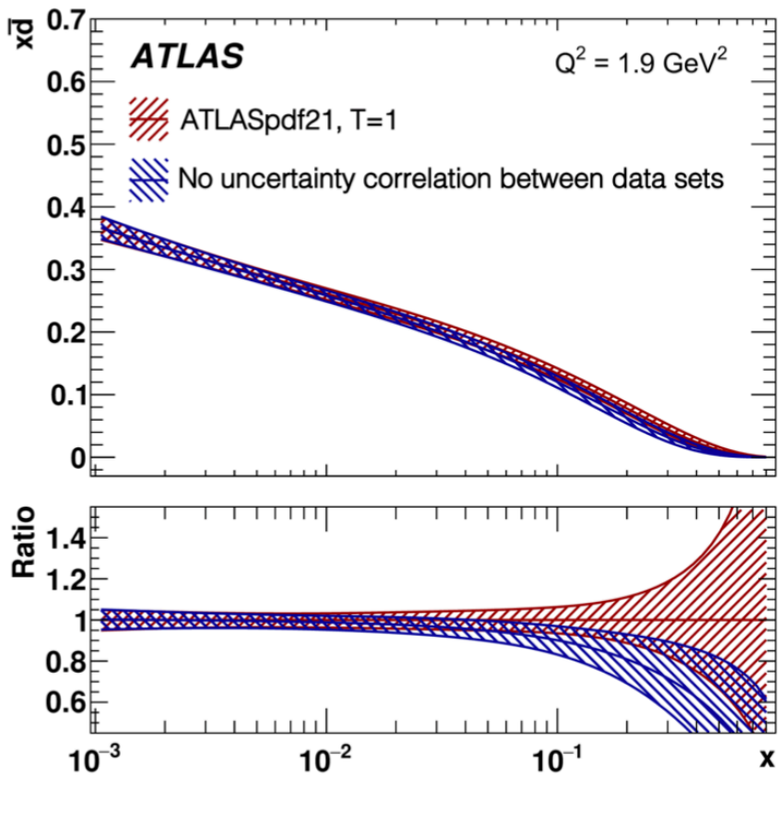

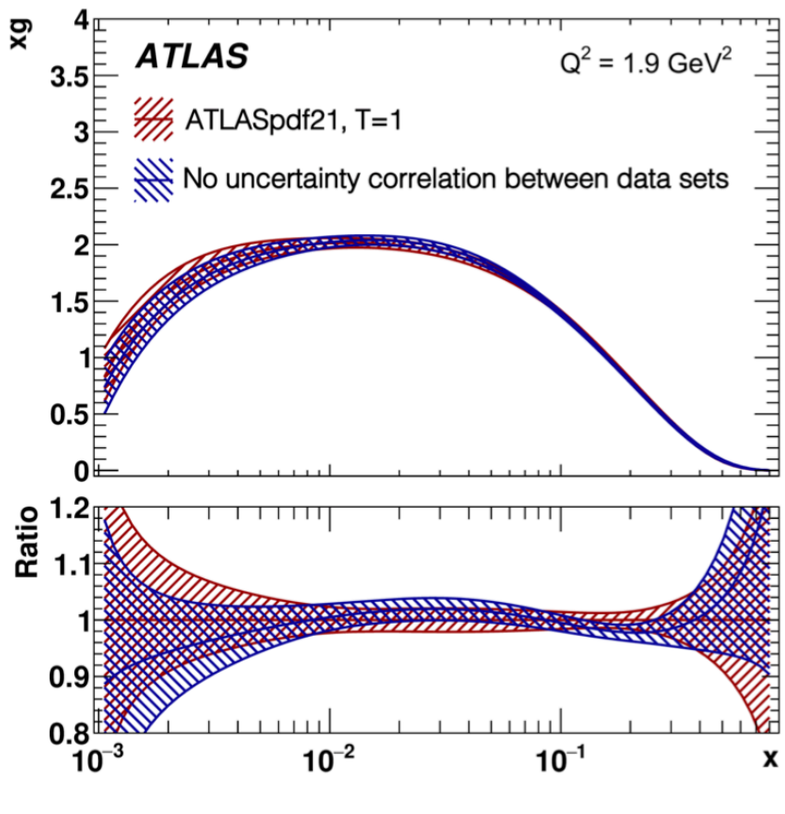

ATLAS is able to assess the correlations of such uncertainties between their datasets and account for them – an ability put to great effect in their new PDF result.

- Such knowledge was not previously available outside ATLAS, making this result a new “vademecum” for global PDF groups.
- It turns out that the impact of such correlations can shift the central values of the PDFs by > 1% in the mid-range momentum region, and by much more than this in the high-x region

Exotic hadrons

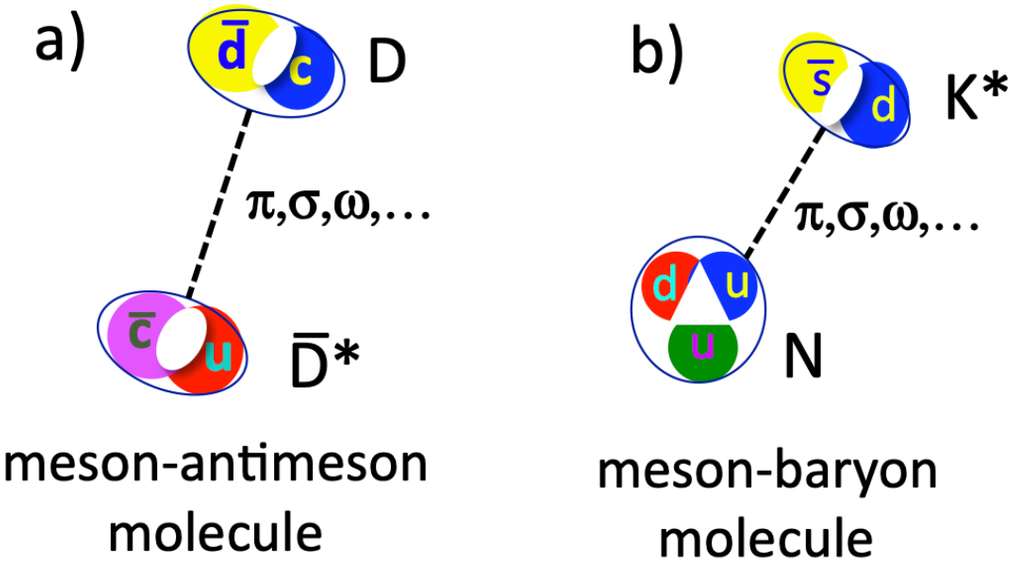

FIG. 7 Illustrations of a **a)** meson-meson and a **b)** meson-baryon molecular-like structure bound by Yukawa-type meson exchange forces. **c)** A sketch of the hadrocharmonium configuration of multiquark states. Here a color-singlet $Q\bar{Q}$ core state interacts with a surrounding 'blob" of gluons and light quarks via QCD versions of Van der Waals type forces. **d)** In adjoint charmonium states, a color-octet $Q\bar{Q}$ pair interacts with surrounding gluons and light quarks via color forces.

Exotic hadrons (charmonium)

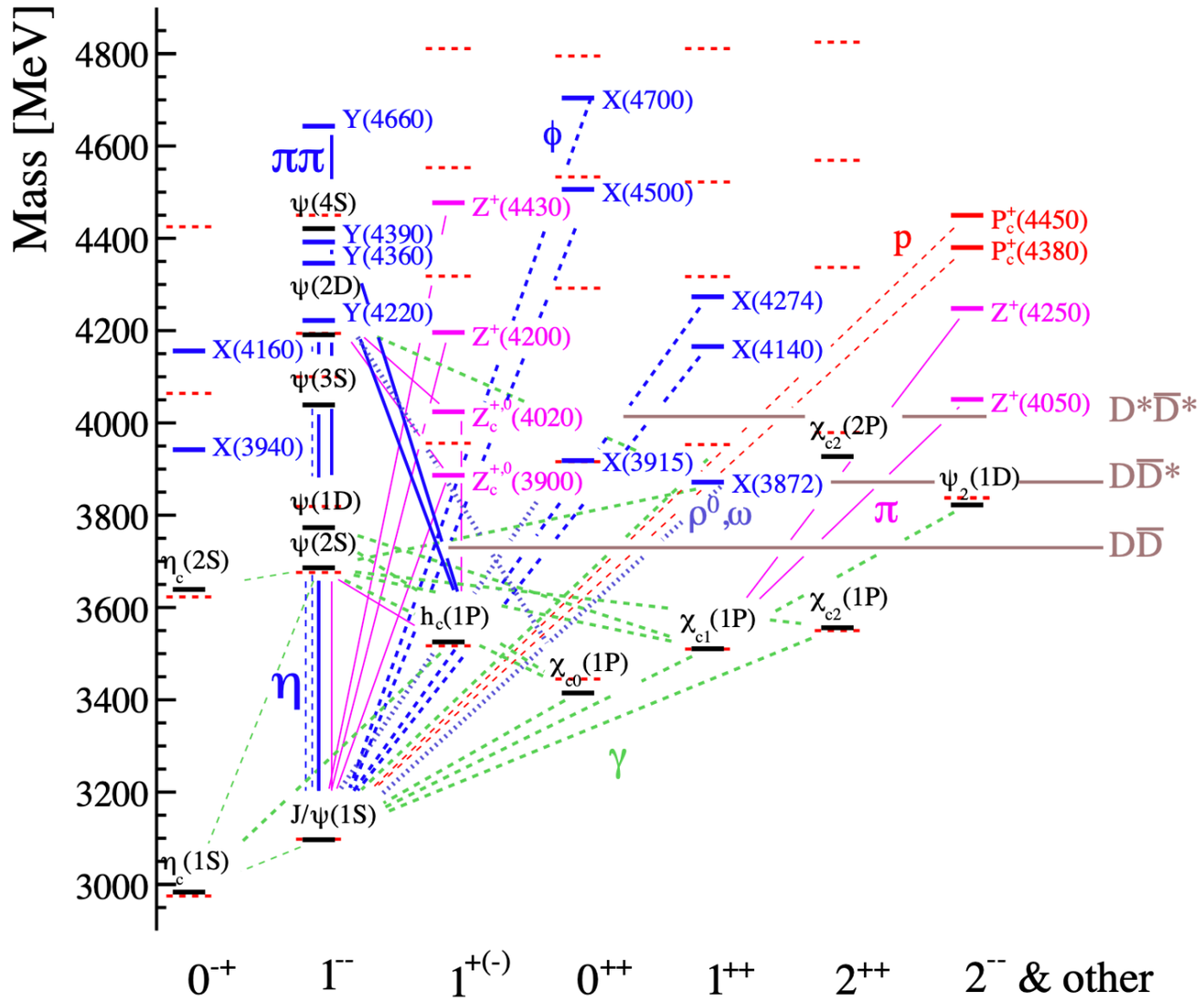

FIG. 65 The current status of the charmonium-like spectrum. The dashed (red) horizontal lines indicate the expected states and their masses based on recent calculations (39) based on the Godfrey-Isgur relativized potential model (40), supplemented by the calculations in ref. (332) for high radial excitations of the P-wave states. The solid (black) horizontal lines indicate the experimentally established charmonium states, with masses and spin-parity (J^{PC}) quantum number assignments taken from ref. (9), and labeled by their spectroscopic assignment. The open-flavor decay channel thresholds are shown with longer solid (brown) horizontal lines. The candidates for exotic charmonium-like states are also shown with shorter solid (blue or magenta) horizontal lines with labels reflecting their most commonly used names. All states are organized according to their quantum numbers given on horizontal axis. The last column includes states with unknown quantum numbers, the two pentaquark candidates and the lightest charmonium 2^{--} state. The lines connecting the known states indicate known photon or hadron transitions between them: dashed-green are γ transitions; (thick E1, thin M1), solid-magenta are π; thin (thick) dashed-blue are η (ϕ); dashed-red are p; dotted-blue are ρ^0 or ω; and solid-blue other $\pi\pi$ transitions, respectively.

Exotic hadrons (bottomonium)

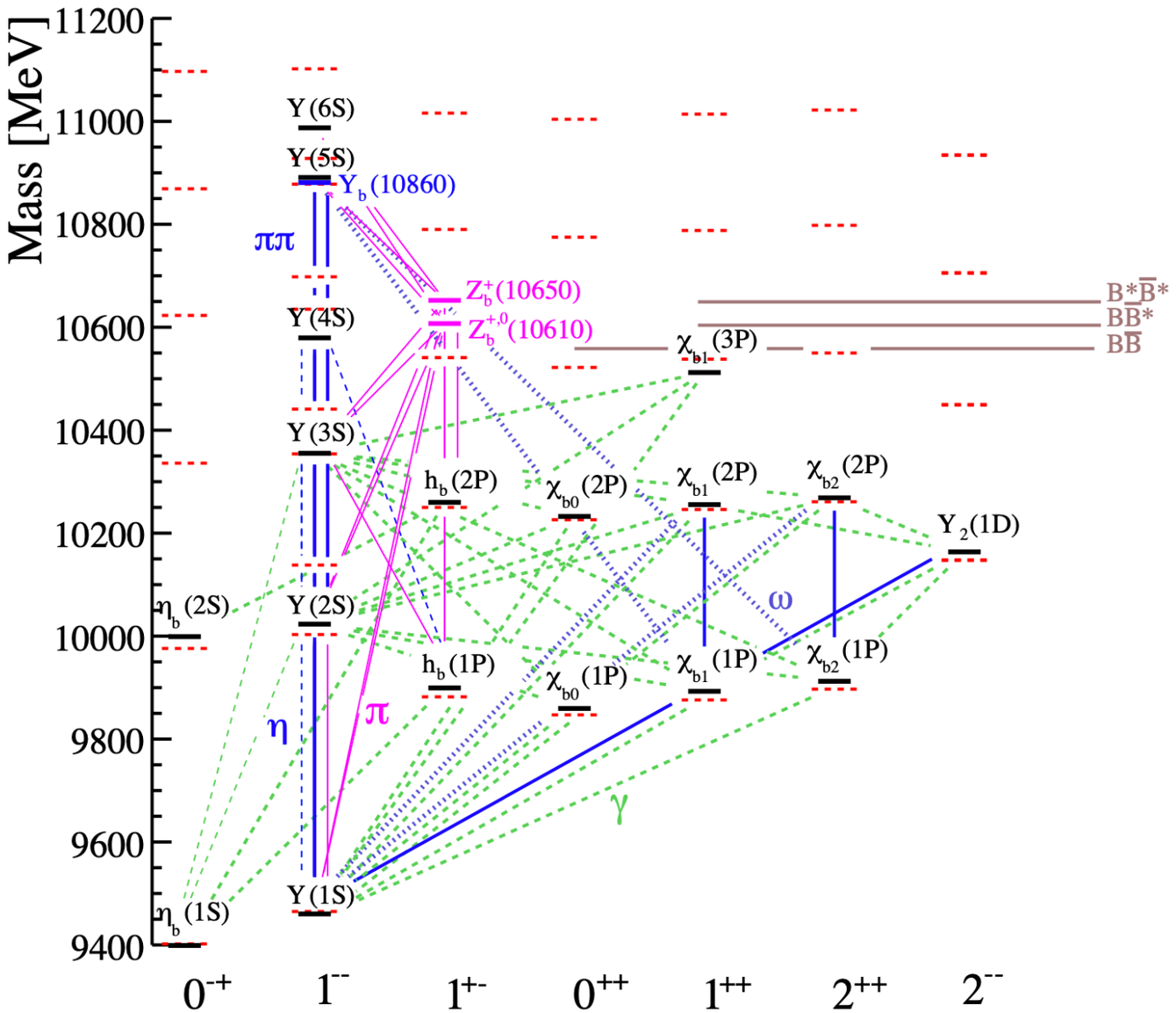

FIG. 66 The current status of the bottomonium-like spectrum. The current status of the bottomonium-like spectrum. The dashed (red) lines indicate the expected states and their masses based on recent calculations (41) based on the Godfrey-Isgur relativized potential model (40). The solid (black) horizontal lines indicate the experimentally established charmonium states, with masses and spin-parity (J^{PC}) quantum number assignments taken from ref. (9), and labeled by their spectroscopic assignment. The open-flavor decay channel thresholds are shown with longer solid (brown) horizontal lines. The candidates for exotic bottomonium-like states are also shown with shorter solid (blue or magenta) horizontal lines with labels reflecting their most commonly used names. The known photon and hadron transitions are also indicated (see the caption of Fig. 65).

ALPHA detector

https://cerncourier.com/a/roman-pots-for-the-lhc/

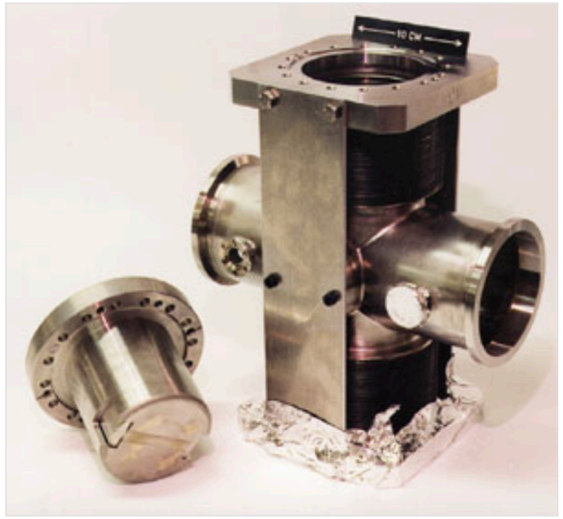

In the Roman Pot technique, the detectors are placed as close to the colliding beams as possible. The pots, which are mounted on either side of the horizontal beam pipe, move vertically in a bellows structure towards the path of the colliding particle beams. One of the pots housing the detectors is shown (left) removed from the bellows structure.

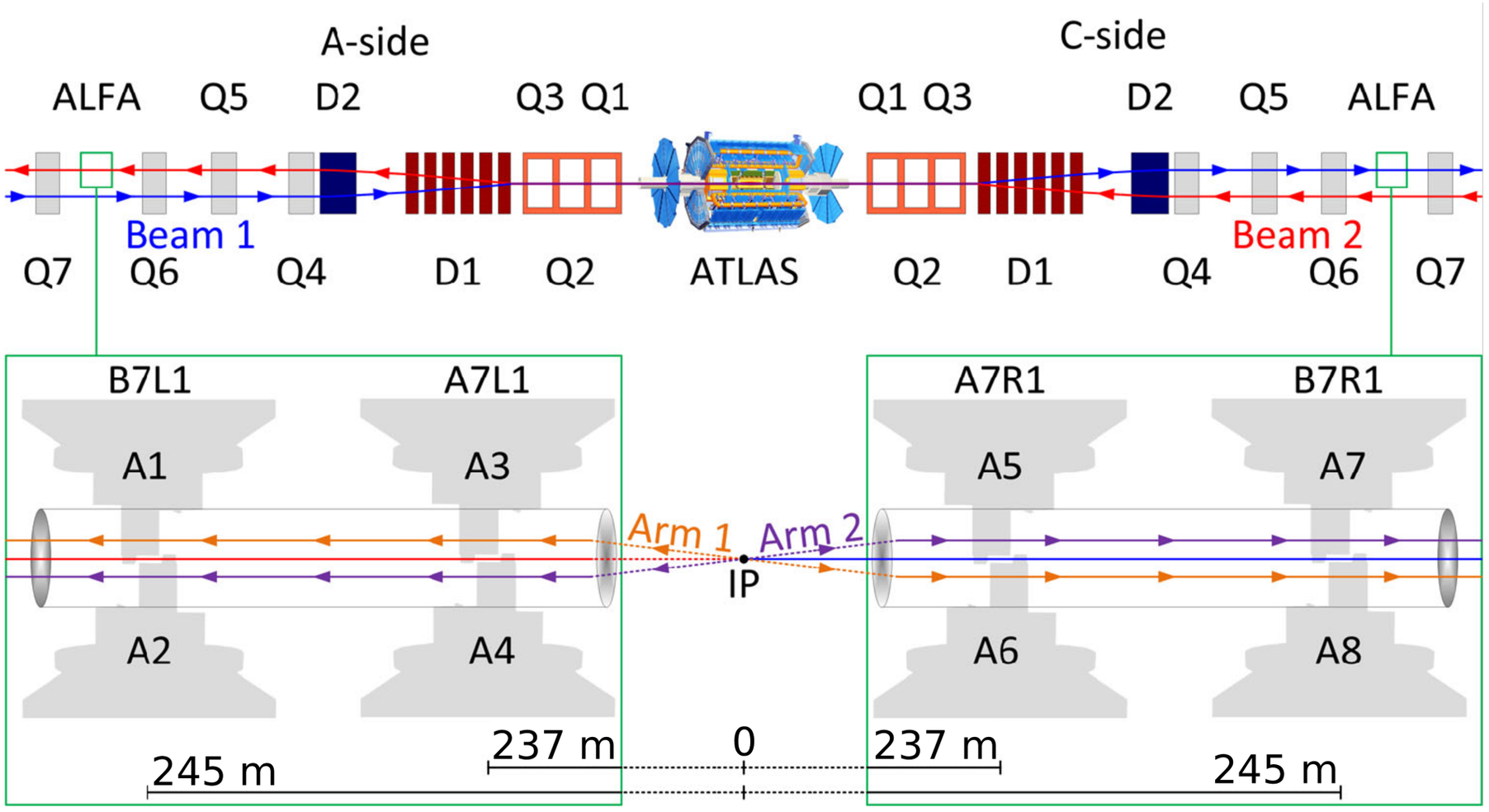

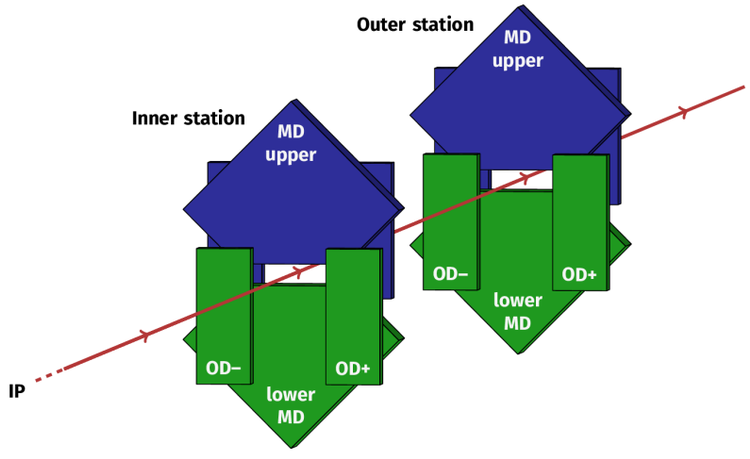

b-fragmentation function with $t\bar{t}$

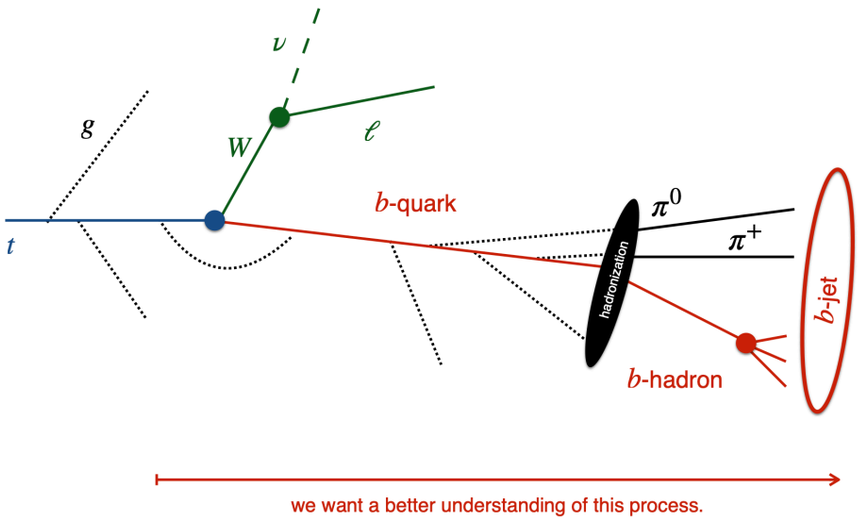

critical for delivering the best physics results with b-jets.

b-tagging efficiency and b-jet response are very sensitive to fragmentation.

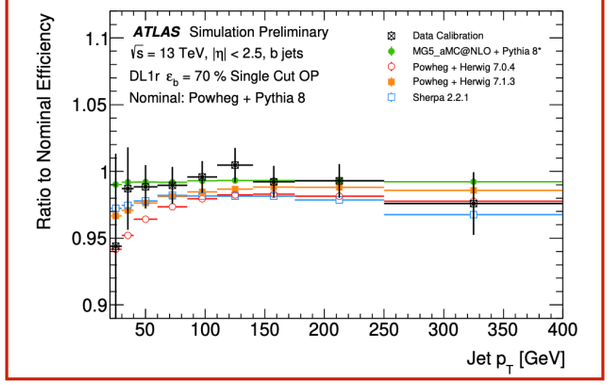

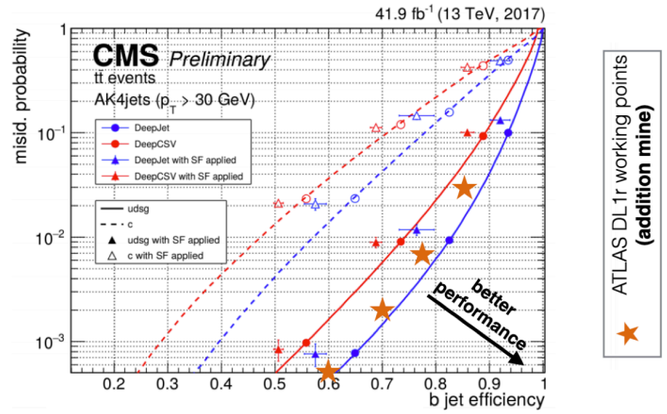

in the machine-learning era, small mismodeling of b-jet internals has large consequences.

may lose ~10% of signal b-jets in data c.f. simulation.

K_s^0 & Λ^0 production

Submitted to EPJC

Measurements of neutral strange particle production interesting

- to test theoretical jet fragmentation functions
- to constrain the underlying event (UE) effects
- ⇾ helpful to to tune strange particle content of MC models

Standard dilepton selection @7TeV data

- classification as inside bjet, inside non-b-jet and outside any jet
- unfolding to particle level

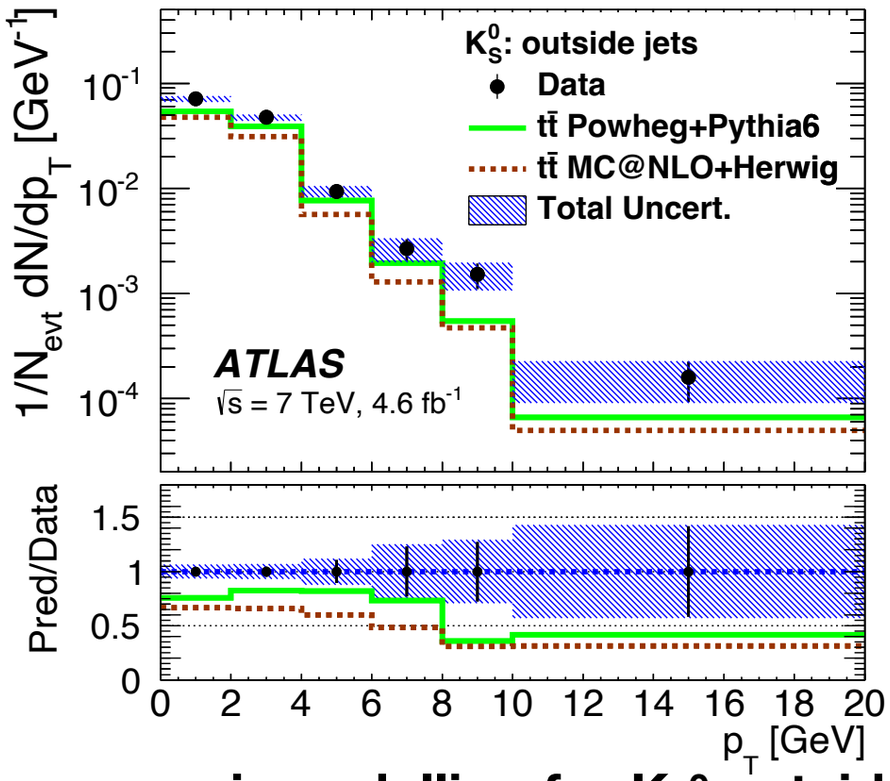

some mismodelling for K_s^0 outside jets

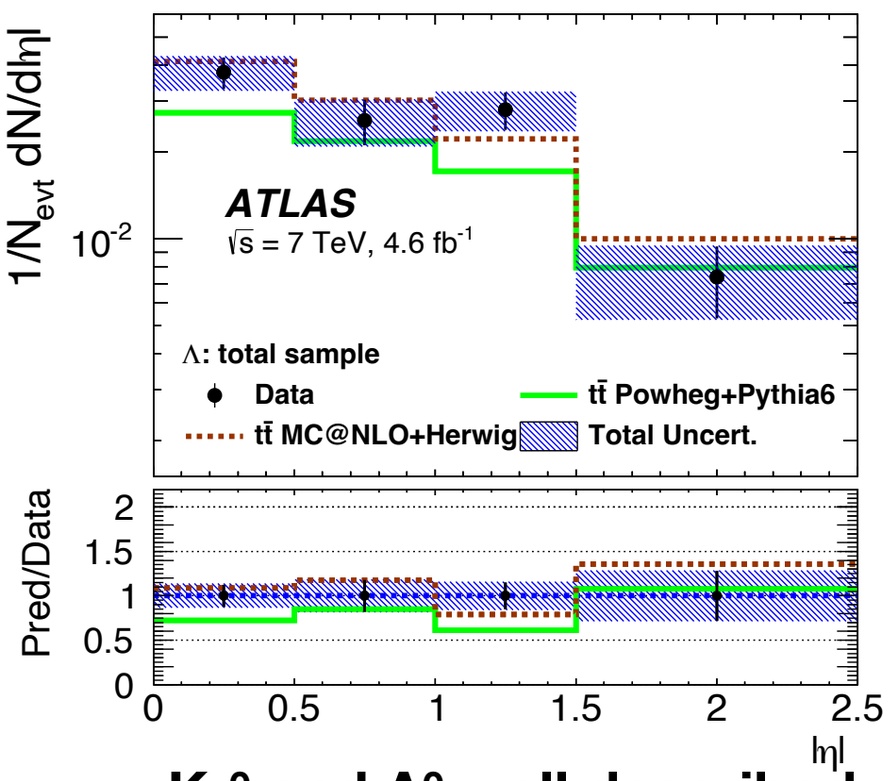

K_s^0 and Λ^0 well described

$t\bar{t}$ differential x-section (l+jets)

ANA-TOPQ-2020-09

After Pre-Approval (particle-level analysis)

Analysis goal: measurement of differential $t\bar{t}$ (l+jets resolved) x-sections at particle and parton level (as separate papers in the pipeline)

- 1D, 2D and 3D x-sections for top and $t\bar{t}$ kinematic observables, Run II data (139/fb)

Comparison with MC (Powheg+Pythia8) and NNLO predictions (computed with MATRIX and from Mitov et al.)

- uncertainties as difference between nominal and "systematically" varied unfolded samples
  - + dominating JES/JER and modelling systematics, Improved w.r.t. already published result (36/fb)
- preliminary result of a PDF fit performed with newly measured x-sections (bottom right)

Future plans (parton-level analysis): extrapolation of m_t, pdf and α_s in simultaneous fit, like CMS recent paper

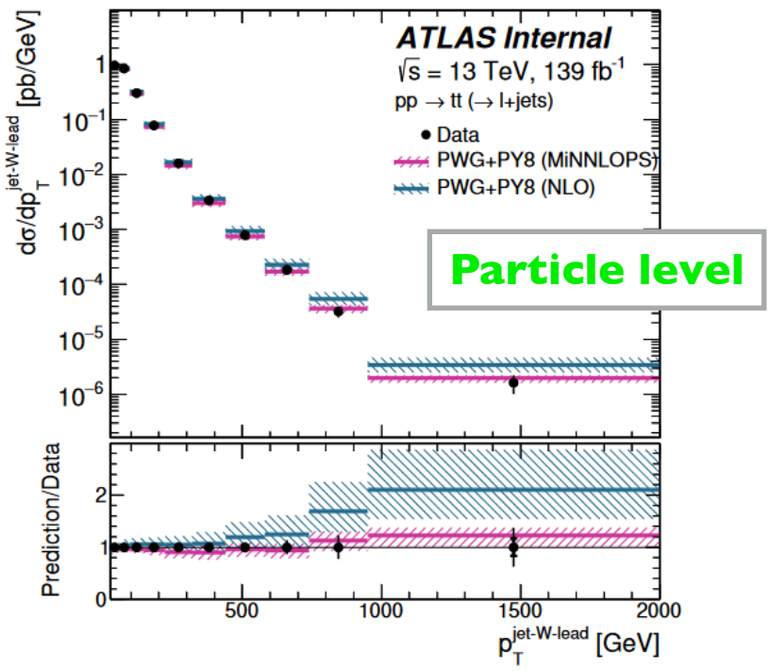

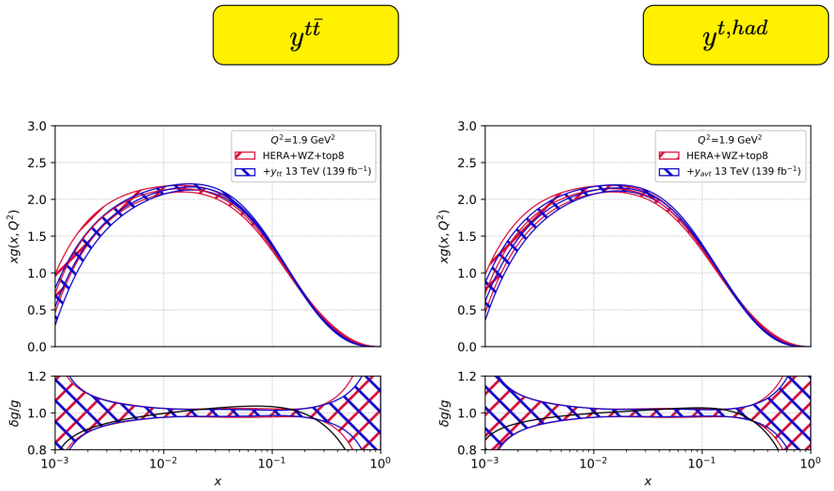

Improvements in uncertainty at high-x gluon PDF softer at higher-x and lower-x for both $y^{t\bar{t}}$ and $y^{t\ had}$

$t\bar{t}$ differential x-section (l+jets)

ANA-TOPQ-2020-09

$p_T^{t\bar{t}}$

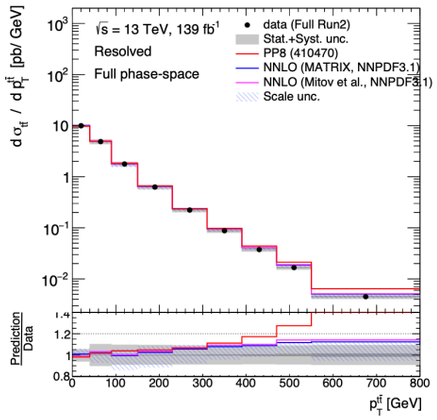

$p_T^{t\bar{t}}$ vs $m^{t\bar{t}}$

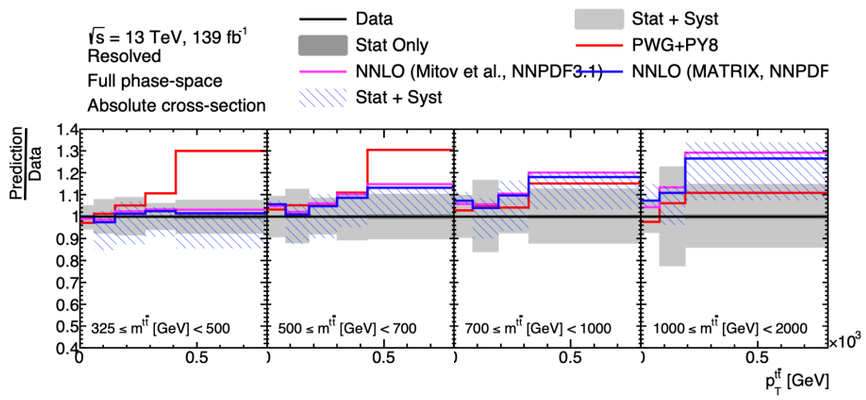

Good compatibility with NNLO predictions

Large differences wrt NLO MC in $p_T^{t\bar{t}}$ and $p_T^{t\bar{t}}$ vs $m^{t\bar{t}}$ distributions

$y^{t\bar{t}}$

$y^{t,had}$

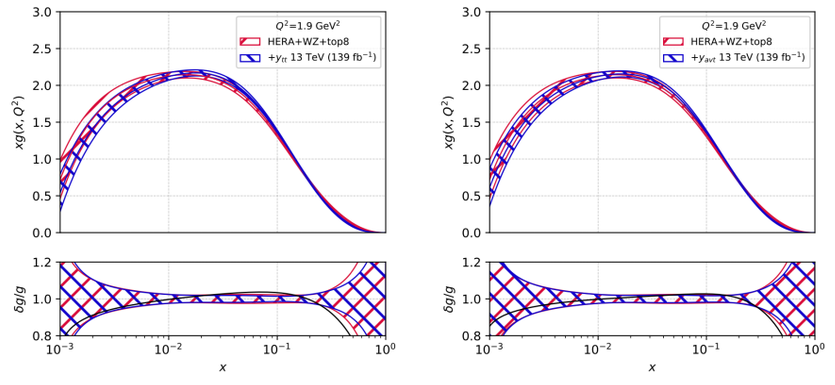

Improvements in uncertainty at high-x

gluon PDF softer at higher-x and lower-x for both $y^{t\bar{t}}$ and $y^{t\ had}$

Top mass with soft-muons

ATLAS-CONF-2019-046

Analysis goal: $m_{\ell\mu}$ invariant mass between hard lepton from W and soft-muon from semi-leptonic b-quark decay as proxy to m_t

- useful in top mass combination since it's not sensitive to hadronic uncertainties

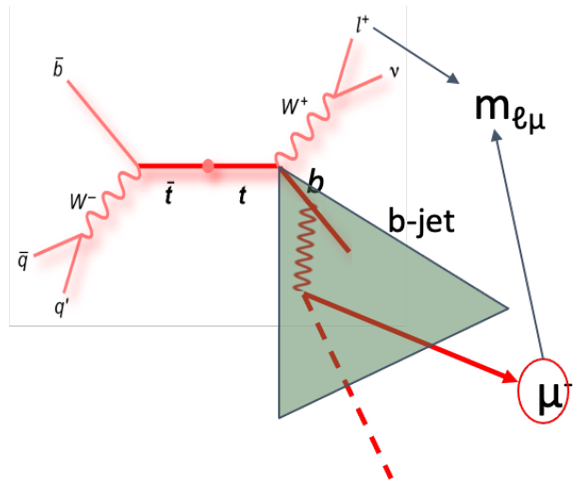

Final topology:

- 1 high-p_T isolated lepton (from $W \to \ell\nu$) + 1 low-p_T muon inside b-jet
- ≥1 b-jet + ≥4 jets + E_T^{miss} cut

Main systematic: modelling of b-quark fragmentation

- b-quark fragmentation in Pythia tuned on LEP data
- production fractions and BRs tuned to Babar/LEP and LHC measurements

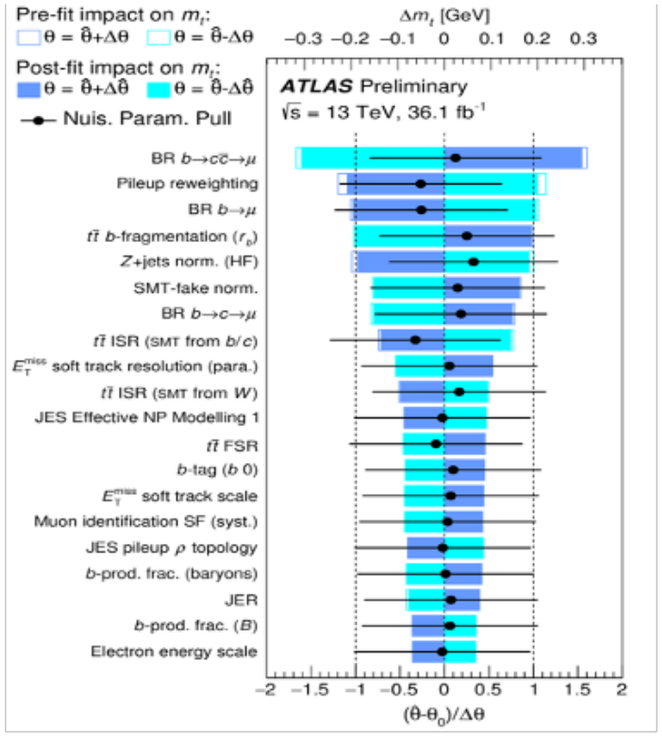

Potentially the most precise top mass analysis in ATLAS (36/fb)

- **m_t = 174.41 ± 0.77 GeV = 174.41 ± 0.39 (stat) ± 0.66 (syst) GeV**

b-quark physics

Why b- and light states- (BLS) physics in ATLAS?

- test of QCD-based prediction: cross section, spectroscopy, asymmetries, etc.
- test of EW physics or search for new physics (rare decays, CPV, Flavour anomalies)

How to study BLS physics?

- typical signatures at hadron colliders
  - + ID system: tracks and reconstruction of secondary vertices
  - + ID system +Muon system: low transverse momentum (p_T) muons
  - + EM calorimeter: rarely photons and electrons
- impossible to trigger all low p_T muons with high-lumi ⇾ employ topological triggers
  - + p_T, η and ϕ of muon ROIs to build topological di-muon quantities (invariant mass or ΔR)
  - + efficient way to reduce bandwidth usage keeping signal efficiency high
  - + gain up to a factor of 3 in di-muon background rejection

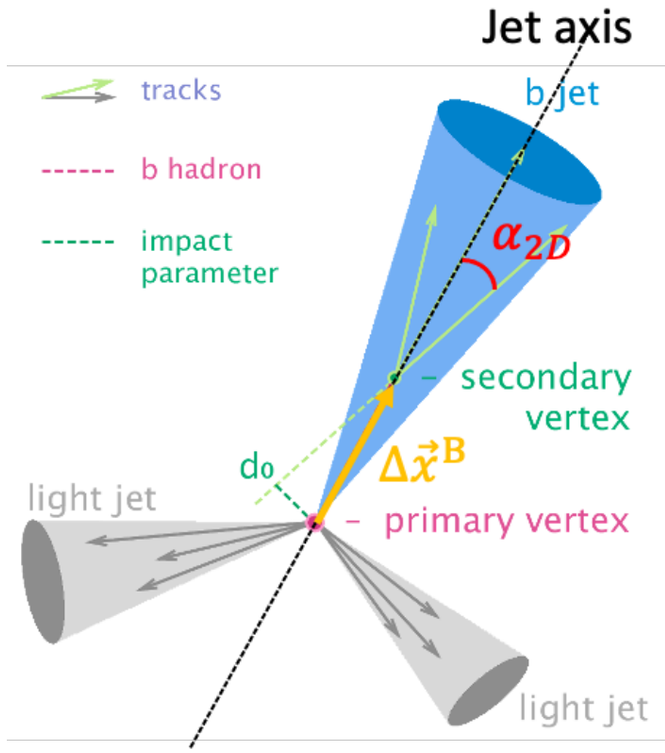

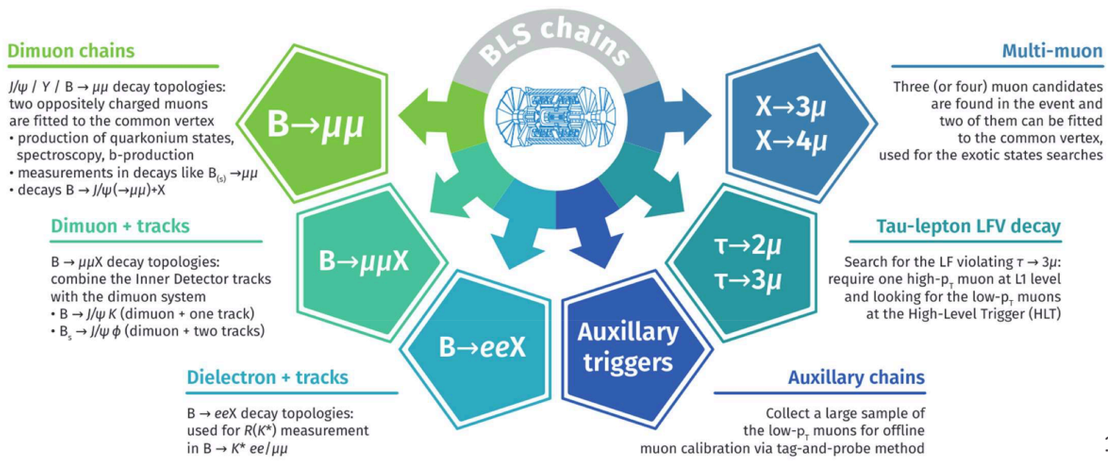

Recent BLS results

More public results here

Short Title	Journal Reference	Date	√s (TeV)	L
search...	search...	search...	search...	
Bc+ to J/psi D(*)(s)+ in full Run2	Submitted to JHEP	2022-03-03	13	139 fb^{-1}
Exclusive b fragmentation at 13 TeV	JHEP 12 (2021) 131	2021-08-26	13	139 fb^{-1}
Bs to J/psi phi run-2	Eur. Phys. J. C 81 (2021) 342	2020-01-20	13	80.5 fb^{-1}
Production ratio of Bc to B+/-	Phys. Rev. D 104 (2021) 012010	2019-12-05	8	20.3 fb^{-1}
Associated production of J/psi and W boson at 8 TeV	JHEP 01 (2020) 095	2019-09-29	8	20.3 fb^{-1}

Short Title	Document number	Date	√s (TeV)	L
search...	search...	search...		
B0(s) to mumu LHC combination	ATLAS-CONF-2020-049	2020-08-04	13	26.3 fb^{-1}
J/psi and psi(2S) differential cross-sections at high pT	ATLAS-CONF-2019-047	2019-09-30	13	139 fb^{-1}
Searches for pentaquarks using Run-1 data	ATLAS-CONF-2019-048	2019-09-27	7, 8	20.6 fb^{-1}, 4.9 fb^{-1}

$B_s^0 \to \mu^+\mu^-$ Combination (ATLAS+CMS+LHCb)
(ATLAS-CONF-2020-049)

$B_s^0 \to \mu^+\mu^-$ and $B^0 \to \mu^+\mu^-$ combination using 2011-2016 LHC data. **2.3σ tension with SM**.
$\tau(B_s^0 \to \mu^+\mu^-) = 1.91\ ^{+0.37}_{-0.35}$

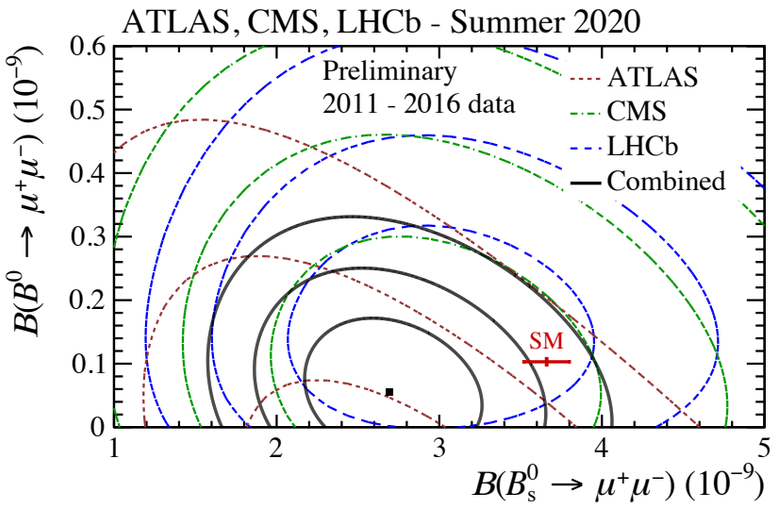

$B_s^0 \to \mu^+\mu^-$ combination published in 2019 (see bottom blue box)

- ongoing analyses:
  - + ITA&&BPHY GLANCE
  - + 5 Run II analyses: 2 Finished, 3 Active

Manpower is the limiting factor

- rare decays / anomalies deserve investigation!
- many open tasks to work on and high visibility guaranteed
- Run I showed some BLS analyses can be competitive with CMS and LHCb